AD_____

AWARD NUMBER: DAMD17-02-1-0291

TITLE: Involvement of 53BP1, a p53 binding protein, in Chk2 phosphorylation of p53 and DNA damage cell cycle checkpoints

PRINCIPAL INVESTIGATOR: Bin Wang, Ph.D.

CONTRACTING ORGANIZATION: Brigham and Women's Hospital
Boston, Massachusetts 02115

REPORT DATE: May 2006

TYPE OF REPORT: Annual Summary

PREPARED FOR: U.S. Army Medical Research and Materiel Command
Fort Detrick, Maryland 21702-5012

REPORT DOCUMENTATION PAGE

Form Approved
OMB No. 0704-0188

1. REPORT DATE *(DD-MM-YYYY)*	**2. REPORT TYPE**	**3. DATES COVERED** *(From - To)*
01-5-2006	Annual Summary	17 Apr 2002 – 16 Apr 2006

4. TITLE AND SUBTITLE

Involvement of 53BP1, a p53 binding protein, in Chk2 phosphorylation of p53 and DNA damage cell cycle checkpoints

5a. CONTRACT NUMBER

5b. GRANT NUMBER
DAMD17-02-1-0291

5c. PROGRAM ELEMENT NUMBER

6. AUTHOR(S)

Bin Wang, Ph.D.

E-Mail: bwang@rics.bwh.harvard.edu

5d. PROJECT NUMBER

5e. TASK NUMBER

5f. WORK UNIT NUMBER

7. PERFORMING ORGANIZATION NAME(S) AND ADDRESS(ES)

Brigham and Women's Hospital
Boston, Massachusetts 02115

8. PERFORMING ORGANIZATION REPORT NUMBER

9. SPONSORING / MONITORING AGENCY NAME(S) AND ADDRESS(ES)
U.S. Army Medical Research and Materiel Command
Fort Detrick, Maryland 21702-5012

10. SPONSOR/MONITOR'S ACRONYM(S)

11. SPONSOR/MONITOR'S REPORT NUMBER(S)

12. DISTRIBUTION / AVAILABILITY STATEMENT
Approved for Public Release; Distribution Unlimited

13. SUPPLEMENTARY NOTES

14. ABSTRACT
53BP1, a p53 binding protein, is involved in DNA damage response. It is phosphorylated in response to DNA damage and rapidly relocalize to sites of damage, forming nuclear foci that colocalize with those formed by phosphorylated histone H2AX, Mre11-Rad50-Nbs1 complex, MDC1, Brca1 and other DNA damage signaling proteins. Our studies aimed to determine the role of 53BP1 in DNA damage response and tumor suppression. We studied the function of 53BP1 in mammalian cells by knocking down expression of 53BP1 using small interfering RNA (siRNA) against 53BP1. We also generated 53BP1-defective (53BP1tr/tr) mouse model with expression of a defective C-terminal truncation of the m53BP1 protein. We have shown that 53BP1 is a key transducer in the DNA damage response signaling. Inhibition of 53BP1 by siRNA in human cancer cell lines resulted in defective S-phase and G2/M checkpoints in response to ionizing irradiation (IR). 53BP1 interacts with tumor suppressors p53, Chk2 and Brca1, and is involved in regulation of these proteins in response to IR. 53BP1tr/tr mice were growth retarded and IR-sensitive. Mouse embryonic fibroblast (MEF) cells generated from 53BP1tr/tr mice were hypersensitive to IR, and exhibited higher level of chromosomal abnormalities when treated with genotoxic stress, indicating a role of 53BP1 in maintaining genomic stability. Thus 53BP1 is likely to play an important role in maintenance of genomic stability and cancer prevention. These studies allowed us gain further insights into the DNA damage response pathway and the tumor suppression pathway in mammalian cells.

15. SUBJECT TERMS
53BP1, Chk2, p53, Checkpoint, DNA damage repair, tumor suppressor, mice knockout

16. SECURITY CLASSIFICATION OF:			**17. LIMITATION OF ABSTRACT**	**18. NUMBER OF PAGES**	**19a. NAME OF RESPONSIBLE PERSON**
a. REPORT	**b. ABSTRACT**	**c. THIS PAGE**			USAMRMC
U	U	U	UU	31	**19b. TELEPHONE NUMBER** *(include area code)*

Table of Contents

Introduction

53BP1 binds to the tumor suppressor protein p53 and has a potential role in DNA damage responses. Through studies of 53BP1-deficient human cells and mouse embryonic fibroblast (MEF) cells, we have shown that 53BP1 is a key transducer in the DNA damage response signaling. Inhibition of 53BP1 by siRNA in human cancer cell lines resulted in defective S-phase and G2/M checkpoints in response to ionizing irradiation (IR). Mouse embryonic fibroblast (MEF) cells generated from 53BP1-/- mice were hypersensitive to IR, and displayed a slight G2/M checkpoint deficiency in response to lower dose of IR. We also showed that 53BP1 binds to p53, Chk2 and Brca1. 53BP1 plays an important role in p53 stabilization, Chk2 phosphorylation in response to IR.

Body

Task1. To determine the role of 53BP1 in Chk2 activation and phosphorylation of p53 (months 1-12)

a. *To identify the association of Chk2 with 53BP1 in response to DNA damage (months 1-6)*
b. *To determine the involvement of 53BP1 in Chk2 phosphorylation and/or stabilization of p53 (months 6-12)*

We have completed this task. In the previous reports, we have shown that 53BP1 associated with Chk2, and the association is a dynamic process. Chk2 binds to 53BP1 in the absence of IR, and dissociates in the presence of IR. 53BP1 is also partially responsible for Chk2 T-68 phosphorylation and p53 stabilization (attached paper Wang et al., 2002). To further understand the role of 53BP1 in Chk2 phosphorylation and p53 stabilization, we seek to find 53BP1 associated proteins, we found that DNA damage repair protein Ku80 interacted with 53BP1. This indicates a role of 53BP1 in non-homologous end joining. Meanwhile, by deletion mutagenesis, we found that 53BP1 could oligomerize in the presence and absence of DNA damage (attached paper, Adams et al., 2005). We also confirmed that p53 binds to the BRCT region of 53BP1. Although BRCT motifs are proposed to be phospho-peptide binding modules, the interaction of p53 with 53BP1 is phosphorylation independent. In collaboration with Dr. Capenter group in UT Medical School, we also found that 53BP1 could be methylated in a glycine-arginine rich (GAR) stretch upstream of the Tudor motif.

Task2. To determine the role of 53BP1 in cell cycle checkpoints in response to DNA damage (months 1-24)

a. *Generation of the 53BP1 somatic knockout cells derived from hTERT-immortalized human epithelia cells (months 1-8)*
b. *Characterization of the sensitivity to DNA, chemotherapeutic agents and transformation potential for 53BP1 null cells (months 9-12)*
c. *To determine if 53BP1 deficiency will affect the G1, S, G2/M checkpoints and affect the known key playes (i.e. ATM, ATR, Chk2, Chk1) (months 12-24)*

We have basically completed this task. **A**, we used an alternative approach to generate 53BP1-deficient human cell line. We have used siRNA against 53BP1 in human cancer cell lines to generate 53BP1-deficient cells. **B**, by analyzing such cells, we were able to show that 53BP1 is involved in S-phase checkpoint and G2/M phase checkpoint. We also found that immortalized 53BP1-/- MEFs were IR-sensitive, but only displayed checkpoint deficiency in response to lower doses of IR. **C**, we showed that Chk2 phsophorylation was partially compromised in the 53BP1-siRNA treated cells. We then tested whether other key players of the DNA damage response, such as ATM, ATR, Chk1, NBS1, SMC1, etc. were affected with inhibition of 53BP1 in response to different types of DNA damage. No difference in activation of ATM, Chk1, or phosphorylation of NBS1 and SMC1 could be detected in the 53BP1 siRNA-treated cells and the control cells. Therefore, 53BP1 seems a specific mediator in regulating Chk2 and p53 in response to IR.

Task3. To determine the role of 53BP1 in development and tumor suppression (1-36)

a. Generation of 53BP1-deficient mince (months 1-12)
b. Characterization of 53BP1 in development (months 12-24)
c. Determination of 53BP1 in tumor suppression (months 24-36)

We mostly finished this task. In collaboration with Dr. Phillip Carpenter group in UT Medical School, we have been able to genotype and analyze the 53BP1-/- mice that were generated by Lexicon Inc. (Woodland, TX). We have shown that 53BP1-/- mice were hypersensitive to IR and cells from these animals exhibited chromosomal abnormalities (attached paper Morales et al., 2003). This suggests a role of 53BP1 in maintaining genomic stability and tumor suppression.

Key Research Accomplishments

- 53BP1 is a checkpoint protein. It is involved in S-phase and G2/M checkpoints
- 53BP1 associates with Chk2 and is involved in its phosphorylation in response to IR
- 53BP1 is involved in p53 stabilization in response to IR
- 53BP1 associates with Brca1 and is involved in its phosphorylation in response to IR
- 53BP1 interacts with DNA damage repair protein Ku80 that is involved in non-homologous end joining
- 53BP1 oligomerize in the presence and absence of IR
- 53BP1 is methylated by PRMT1 in glycine-arginine rich (GAR) stretch upstream of the tudor motif

Reportable Outcomes

Adams MM, Wang B, Xia Z, Morales JC, Lu X, Donehower LA, Bochar DA, Elledge SJ, Carpenter PB. (2005) ***Cell Cycle*** 4(12):1854-61

Wang B, Matsuoka S, Carpenter PB, Elledge SJ. (**2002**) 53BP1, a mediator of the DNA damage checkpoint. ***Science*** 298:1435-8.

Stewart GS, Wang B, Bignell CR, Taylor AM, Elledge SJ. (**2003**) MDC1 is a mediator of the mammalian DNA damage checkpoint. ***Nature*** 421:961-6.

Morales JC, Xia Z, Lu T, Aldrich MB, Wang B, Rosales C, Kellems RE, Hittelman WN, Elledge SJ, Carpenter PB (**2003**) Role for the BRCT protein 53BP1 in maintaining genomic stability. ***J Biol Chem.***

Conclusions

We have shown that 53BP1 is one of the functional homologs of yeast Rad9, functioning as a mediator of DNA damage response signaling. We also showed that 53BP1 is involved in regulation of three tumor suppressors, p53, Chk2 and Brca1. These evidences supports that 53BP1 may be a new tumor suppressor protein. Through these studies we are able to gain further insights into the DNA damage response pathway and the tumor suppression pathway in mammalian cells.

[Cell Cycle 4:12, 1854-1861, December 2005]; ©2005 Landes Bioscience

Report

53BP1 Oligomerization is Independent of its Methylation by PRMT1

Melissa M. Adams[1]
Bin Wang[2]
Zhenfang Xia[1]
Julio C. Morales[1]
Xiongbin Lu[3]
Lawrence A. Donehower[2]
Daniel A. Bochar[4]
Stephen J. Elledge[2]
Phillip B. Carpenter[1,*]

[1]Department of Biochemistry and Molecular Biology; University of Texas Health Science Center; Houston, Texas USA

[2]Howard Hughes Medical Institute; Department of Genetics; Harvard Partners Center for Genetics and Genomics; Harvard Medical School; Boston, Massachusetts USA

[3]Department of Molecular Virology and Microbiology; Baylor College of Medicine; Houston, Texas USA

[4]Department of Biological Chemistry; University of Michigan; Ann Arbor, Michigan USA

*Correspondence to: Phillip B. Carpenter; Department of Biochemistry and Molecular Biology; UT Health Science Center; 6431 Fannin; MSB 6.200; Houston, Texas 77030, USA; Tel.: 713.500.6032; Fax: 713.500.0652; Email. Phillip.B.Carpenter@uth.tmc.edu

Received 10/25/05; Accepted 10/28/05

Previously published online as a Cell Cycle E-publication:
http://www.landesbioscience.com/journals/cc/abstract.php?id=2282

KEY WORDS

arginine methylation, tumor suppressor, cell cycle, oligomerization, DNA repair

ACKNOWLEDGEMENTS

We thank Dr. Mark Bedford (University of Texas MD Anderson) and Dr. E. Ruley (Vanderbilt) for the generous gift of plasmids and cell lines as described in the text. This work was supported by NIH Grant GM65812 (P.B.C.), the Robert A. Welch Foundation (AU-1509; P.B.C.), NIEHS grant ES09650 (L.A.D.), and an NIH grant to S.J.E. B.W. was supported by a US Army breast cancer postdoctoral fellowship. S.J.E. is an Investigator of the Howard Hughes Medical Institute.

ABSTRACT

p53 binding protein 1 (53BP1) participates in the repair of DNA double stranded breaks (DSBs) where it is recruited to or near sites of DNA damage. Although little is known about the biochemical functions of 53BP1, the protein possesses several motifs that are likely important for its role as a DNA damage response element. This includes two BRCA1 C-terminal repeats, tandem Tudor domains, and a variety of phosphorylation sites. Here we show that a glycine-arginine rich (GAR) stretch of 53BP1 lying upstream of the Tudor motifs is methylated. We demonstrate that arginine residues within this region are important for asymmetric methylation by the PRMT1 methyltransferase. We further show that sequences upstream of the Tudor domains that do not include the GAR stretch are sufficient for 53BP1 oligomerization in vivo. Thus, although Tudor domains bind methylated proteins, 53BP1 homo-oligomerization occurs independently of Tudor function. Lastly, we find that deficiencies in *53BP1* generate a "hyper-rec" phenotype. Collectively, these data provide new insight into 53BP1, an important component in maintaining genomic stability.

INTRODUCTION

DNA damage-response mechanisms ensure the fidelity of chromosomal transmission and their failure may lead to the development of diseases such as cancer due to the inherent oncogenic potential of unrepaired, DNA double-stranded breaks (DSBs). DSBs arise through both programmed and unprogrammed mechanisms and are repaired by either of two principle mechanisms: homologous recombination (HR) or nonhomologous end joining (NHEJ). Programmed DSBs occur during the development of the immune system where both T and B cells undergo V(D)J and/or class switch recombination (CSR) in order to generate a wide variety of T cell receptors and immunoglobulins.[1] Both programmed and non-programmed breaks, the latter of which may be formed through exposure to ionizing radiation (IR), free radicals, or through the stalling of replication forks in S-phase, activate phosphoinositide-like kinases (PIKs) such as the DNA-dependent protein kinase (DNA-PK), ATM (mutated in ataxia-telangiectasia), and ATR (ATM and Rad3-related) that transduce damage signals to various effector molecules.[2,3] The PIKs have overlapping substrate specificities and phosphorylate serine (S) and/or threonine (T) residues at S/TQ motifs[2,3] that are found in a variety of DNA repair/cell cycle proteins, including the histone variant H2AX, components of the Mre11/Rad50/Nbs1 (MRN) complex, and p53-binding protein 1 (53BP1).

Mice defective in 53BP1 display phenotypes consistent with a role for the protein in DSB repair, including sensitivity to ionizing radiation (IR) and immunodeficiencies through impaired CSR.[4-7] Cells "knocked down" in 53BP1 expression exhibit defective cell cycle checkpoints and reduced phosphorylation of of various ATM substrates including BRCA1, Chk2, and Smc1.[8-10] Chk1 controls the localization of 53BP1 to sites of stalled replication forks where it recruits the Bloom's syndrome protein BLM and p53 to these abnormal DNA structures.[11] In addition, 53BP1 possesses a kinetochore binding domain (KBD) that is sufficient for localization to the kinetochore during mitosis.[12] 53BP1 is rapidly phosphorylated in response to IR and accumulates at sites of irradiation-induced foci (IRIF; reviewed in ref .13), an activity dependent upon the phosphorylation of H2AX (α-H2AX^{8}). Accumulation of 53BP1 at IRIF is dependent upon functional Mdc1, a mediator of the DNA damage response that has been shown to bind to Mre11 and H2AX.[14,15] ATM targets 53BP1 at several S/TQ motifs that predominantly lie in a cluster within the N-terminal half of the protein. These modifications are not required for the

accumulation of the protein at sites of DNA damage.[9,16] Rather, the Tudor domains appear to be sufficient for localization of 53BP1 to IRIF.[17] The Tudor motif has been shown to be structurally similar to the chromodomain, a motif known to bind methylated proteins.[18] Indeed, the Tudor domain of 53BP1 directly interacts with methylated lysine 79 (K79) of histone H3, a reaction catalyzed by the Dot1 methyltransferase.[17] As K79 maps to the histone core and is likely to be sterically inaccessible, changes in chromatin structure, perhaps as induced by DSBs, have been proposed to be detected by 53BP1, leading to the notion that 53BP1 senses DSBs.[17,19] In addition to the Tudor domains, 53BP1 possesses an upstream region that binds DNA and facilitates end joining in vitro,[20] events that are likely important in DSB repair. This region contains an RG-rich cluster (GAR) that has been associated with S-adenosyl-methionine (AdoMet)-dependent protein arginine methyltransferases (PRMTs).[21] Arginine, by virtue of its guanidino side group, may be di-methylated in an asymmetric or symmetric fashion, predominantly by PRMT1 (asymmetric) or PRMT5 (symmetric), respectively.[21] PRMT-dependent methylation has been implicated in a variety of cellular processes including protein-protein interactions, signal transduction, RNA metabolism, nuclear transport, and more recently DNA repair.[21]

Although a variety of reports have implicated 53BP1 as a mediator in the cellular response to DSBs, the precise role(s) of the protein within these pathways has yet to be clearly defined. Moreover, little is known about how 53BP1 functions at the biochemical level. To shed more light on this, we demonstrate that 53BP1 is methylated in vivo. In particular, we find that PRMT1 methylates 53BP1 on arginine residues within its GAR stretch. Intriguingly, we found that 53BP1 formed oligomers in vivo and that this occurred independently of both GAR methylation and the Tudor motifs. Mutation of GAR arginine residues to lysine residues reduced, but did not abolish, DNA binding. We additionally demonstrate that *53BP1*-deficient cells exhibit a hyper-rec phenotype indicative of aberrant recombination. Collectively, our results provide new insights into the role of 53BP1 within the DNA damage response.

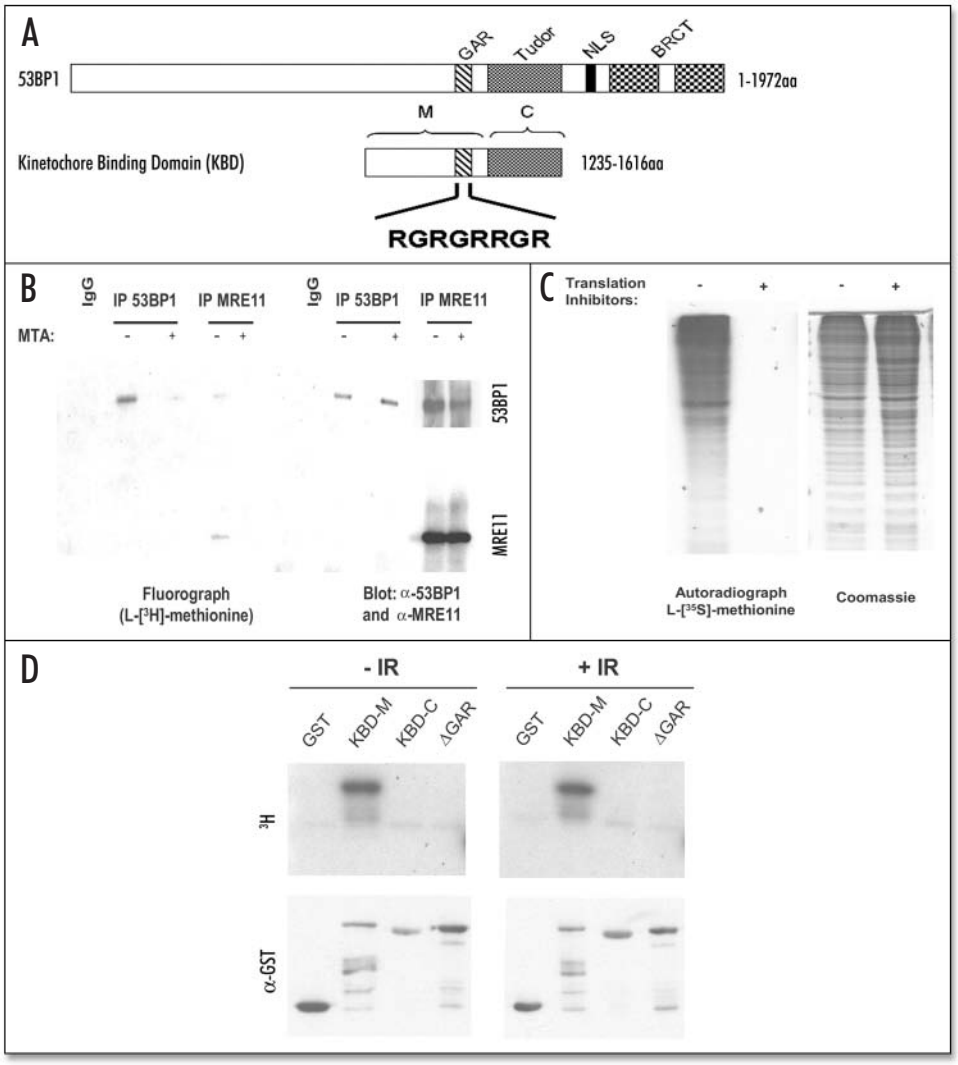

Figure 1. In vivo methylation of 53BP1. (A) Diagram of the domain organization of 53BP1 (not drawn to scale). In addition to its two, C-terminal repeating BRCT repeats and a nuclear localization signal (NLS), 53BP1 possesses a GAR stretch (KBD-M) that lies upstream of the tandem Tudor motifs (KBD-C). Both the GAR stretch and the Tudor motifs lie in a region (kinetochore binding domain [KBD]) previously shown to be sufficient for the localization of 53BP1 to the kinetochore.[12] (B) In vivo methylation of 53BP1 in HeLa cells. HeLa cells were labeled with L-[methyl-^{3}H]-methionine either in the presence or absence of the methyltransferase inhibitor MTA as described in Materials and Methods. The samples were processed for immunoprecipitation with α-53BP1 and α-Mre11 and either subjected to fluorography to detect ^{3}H incorporation into proteins (left) or Western blotting as a control (right). (C) Inhibition of protein synthesis during incorporation of L-[methyl-^{3}H]-methionine by the translational inhibitors cycloheximide and chloramphenicol. Left, autradiography showing the efficacy of translation inhibition. Right, Coomassie staining to show loading control. (D) In vitro methylation of 53BP1 within its GAR stretch. GST fusion proteins encompassing the GAR stretch (KDB-M), an in-frame deletion of the GAR sequences (ΔGAR), and a region containing the Tudor motifs (KBD-C) were purified and tested for their ability to serve as substrates for methyltransferases endogenous to mammalian nuclear extracts that were either left untreated or treated with 10 Gy IR as shown (see Materials and Methods). Top, fluorography showing methylation of KBD-M. Bottom, Western blot with α-GST as a control for protein loading.

MATERIALS AND METHODS

In vivo and in vitro methylation assays and preparation of GST fusion proteins. In vivo methylation assays were performed essentially as described by Liu and Dreyfuss.[22] Briefly, HeLa cells were metabolically labeled with L-[^{3}H-methyl]-methionine in methionine free, DMEM media for three hours in the presence of cyclohexamide (100 μg/mL) and chloramphenicol (40 μg/mL). L-[^{35}S]-methionine was also used as a control under the same conditions. Nuclear extracts derived from these cells were subject

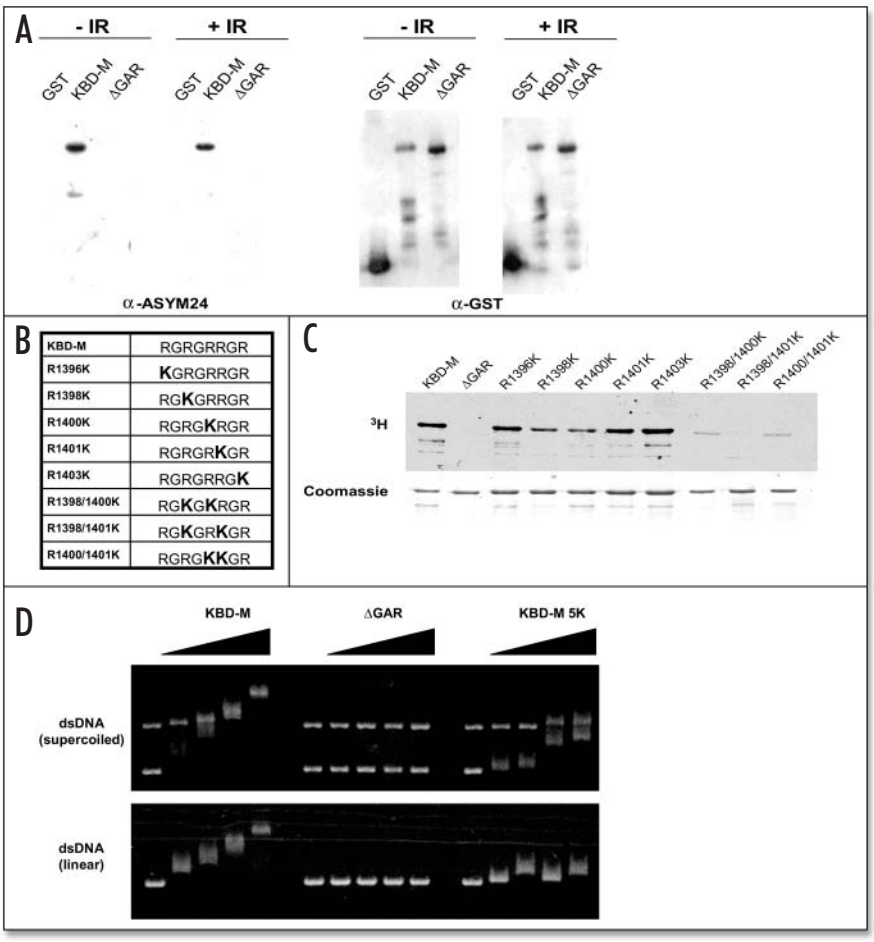

Figure 2. Asymmetric dimethylation of arginine residues within the GAR stretch of 53BP1. (A) Asymmetric methylation of arginine residues within the GAR stretch of 53BP1. KBD-M, ΔGAR, and control GST proteins were methylated as described above, except that "cold" SAM was used. After separation on SDS PAGE, the samples were immunoblotted with antibodies that specifically recognized asymmetrically dimethylated arginine residues (left) or GST for a loading control (right). (B) Schematic table showing the GAR stretch within KBD-M and various mutations used in this study. (C) In vitro methylation of KBD-M and mutant derivatives as shown in (B) reveals that multiple arginine residues within GAR are important for methylation. Top, fluorgraph showing ^{3}H incorporation into KBD-M and its mutant derivatives. Bottom, Coomassie staining of protein samples as loading controls. (D) DNA binding of KBD-M and mutant derivatives. Agarose electrophoretic mobility shift assays were employed to characterize the ability of recombinant KBD-M, ΔGAR, and KBD-M 5K to bind DNA. 200 ng of dsDNA was incubated with increasing amounts of 1x, 2x, 5x or 10x protein. Top panel, binding to supercoiled plasmid DNA and lower panel, binding to plasmid DNA linearized with *Eco* RI.

to immunoprecipitation with antibodies directed against 53BP1 (Bethyl labs), Mre11 (Novus), or a control IgG (Santa Cruz). The immunoprecipitates were washed in NETN (20 mM Tris, pH 8.0, 200 mM NaCl, 1.0% NP-40) and boiled in SDS solubilizer prior to electrophoresis and processing for fluorography with Amplify (Amersham).

GST fusion proteins were overexpressed in *E. coli* strain BL21(DE3)-RIL cells (Stratagene) by induction with 0.4 mM IPTG. Cells were resuspended in PBS containing 1.0 mM PMSF and sonicated on ice. Soluble lysate was used to batch purify expressed GST proteins using glutathione agarose (Sigma), followed by washing in PBS, and elution with 10 mM reduced glutathione in 50 mM Tris-HCl, pH 8.0. We used this *E. coli* expression system to purify various derivatives of 53BP1 fused to GST for in vitro methylation assays. We generated KBD-M (residues 1319-1479) as previously described,[20] KBD-C, spanning residues 1480-1616,[20] and ΔGAR, a derivative of KBD-M with residues 1384-1407 deleted in frame. KBD-M was used as the parental template for site directed mutagenesis (QuickChange, Stratagene) to generate arginine to lysine mutants. Purified GST proteins were incubated in parallel with 500 μg 293T nuclear extract in the presence of 3.0 μCi [methyl-^{3}H] S-adenosyl-L-methionine (Amersham) for 1.5 hours at 37°C. Fusion proteins were isolated after incubation with glutatione agarose (Sigma), washed with PBS, and prepared for electrophoresis. The samples were separated by SDS-PAGE and transferred to PVDF membrane for either Western blotting with α-GST, α-ASYM24 (Upstate), or α-SYM10 (Upstate) or sprayed with EN^{3}HANCE (Perkin-Elmer) for visualization of methylated proteins. In some cases, nuclear extracts were derived from *PRMT1*-deficient ES cells (*PRMT1*$^{-/-}$) or a wild-type counterpart. *PRMT1*$^{-/-}$ and *PRMT1*$^{+/+}$ ES cells were the generous gift of Dr. Earl Ruley (Vanderbilt University) and have been described.[23]

For in vitro methylation reactions with individual PRMT enzymes, constructs encoding GST-PRMT1, PRMT3, PRMT4, and PRMT6 were obtained from M. T. Bedford (University of Texas, MD Anderson). Recombinant PRMTs were expressed in *E. coli* and purified as described above. Control reactions for PRMT enzyme activity (PRMT1, 3, 4) utilized core histones purified from HeLa cells[24] or a fibrillarin GAR sequence (PRMT6).[25] Methylation reactions contained 0.5 μM S-Adenosyl-L-[methyl-^{3}H] methionine (55 Ci/mmol, PerkinElmer), 2.0 mM EDTA, 1.0 mM DTT, 0.1 μg/μl BSA in 50 mM Tris pH 8.0. Reactions were incubated for one hour at 37 °C and processed for SDS-PAGE. Proteins were visualized by Coomassie staining to verify an equal loading of substrate in each reaction. Gels were then subjected to fluorography.

53BP1 oligomerization. Purified plasmid DNA (6 μg) was transfected into 293T cells using Lipofectamine 2000 (Invitrogen). Fourty-eight hours posttransfection, the material was treated with 10 Gy IR or left untreated prior to performing immunoprecipitation analysis with anti-Flag (Sigma) or anti-HA (Santa Cruz) antibodies. To make specific mutations in 53BP1, we primarily used the parental plasmid pCMH6K53BP1 that encodes HA-53BP1[26] as a template for site-directed mutagenesis (Quick-Change, Stratagene) with specific primers designed to generate in-frame deletions or to mutate various regions of 53BP1 as discussed in the text. All constructs encoded for 53BP1 proteins that possessed its natural nuclear localization signal (NLS)[12] or had the SV40 NLS placed at the amino terminus (53BP1-393 and 53BP1-391). AQ24 (a total of 24 putative phosphorylation sites) changed all S and/or T residues in S/TQ motifs to AQ sites beginning with residue 6 and ending with residue 1943. All constructs were sequenced to verify the changes. Primer sequences will be made available upon request.

Assaying for aberrant recombination. Murine embryonic fibroblasts (MEFs) were prepared at day 13.5 (E13.5) from timed matings as previously described.[5] For HR assays, one million viral particles containing the retroviral reporter pLNCX-GZ [27] was used to infect *53BP1*$^{+/+}$, *53BP1*$^{+/-}$, or *53BP1*$^{-/-}$ MEFs that were genotyped as previously described.[5] Fourty-eight hours postinfection, the medium was changed to that containing G418 and Zeocin. Cells were selected for approximately two weeks post-infection and then scored for the expression of GFP in G418 and Zeocin. In addition to pLNCX-GZ being able to confer resistance to G418 (Neo), *53BP1*$^{-/-}$ MEFs, as we have previously described, are also resistant to G418.[5] Therefore, because of zeocin selection, we were precluded from determining the cell number at later, post-infection time points where recombination events take place. Thus, we used the starting cell numbers to determine the recombination frequency. Although these values are not correct in the absolute sense, the

fact that *53BP1*$^{-/-}$ MEFs grow much slower than their wild-type counterparts[5] indicates that the calculated recombination frequency is actually lower than the absolute value.

Other procedures. DNA binding assays and immunofluorescence were performed as previously described.[5,20]

RESULTS

In vivo and in vitro methylation of 53BP1. In addition to its BRCT and Tudor motifs, 53BP1 possesses a glycine and arginine rich stretch, known as a GAR domain (Fig. 1A). As these sequences have been shown to be substrates for protein arginine methyltransferases (PRMTs), we determined whether 53BP1 was a target for protein arginine methylation in vivo. To perform this, we metabolically labeled HeLa cells with L-[^{3}H-methyl]-methionine in the presence of the translation inhibitors cyclohexamide and chloramphenicol according to the method of Liu and Dreyfuss.[22] We also examined methylation in the presence of 5' deoxy-5' methylthioadenosine (MTA), an established inhibitor of AdoMet-dependent methyltransferases. After labeling, we used antibodies directed against either 53BP1 (α-53BP1) or Mre11 (α-MRE11), a control protein known to be methylated on arginine residues,[28] to immunoprecipitate and detect any incorporation of ^{3}H label into 53BP1 and Mre11. Importantly, we found that both 53BP1 and, as expected, Mre11 were methylated in vivo and that this was significantly reduced in MTA-treated samples (Fig. 1B). We confirmed that the autoradiographic signal was derived from methylation and not ongoing protein synthesis as there was no detectable protein synthesis in the presence of the translation inhibitors (Fig. 1C). Additionally, we found that 53BP1 was detected in α-Mre11 immunoprecipitates and this interaction was not influenced by our MTA treatment (Fig. 1B). Collectively, these data establish that 53BP1 is methylated in vivo.

To further characterize the potential targets of methylation within 53BP1, we performed an in vitro methylation assay using mammalian cell nuclear extracts and various derivatives of 53BP1 fused to glutathione-S-transferase (GST) (Fig. 1D). These fusions encoded for regions of 53BP1 that possess potential arginine methylation sites within the GAR domain (KBD-M), a modified version of the latter that deleted these residues (ΔGAR), and a region possessing the Tudor domains (KBD-C). After incubation of purified KBD-M, KBD-C, and ΔGAR and the control protein GST in nuclear extracts in the presence of the methyl donor [^{3}H]AdoMet, the recombinant proteins were retrieved with affinity resin, washed, and processed for electrophoresis. Immunoblotting a portion of this sample with an antibody that recognized GST (α-GST) indicated that equivalent amounts of protein were used in the methylation assay (Fig. 1D). Only KBD-M incorporated ^{3}H when incubated in mammalian nuclear extracts. In contrast to KBD-M, KBD-C, the region containing the tandem Tudor motifs, and GST, as expected, failed to incorporate any label (Fig. 1D). Additionally, we observed no changes in the level of KBD-methylation in extracts derived from cells that were pre-treated with IR (Fig. 1D). Our data indicates that 53BP1 residues 1319-1480, a region that contains the GAR stretch, but not the Tudor motifs, serve as susbstrate(s) for methyltransferase(s) enzymes in mammalian extracts.

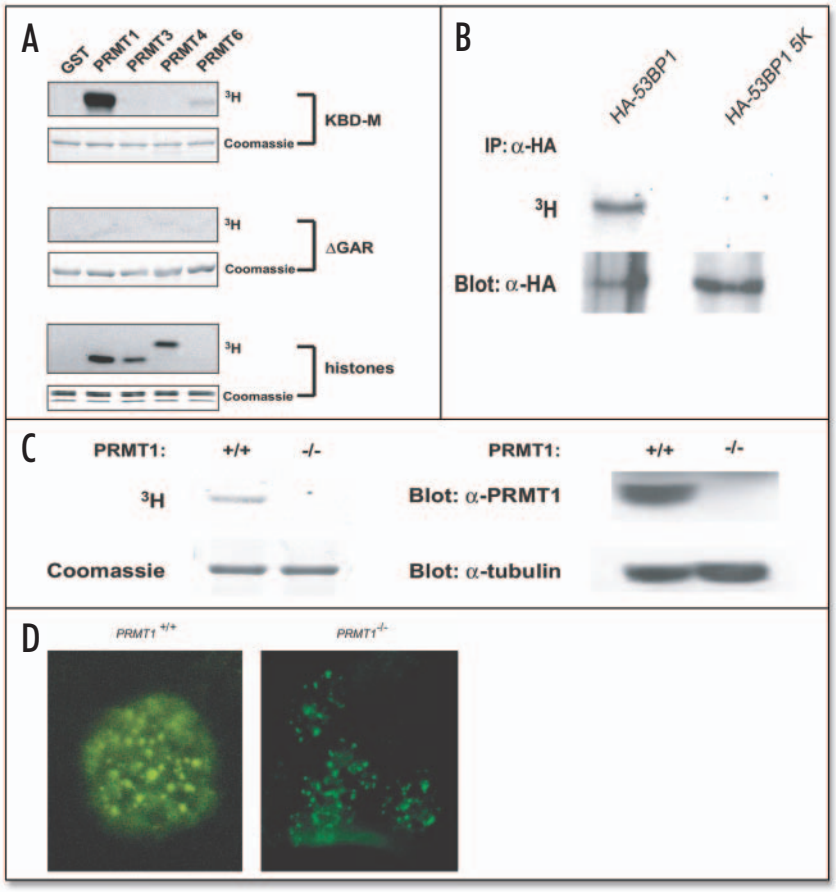

Figure 3. PRMT1 methylates 53BP1. (A) Direct methylation of 53BP1 within the GAR stretch by PRMT1 methyltrasnsferase. PRMT1, 3, 4 and 6 and GST were purified as described in Materials and Methods and used to methylate KBD-M (top), ΔGAR (middle), or histone control (bottom). After incubation of proteins in the presence of [^{3}H] SAM, the samples were processed for fluorography and Coomassie staining as a loading control. (B) Direct methylation of full-length 53BP1 and a derivative in which all arginines within the GAR region are mutated to lysine (53BP1 5K) by PRMT1. HA-tagged proteins were expressed in 293T cells and isolated by immunoprecipitation with anti-HA antibody as described in Materials and Methods. (C) Loss of 53BP1 methylation in *PRMT1*-deficient cells. Recombinant KBD-M was incubated in *PRMT1*$^{+/+}$ and *PRMT1*$^{-/-}$ nuclear extracts and processed for fluorgraphy and Coomassie staining as shown. Immunoblotting of whole cell extracts with an antibody that recognizes PRMT1 (Upstate) was used to verify the inability of *PRMT1*$^{-/-}$ cells to produce PRMT1 enzyme. Alpha-tubulin was used as a loading control. (D) Indirect immunofluorscence showing 53BP1 foci formation after treatment with 10 Gy IR in PRMT1$^{+/+}$ and PRMT1$^{-/-}$ ES cells.

Asymmetric methylation of 53BP1 arginine residues within the GAR domain. Due to the nature of the guanidino side group of arginine, methylation of this residue can occur in either an asymmetric or symmetric fashion.[21] To determine the type(s) of arginine methylation occuring in 53BP1, we used commercially available antibodies (see Materials and Methods) capable of distinguishing between asymmetric and symmetric, dimethylarginine residues. KBD-M, ΔGAR and GST were methylated in vitro as described above and processed for immunoblotting in parallel using either αASYM24 (asymmetric) or αSYM10 (symmetric) antibodies. An antibody recognizing GST (α-GST) was used to verify equal input of protein in each reaction (Fig. 2A). We found that αASYM24, but not αSYM10, recognized KBD-M only after methylation in mammalian nuclear extracts and that the levels of methylation were not influenced by treatment with IR (Fig. 2A and data not shown). In contrast, no cross reactivity was observed with αASYM24 when ΔGAR and GST were used as substrates in the methyltransferase assay (Fig. 2A). In addition, αSYM10 failed to recognize any methylated substrates (data not shown). We conclude that arginine sequences within the GAR stretch of KBD-M are asymmetrically methylated by enzymes in mammalian nuclear extracts.

The GAR stretch between 53BP1 residues 1396-1403 contains five arginine residues, each of which may be considered the potential target of methyltransferase enzymes (Fig. 2B). To further evaluate the arginine residues important for methylation, we generated a series of mutants within the GAR stretch (Fig. 2B). As enzyme-substrate interactions are often

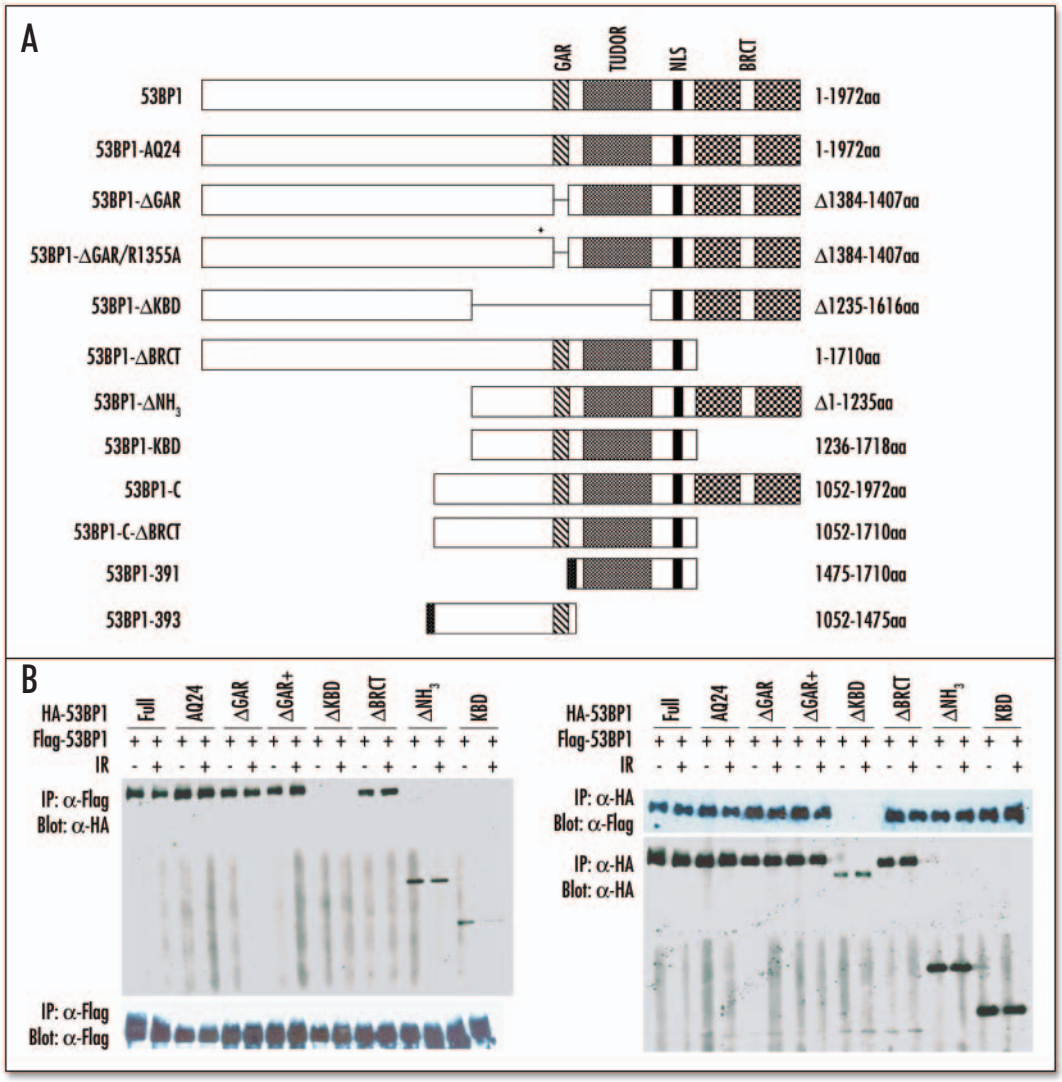

Figure 4A and B. 53BP1 oligomerization in vivo is independent of methylation and DNA damage. (A) Diagram of HA-53BP1 and various mutant derivatives used to measure 53BP1 oligomerization potential (not drawn to scale). Note that 53BP1-ΔGAR+ contains an additional mutation (R1355A) in an arginine residue that lies outside of the GAR stretch. 53BP1-ΔKBD has an in-frame deletion that removes residues 1236-1615. (B) The KBD region of 53BP1 is necessary for oligomerization as revealed by reciprocal co-immunoprecipitation experiments from extracts co-transfected into 293T cell with two differentially tagged, 53BP1 expression vectors. Full-length, Flag-53BP1 was co-transfected with full-length, HA-53BP1 or any of the mutant derivatives shown in (A). The cells were treated with 10 Gy IR 48 hours post-infection and then processed for immunoprecipitation and Western blotting with α-Flag and α-HA as shown.

influenced by charge, we mutated the arginine residues in the GAR stretch to lysines to conserve charge and tested for their ability to serve as methyltransferase substrates in our in vitro assay system. Representative results from several experiments are shown (Fig. 2C). By themselves, no single mutation within the GAR region is solely responsible for methylation as shown. Two mutations, R1396K and R1403K, exhibited almost no reduction in levels of methylation as compared to the parental KBD-M protein, suggesting that these two residues are dispensible for methylation. In contrast, the single mutants R1398K, R1400K and R1401K reproducibly showed decreased levels of methylation relative to KBD-M protein, indicating that these residues are important for 53BP1 methylation (Fig. 2C). In addition, double mutations in residues 1398 and 1400 (R1398/1400K), R1400/1401K, and R1398/1401K resulted in a substantial decrease in methylation, suggesting that two or more arginines are methylated in this region (Fig. 2C). We conclude that multiple arginine residues within the GAR region, in particular 1398, 1400, and 1401, of 53BP1 are either methylated or play an important role in 53BP1 methylation, perhaps through enzyme recognition.

As KBD-M possesses both methylation and DNA binding activities,[20] we tested the relationship between GAR methylation and DNA binding. To perform this, we purified KBD-M, ΔGAR, and a derivative that replaced all five arginines within the GAR sequences with lysine residues (KBD-M 5K). These proteins were used to assess their ability to bind supercoiled or linearized dsDNA as determined through a gel mobility shift assay. As expected, KBD-M readily bound DNA (Fig. 2D), but in contrast, ΔGAR did not. KBD-M 5K, however, bound DNA although with lesser affinity. We conclude that arginine residues within the GAR stretch of 53BP1 contribute to DNA binding.

PRMT1-dependent methylation of 53BP1. To identify the enzyme(s) that asymmetrically methylate 53BP1, we performed in vitro methylation reactions with various purified PRMT enzymes and recombinant 53BP1 proteins in the presence of [^{3}H]Ado-Met as described in Materials and Methods. We used PRMT1, 3, 4 and 6 enzymes as they are known to asymmetrically target arginine residues.[21] Purified PRMT 1, 3 and 4 methylated their previously identified, cognate histone substrates, and PRMT6 recognized the fibrillarin GAR sequence as previously described (Fig. 3A and data not shown). We found that only PRMT1 significantly methylated KBD-M (Fig. 3A). This methylation was abolished when ΔGAR was used as a substrate, indicating that PRMT1 directly methylates 53BP1 within the GAR stretch. We also found that PRMT1 could methylate full-length 53BP1 (Fig. 3B) and that this activity was lost when the five arginine residues within the GAR region were mutated to lysine residues (Fig. 3B). To further evaluate the role of PRMT1 in 53BP1 methylation, we used nuclear extracts derived from *PRMT1*-deficient (*PRMT1*$^{-/-}$) ES cells (23) in in vitro methylation assays with KBD-M. We found that PRMT1$^{+/+}$ extracts were capable of methylating KBD-M (Fig. 3C). In contrast, no incorporation of methyl groups into KBD-M was observed in *PRMT1*$^{-/-}$ cells indicating that PRMT1 methylates arginine residues of 53BP1 within the GAR stretch. We also found that 53BP1 IRIF formation occurred independently of PRMT1 function (Fig. 3D), suggesting that GAR methylation may function outside of the DSB repair activities of 53BP1.

53BP1 oligomerization is independent of GAR sequences and methylation. 53BP1 interacts with a variety of proteins and is a resident of various complexes of DNA damage response elements. To examine if 53BP1 could oligomerize with itself, we used two differentially tagged 53BP1 expression vectors designated as HA-53BP1 (pCMH6K53BP1[20]) and Flag-53BP1. Both vectors produce 53BP1 proteins that localize to IRIF demonstrating

the expressed tagged proteins are active for a major aspect of 53BP1 function (ref. 5 and data not shown). HA-53BP1 and Flag-53BP1 were co-transfected into 293T cells and the samples were either treated with 10 Gy IR or left untreated before processing for reciprocal co-immunoprecipitation and Western blotting experiments. Immunoblotting indicated that each tagged 53BP1 protein was expressed in mammalian cells (Fig. 4B). Immunoprecip-itation with α-FLAG followed by Western blotting with α-HA revealed that HA-53BP1 formed complexes with Flag-53BP1 (Fig. 4B). Correspondingly, Flag-53BP1 was detected in α-HA immunoprecipitates (Fig. 4B). We conclude that 53BP1 oligomerizes with itself in vivo.

To assess the structural features of 53BP1 responsible for mediating its self-oligomerization, we generated HA-tagged 53BP1 constructs expressing proteins with deletions and/or mutations in various structural domains as shown in Fig. 4A. We used these constructs and full length, Flag-53BP1 to assess 53BP1 oligomerization potential in co-transfection assays. In addition to the previously described GAR stretch, 53BP1 possesses numerous S/TQ phosphorylation sites, some of which are known to be targeted in vivo.[9,16] Moreover, 53BP1 has repeating C-terminal BRCT motifs and a kinetochore binding domain (KBD) that spans both the GAR stretch and Tudor domains.[12] Full length, wild-type Flag-53BP1 was co-transfected with any one of several mutant HA-53BP1 derivatives. The samples were processed and analyzed for their oligomerization potential as described above. Our data indicates that a region encompassing the KBD was essential for mediating 53BP1 self-oligomerization (Fig. 4B). An additional experiment revealed that the GAR stretch was dispensible for 53BP1 oligomerization (Fig. 4C). Therefore, oligomerization of 53BP1 is independent of its methylation. Moreover, several other important structural elements of 53BP1, including the BRCT motifs, and 24 S/TQ phosphorylation sites were also dispensible for oligomerization (Figs. 4B,C). In fact, deletion of the first 1,235 residues of 53BP1, which contains numerous S/TQ sites, had no impact on its self oligomerization. Consistent with the latter, 53BP1 oligomerization occurred in ATM-deficient cells (not shown). In addition, we found that the formation and stabilization of 53BP1 oligomers was independent of IR (Figs. 4B and C). To further examine the sequence requirements for 53BP1 oligomerization, we generated 53BP1-391 and 53BP1-393, two constructs that express 53BP1 truncations within the KBD (Fig. 4A). In particular, 53BP1-391 possesses the Tudor motifs and 53BP1-393 contains the upstream GAR stretch. We used these two constructs in co-transfection assays with Flag-53BP1 and found that 53BP1 residues 1052-1475 were required for oligomerization (Fig. 4D). We also found that differentially-tagged 53BP1-393 constructs co-transfected into 53BP1-deficient MEF cells were capable of forming oligomers, indicating that residues upstream of the Tudor domains (1052-1475) are sufficient for 53BP1 oligomerization (Fig. 4E). Collectively, our data clearly demonstrates that 53BP1 oligomerization occurs independently of methylation and Tudor domain function.

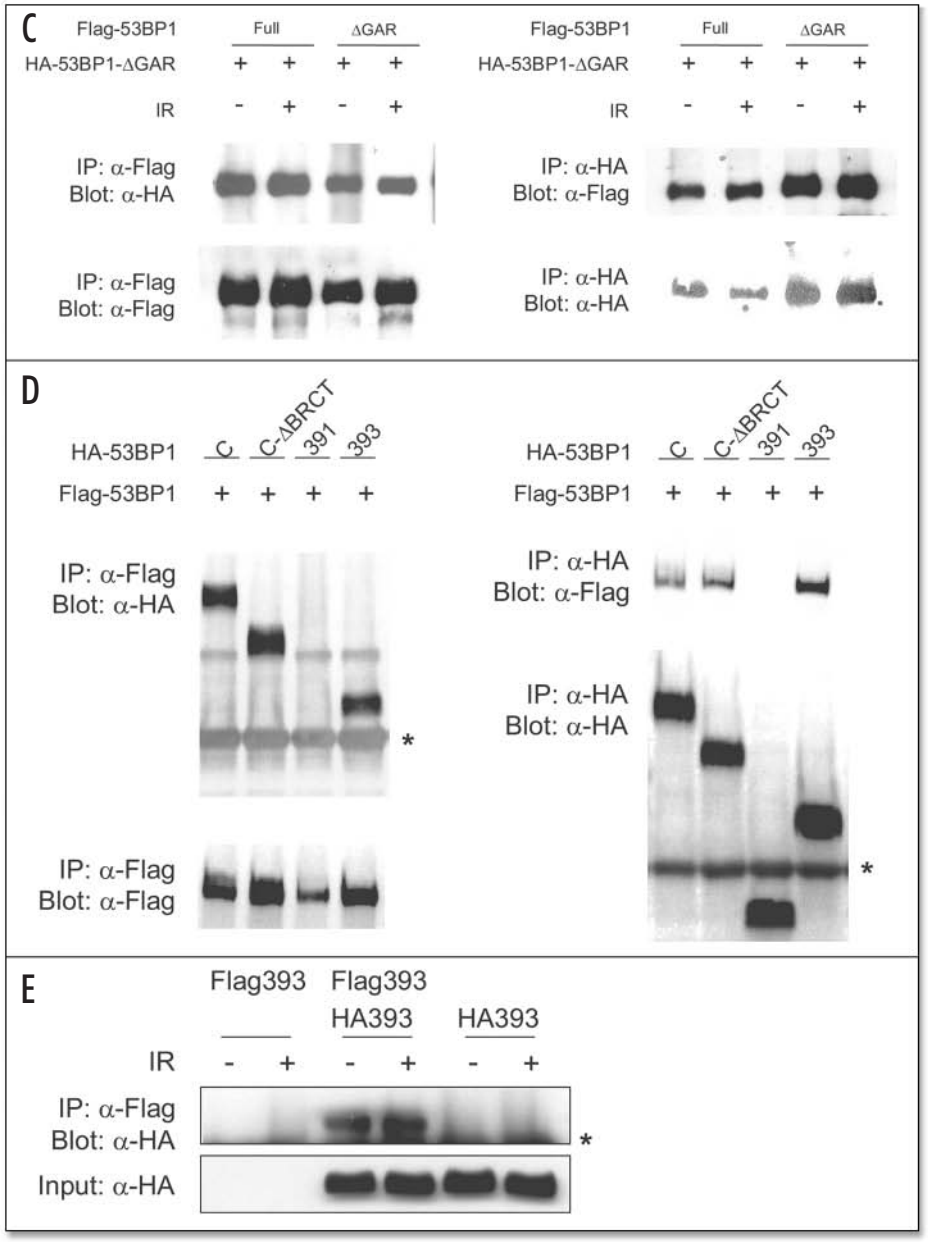

Figure 4C–E. 53BP1 oligomerization in vivo is independent of methylation and DNA damage. (C) Deletion of the GAR stretch of 53BP1 has no impact on its oligomerization. Both HA- and Flag-tagged 53BP1 constructs deleted fro the GAR stretch were co-transfected into 293T cells and processed for reciprocal co-immunoprecipitation/Western blotting analysis as shown. (D) A region of 53BP1 upstream of the Tudor motifs is sufficient for 53BP1 oligomerization. Plasmid DNA encoding HA-tagged 53BP1-393, 53BP1-391, and 53BP1-C-ΔBRCT was co-transfected with Flag-53BP1 and processed for reciprocal co-immunoprecipitation/Western blotting analysis as shown. The asterisk represents the Ig heavy chain. (E) A region upstream of the Tudor motifs is sufficient for 53BP1 oligomerization. 53BP1 residues 1052–1475 were tagged with either HA (HA393 or 53BP1-393 as in [A]) or Flag (Flag393) and transfected into 53BP1-deficient cells as shown. Samples were immunoprecipitated with α-Flag and immunoblotted with α-HA as shown. The asterisk represents Ig heavy chain.

53BP1 suppresses HR and aberrant recombination. In addition to the GAR stretch within KBD-M, this region of 53BP1 possesses DNA binding and end joining activities.[20] These two functions are conceivably important to the DSB repair activities of 53BP1. As both HR and NHEJ mediate DSB repair, we sought to further examine the role of 53BP1 in these processes. To test if 53BP1 functions in spontaneous, as opposed to break-induced, HR, we used a previously described retroviral reporter system designed to model HR.[27] In this system, the retroviral vector pLNCX-GZ contains

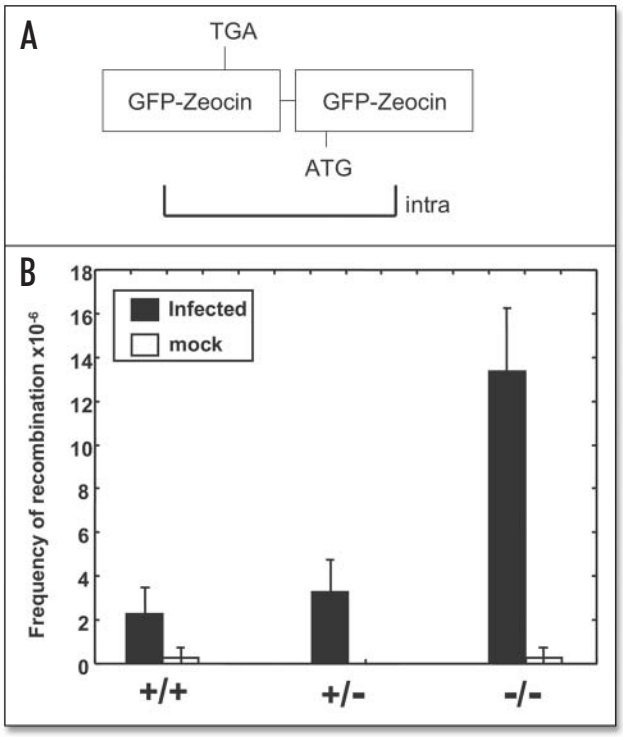

Figure 5. 53BP1 suppresses aberrant homologous recombination (HR). (A) Schematic representation of the reporter construct used to assess spontaneous recombination in *53BP1*$^{-/-}$ MEFs as adapted from reference 27. Note that this assay measures intramolecular recombination (B) Hyper-recombination phenotype in *53BP1*$^{-/-}$ embryonic fibroblasts (MEFs). Blind samples of *53BP1*$^{+/+}$, *53BP1*$^{+/-}$ and *53BP1*$^{-/-}$ MEFs were infected with the HR reporter virus pCLNCX-G2 as described in Experimental Procedures. The data represents the average of three independent experiments. Recombination frequency was scored as described in Materials and Methods. Error bars represent the standard deviation. The mock sample represents uninfected samples.

tandem repeats of mutated versions of a GFP-Zeocin fusion gene and is introduced and selected for in target cells. Intramolecular recombination between the tandem homologous repeats generates a functional GFP-ZeoR marker that can be readily scored and used to determine the frequency of HR in a given target cell (Fig. 5A). Because the tandem repeating GFP units are homologous sequences, GFP-Zeocin expression models HR.[27] Moreover, only intrachromosomal HR between the tandem repeats has to occur to generate a GFP^{+}, Zeo^{R} cell. As this recombination event generates a new genetic structure, it may be seen as an aberrant HR event. To examine the role of 53BP1 in these processes, we used these viral particles to infect primary fibroblast cells (MEFs) of genotypes *53BP1*$^{+/+}$, *53BP1*$^{+/-}$ and *53BP1*$^{-/-}$ derived from timed matings (E13.5) of animals heterozygous for *53BP1* (*53BP1*$^{+/-}$). Uninfected cells were used as a negative control (mock). One million colony forming units of fully packaged virus particles containing pLNCX-GZ were used in parallel to infect exponentially growing cultures of *53BP1*$^{+/+}$, *53BP1*$^{+/-}$ and *53BP1*$^{-/-}$ cells. We reproducibly observed that cells deficient in *53BP1*, but not in the wild-type or heterozygous ones, exhibited a nearly 5-fold increase (see Materials and Methods) in the levels of spontaneous HR (Fig. 5B). We conclude that 53BP1 functions to suppress spontaneous HR, a phenotype previously observed for other DNA damage response elements, including members of the recQ helicase family BLM and p53.[27,29]

DISCUSSION

This paper reports multiple, novel aspects concerning the biology of the 53BP1 DNA damage response element. We have shown that 53BP1 is asymmetrically methylated on multiple arginine residues by the PRMT1 methyltransferase within a GAR stretch that lie upstream of the Tudor motifs. Thus sequences that encompass KBD-M mediate DNA binding, arginine methylation, and homo-oligomerization. 53BP1 methylation occurs independently of its ability to oligomerize and both methylation and oligomerization appear to occur independently of DNA damage (IR) and 53BP1 focus formation. We have additionally shown that *53BP1*-deficiency leads to a hyper-rec phenotype. The implications for these findings are discussed below.

While our experiments were in progress, an independent study concluded that in vitro the Tudor domain of 53BP1 binds a synthetically methylated peptide modeled after the 53BP1 GAR region.[30] Moreover, this peptide contained five symmetrically-methylated arginine residues. Although these authors reported little significant difference, if any, in the binding constants between the Tudor domain and methylated peptide vs. the Tudor domain and control, non-methylated peptide (Kd = 3.9 ± 2.2 mM and 5.8 ± 2.7 mM for the nonmethylated and methylated peptides, respectively), they suggested, but provided no supporting experimental evidence, that 53BP1 methylation may promote intra- or inter-molecular associations through its Tudor domains.[30] In contrast, we have clearly shown that although 53BP1 is asymmetrically methylated by PRMT1 and does indeed oligomerize, it is not symmetrically methylated and oligomerization occurs independently of methylation and Tudor function. In fact, the region upstream of the Tudor domains is sufficient for 53BP1 oligomerization. Thus, 53BP1 oligomerization occurs independently of methylation and our data suggests that both processes are independent of treatment with IR, a major effector of 53BP1 function. Moreover, they do not appear to play a significant role in the ability of 53BP1 to form IRIF, a major role for the protein in DNA repair. Because 53BP1 methylation is independent of Tudor function, it likely does not influence DSB repair, an idea reinforced by the presence of 53BP1 IRIF in PRMT1-deficient cells. Thus, although Dot1-dependent methylation of histone H3 is required for 53BP1 IRIF formation,[17] methylation of 53BP1 per se is not. As both methylation and oligomerization are potentially constitutive processes, one possibility is that they both play a structural role in 53BP1 function. We did, however, observe that mutation of GAR arginine residues to lysines within KBD-M reduced the ability of the protein to bind DNA. Although it is tempting to speculate that methylation of 53BP1 within the GAR region is required for DNA binding, it is important to note that KBD-M binds DNA despite the fact that it is not methylated in our assay as it is derived from *E. coli*.

Although the Tudor domains of 53BP1 do not appear to bind 53BP1 to form homo-oligomers, they have been shown to bind directly to methylated lysine 79 of histone H3.[17] Given this and the relationship between 53BP1 and various proteins well documented to influence chromatin biology (i.e., HDAC4, H2AX, and SMC1), the Tudor domain of 53BP1 may also bind to other methylated targets that influence chromatin structure, perhaps in the context of DSB repair (i.e., histone tails). It is possible that 53BP1 methylation and oligomerization influence aspects of chromatin biology and/or DSB repair that 53BP1 participates in through protein-protein interactions analogous to chromodomain function. In this light, a recent report demonstrated that the C-terminal half of 53BP1

conferred dominant-negative activity on 53BP1 by abrogating Chk2 phosphorylation.[31] This phenomenon could be explained by the fact that the region sufficient for 53BP1 oligomerization lies in the C-terminal half of the protein. Interestingly, a fusion protein between 53BP1 and the platelet derived growth factor (PDGF) was recently identified in a patient with a myeloproliferative disorder.[32] The 53BP1-PDGF fusion was found to contain the sequences sufficient for 53BP1 oligomerization as it contained the first 1,691 residues before the breakpoint fusion with PDGF.[32] As these fusions typically encode proteins that contain oligomerization motifs important for activation of constitutive tyrosine kinase activity, we suggest that the oligomerization sequences in 53BP1 contribute to the activation of the 53BP1-PDGF fusion protein.

In a separate line of inquiry, we found that fibroblasts deficient in 53BP1 function display nearly 5-fold increased levels of HR as measured in an established retroviral GFP-Zeocin system. This assay measures spontaneous HR and is therefore an indicator of the initiation of this event. It should be noted that the pLNCX-GZ retroviral system is different than previously described HR assays that use the I-*Sce I* endonuclease to introduce DNA breaks. As I-*Sce I* introduces DSBs, it therefore measures break-induced HR (BIR). 53BP1 has been shown to have no role in BIR.[7] Interestingly, the increase in HR observed in *53BP1*$^{-/-}$ cells is similar to p53 mutants as well as mutants in genes encoding members of the recQ family (i.e. BLM). Based upon this, we suggest that 53BP1 cooperates with p53 to suppress aberrant recombination. We imagine that 53BP1, like p53 and BLM, could be involved with the recognition and processing of Holliday structures, perhaps as they are formed during the response to stalled replication forks in S phase. Consistent with this, 53BP1 has been shown to recruit both BLM and p53 to sites of stalled DNA replication forks in a manner that depends upon functional Chk1 activity,[11] indicating that 53BP1 operates at the interface of DNA replication, recombination, and repair. Further experiments will be needed to address the role of 53BP1 methylation and DNA binding in spontaneous HR.

References

1. Lombard DB, Chua KF, Mostoslavsky R, Franco S, Gostissa M, Alt FW. DNA repair, genome stability, and aging. Cell 2005; 120:497-512.
2. Abraham RT. Cell cycle checkpoint signaling through the ATM and ATR kinases. Genes Dev 2001; 15:2177-96.
3. Zhou BB, Elledge SJ. The DNA damage response: putting checkpoints in perspective. Nature 2000; 408:433-9.
4. Manis JP, Morales JC, Xia Z, Kutok JL, Alt FW, Carpenter PB. 53BP1 links DNA damage-response pathways to immunoglobulin heavy chain class-switch recombination. Nat Immunol 2004; 5:481-7.
5. Morales JC, Xia Z, Lu T, Aldrich MB, Wang B, Rosales C, Kellems RE, Hittelman WN, Elledge SJ, Carpenter PB. Role for the BRCA1 C-terminal repeats (BRCT) protein 53BP1 in maintaining genomic stability. J Biol Chem 2003; 278:14971-7.
6. Ward IM, Minn K, van Deursen J, Chen J. p53 Binding protein 53BP1 is required for DNA damage responses and tumor suppression in mice. Mol Cell Biol 2003; 23:2556-63.
7. Ward IM, Reina-San-Martin B, Olaru A, Minn K, Tamada K, Lau JS, Cascalho M, Chen L, Nussenzweig A, Livak F, Nussenzweig MC, Chen J. 53BP1 is required for class switch recombination. J Cell Biol 2004; 165:459-64.
8. DiTullio RA, Jr., Mochan TA, Venere M, Bartkova J, Sehested M, Bartek J, Halazonetis TD. 53BP1 functions in an ATM-dependent checkpoint pathway that is constitutively activated in human cancer. Nat Cell Biol 2002; 4:998-1002.
9. Fernandez-Capetillo O, Chen HT, Celeste A, Ward I, Romanienko PJ, Morales JC, Naka K, Xia Z, Camerini-Otero RD, Motoyama N, Carpenter PB, Bonner WM, Chen J, Nussenzweig A. DNA damage-induced G2-M checkpoint activation by histone H2AX and 53BP1. Nat Cell Biol 2002; 4:993-7.
10. Wang B, Matsuoka S, Carpenter PB, Elledge SJ. 53BP1, a mediator of the DNA damage checkpoint. Science 2002; 298:1435-8.
11. Sengupta S, Robles AI, Linke SP, Sinogeeva NI, Zhang R, Pedeux R, Ward IM, Celeste A, Nussenzweig A, Chen J, Halazonetis TD, Harris CC. Functional interaction between BLM helicase and 53BP1 in a Chk1-mediated pathway during S-phase arrest. J Cell Biol 2004; 166:801-13.
12. Jullien D, Vagnarelli P, Earnshaw WC, Adachi Y. Kinetochore localisation of the DNA damage response component 53BP1 during mitosis. J Cell Sci 2002; 115:71-9.
13. Mochan TA, Venere M, DiTullio RA, Jr., Halazonetis TD. 53BP1, an activator of ATM in response to DNA damage. DNA Repair (Amst) 2004; 3:945-52.
14. Bekker-Jensen S, Lukas C, Melander F, Bartek J, Lukas J. Dynamic assembly and sustained retention of 53BP1 at the sites of DNA damage are controlled by Mdc1/NFBD1. J Cell Biol 2005; 170:201-11.
15. Stewart GS, Wang B, Bignell CR, Taylor AM, Elledge SJ. MDC1 is a mediator of the mammalian DNA damage checkpoint. Nature 2003; 421:961-6.
16. Ward IM, Minn K, Jorda KG, Chen J. Accumulation of checkpoint protein 53BP1 at DNA breaks involves its binding to phosphorylated histone H2AX. J Biol Chem 2003; 278:19579-82.
17. Huyen Y, Zgheib O, Ditullio RA, Jr., Gorgoulis VG, Zacharatos P, Petty TJ, Sheston EA, Mellert HS, Stavridi ES, Halazonetis TD. Methylated lysine 79 of histone H3 targets 53BP1 to DNA double-strand breaks. Nature 2004; 432:406-11.
18. Maurer-Stroh S, Dickens NJ, Hughes-Davies L, Kouzarides T, Eisenhaber F, Ponting CP. The Tudor domain 'Royal Family': Tudor, plant Agenet, Chromo, PWWP and MBT domains. Trends Biochem Sci 2003; 28:69-74.
19. Mochan TA, Venere M, DiTullio RA, Jr., Halazonetis TD. 53BP1 and NFBD1/MDC1-Nbs1 function in parallel interacting pathways activating ataxia-telangiectasia mutated (ATM) in response to DNA damage. Cancer Res 2003; 63:8586-91.
20. Iwabuchi K, Basu BP, Kysela B, Kurihara T, Shibata M, Guan D, Cao Y, Hamada T, Imamura K, Jeggo PA, Date T, Doherty AJ. Potential role for 53BP1 in DNA end-joining repair through direct interaction with DNA. J Biol Chem 2003; 278:36487-95.
21. Boisvert FM, Cote J, Boulanger MC, Richard S. A Proteomic Analysis of Arginine-methylated Protein Complexes. Mol Cell Proteomics 2003; 2:1319-30.
22. Liu Q, Dreyfuss G. In vivo and in vitro arginine methylation of RNA-binding proteins. Mol Cell Biol 1995; 15:2800-8.
23. Pawlak MR, Scherer CA, Chen J, Roshon MJ, Ruley HE. Arginine N-methyltransferase 1 is required for early postimplantation mouse development, but cells deficient in the enzyme are viable. Mol Cell Biol 2000; 20:4859-69.
24. Cote J, Utley RT, Workman JL. Basic analysis of transcription factor binding to nucleosomes. Methods Mol Gen 1995; 6:108-27.
25. Frankel A, Yadav N, Lee J, Branscombe TL, Clarke S, Bedford MT. The novel human protein arginine N-methyltransferase PRMT6 is a nuclear enzyme displaying unique substrate specificity. J Biol Chem 2002; 277:3537-43.
26. Iwabuchi K, Li B, Massa HF, Trask BJ, Date T, Fields S. Stimulation of p53-mediated transcriptional activation by the p53-binding proteins, 53BP1 and 53BP2. J Biol Chem 1998; 273:26061-8.
27. Lu X, Lozano G, Donehower LA. Activities of wildtype and mutant p53 in suppression of homologous recombination as measured by a retroviral vector system. Mutat Res 2003; 522:69-83.
28. Boisvert FM, Dery U, Masson JY, Richard S. Arginine methylation of MRE11 by PRMT1 is required for DNA damage checkpoint control. Genes Dev 2005; 19:671-6.
29. van Brabant AJ, Stan R, Ellis NA. DNA helicases, genomic instability, and human genetic disease. Annu Rev Genomics Hum Genet 2000; 1:409-59.
30. Charier G, Couprie J, Alpha-Bazin B, Meyer V, Quemeneur E, Guerois R, Callebaut I, Gilquin B, Zinn-Justin S. The Tudor tandem of 53BP1: a new structural motif involved in DNA and RG-rich peptide binding. Structure (Camb) 2004; 12:1551-62.
31. Yoo E, Kim BU, Lee SY, Cho CH, Chung JH, Lee CH. 53BP1 is associated with replication protein A and is required for RPA2 hyperphosphorylation following DNA damage. Oncogene 2005; 24:5423-30.
32. Grand FH, Burgstaller S, Kuhr T, Baxter EJ, Webersinke G, Thaler J, Chase AJ, Cross NC. p53-Binding protein 1 is fused to the platelet-derived growth factor receptor beta in a patient with a t(5;15)(q33;q22) and an imatinib-responsive eosinophilic myeloproliferative disorder. Cancer Res 2004; 64:7216-9.

were resistant to the growth-inhibitory effects of IFN-α and proliferated in the presence of 50 U/ml of IFN-α at a rate comparable to that of untreated controls (Fig. 3B). Cells possessing mutations in the vIL-6 promoter at either ISRE-1 or ISRE-2 had diminished IFN resistance and reduced proliferation at low concentrations of IFN-α.

Feedback inhibition of IFN signaling by vIL-6 provides a clear example of how virus subversion of host cell defenses can lead to cell proliferation. Why does cellular IL-6 not achieve the same effect? Both hIL-6 and vIL-6 can initiate IL-6 signaling in BCP-1 cells, as measured by electrophoretic mobility–shift assays in which the gamma-inteferon activation sequence (GAS) element from the interferon regulatory factor 1 (IRF-1) promoter is used as a probe, although vIL-6 signaling is more robust (*18*). The answer may lie in differences in receptor usage by the two cytokines. IFN-α treatment results in down-regulation of gp80 surface expression but has no effect on gp130 surface expression (Fig. 4A), an effect previously noted for other B cell lines, including the IL-6–dependent U266 multiple myeloma cell line (*26*). IFN-α also blocks hIL-6–induced but not vIL-6–induced gp130 tyrosine phosphorylation (Fig. 4B), demonstrating that the blockage occurs at the receptor level. gp80 mRNA expression is not markedly altered by IFN-α treatment, suggesting that gp80 blockade is largely due to posttranscriptional inhibition (fig. S4). This leads to a model (Fig. 4C) in which viral evolution has generated a modified cytokine that escapes regulatory control of IL-6 signaling by IFN-α. Infected cells that normally would either arrest or undergo apoptosis in response to IFN signaling continue to proliferate in the presence of vIL-6, resulting in a virus-human autocrine feedback circuit.

vIL-6 inhibits tumor-suppressor pathways activated during immune signaling, but it is important to emphasize that this is not solely responsible for PEL tumorigenesis, which results from multiple, combined viral and host cell genetic influences. Viruses have evolved a variety of ways to overcome host defenses against infection, including abrogating IFN signaling pathways (*27*, *28*). KSHV itself possesses another protein, vIRF-1, to inhibit IFN-mediated transcription. By sensing levels of IFN-α signaling, KSHV reacts to and modifies its cellular environment through vIL-6, exhibiting a fundamental property of biological systems called irritability that has been previously used to distinguish viruses from higher forms of life (*29*). In addition to immune evasion, it is possible that this mechanism plays a role in maintaining viral latency by preventing IFN induction of lytic replication. The autocrine loop established by vIL-6 illustrates mechanistically how interference with antiviral defenses can contribute to tumor cell proliferation and provides an attractive target for novel therapies directed against KSHV-related hematopoietic tumors.

References and Notes

1. P. S. Moore, Y. Chang, *Trends Genet.* **14,** 144 (1998).
2. P. S. Moore *et al.*, *Science* **274**, 1739 (1996).
3. F. Neipel *et al.*, *J. Virol.* **71**, 839 (1997).
4. J. Nicholas *et al.*, *Nature Med.* **3**, 287 (1997).
5. K. D. Jones *et al.*, *Blood* **94**, 2871 (1999).
6. C. Parravinci *et al.*, *Am. J. Pathol.* **151**, 1517 (1997).
7. J. Teruya-Feldstein *et al.*, *Lab. Invest.* **78**, 1637 (1998).
8. Y. Aoki *et al.*, *Blood* **93**, 4034 (1999).
9. J. Osborne *et al.*, *Hum. Immunol.* **60**, 921 (1999).
10. T. Hideshima *et al.*, *Clin. Cancer Res.* **6**, 1180 (2000).
11. T. Taga, T. Kishimoto, *Annu. Rev. Immunol.* **15**, 797 (1997).
12. J. Molden *et al.*, *J. Biol. Chem.* **272**, 19625 (1997).
13. J. Mullberg *et al.*, *J. Immunol.* **164**, 4672 (2000).
14. D. Chow *et al.*, *Science* **291**, 2150 (2001).
15. G. R. Stark *et al.*, *Annu. Rev. Biochem.* **67**, 227 (1998).
16. T. Taniguchi *et al.*, *Annu. Rev. Immunol.* **19**, 623 (2001).
17. Materials and methods are available as supporting material on *Science* Online.
18. M. Chatterjee, J. Osborne, G. Bestetti, Y. Chang, P. S. Moore, data not shown.
19. O. Sangfelt *et al.*, *Oncogene* **14**, 415 (1997).
20. W. S. El-Deiry *et al.*, *Cell* **75**, 817 (1993).
21. R. Renne *et al.*, *Nature Med.* **2**, 342 (1996).
22. R. Sun *et al.*, *Proc. Natl. Acad. Sci. U.S.A.* **95**, 10866 (1998).
23. J. Chang *et al.*, *Virology* **266**, 17 (2000).
24. J. J. Russo *et al.*, *Proc. Natl. Acad. Sci. U.S.A.* **93**, 14862 (1996).
25. E. Meurs, A. G. Hovanessian, *EMBO J.* **7**, 1689 (1988).
26. M. Schwabe *et al.*, *J. Clin. Invest.* **94**, 2317 (1994).
27. N. C. Reich *et al.*, *J. Virol.* **62**, 114 (1988).
28. T. E. Morrison *et al.*, *Immunity* **15**, 787 (2001).
29. M. J. Pelsczar, R. D. Reid, *Microbiology* (McGraw-Hill, New York, 1972), p. 5.

30. We thank R.D. Wood, C. Schindler, A. Pernis, E. Marcantonio, J. Nicholas, S. Kalachikov, and D. Baker for helpful discussions on experimental design or reagents used in this study and D. Holland and B. Frizell for help with the manuscript. This work was supported by National Cancer Institute grants CA76586 and CA87661.

Supporting Online Material

www.sciencemag.org/cgi/content/full/298/5597/1432/DC1

Materials and Methods
Figs. S1 to S4
Table S1
References

10 June 2002; accepted 24 September 2002

53BP1, a Mediator of the DNA Damage Checkpoint

Bin Wang,[1] Shuhei Matsuoka,[1] Phillip B. Carpenter,[4] Stephen J. Elledge[1,2,3]*

53BP1 binds to the tumor suppressor protein p53 and has a potential role in DNA damage responses. We used small interfering RNA (siRNA) directed against 53BP1 in mammalian cells to demonstrate that 53BP1 is a key transducer of the DNA damage checkpoint signal. 53BP1 was required for p53 accumulation, G_2-M checkpoint arrest, and the intra-S-phase checkpoint in response to ionizing radiation. 53BP1 played a partially redundant role in phosphorylation of the downstream checkpoint effector proteins Brca1 and Chk2 but was required for the formation of Brca1 foci in a hierarchical branched pathway for the recruitment of repair and signaling proteins to sites of DNA damage.

53BP1 was identified through its ability to bind to the tumor suppressor protein p53 through 53BP1's COOH-terminal BRCT (Brca1 carboxyl-terminus) repeats (*1*, *2*), which are found in many DNA damage response proteins (*3–8*). 53BP1 responds to DNA double-strand breaks (*9–12*), quickly relocalizing to discrete nuclear foci upon exposure to ionizing radiation (IR). These foci colocalize with those of the Mre11-Nbs1-Rad50 complex and phosphorylated γ-H2AX, which are thought to facilitate the recruitment of repair factors to damaged DNA (*9–11*). In response to IR, 53BP1 is phosphorylated in an ataxia telangiectasia mutated (ATM)–dependent manner (*10–12*), but its role in the DNA damage response is unclear.

To determine 53BP1's role, we used small interfering RNAs (siRNAs) in the form of two independent, nonoverlapping, 21–base pair RNA duplexes that target 53BP1 to inhibit its expression (*13*, *14*). U2OS cells were transfected with these siRNA oligonucleotides (oligos) and, within 3 days posttransfection, a portion of cells had undergone cell death (fig. S1). A similar phenotype was also observed in two other cell lines, Hct116 and Saos2 (*15*).

To determine whether 53BP1 plays a role in DNA damage cell cycle checkpoints, we examined the response of 53BP1-inhibited cells to IR. IR induces the intra-S-phase

[1]Verna and Mars McLean Department of Biochemistry and Molecular Biology, [2]Department of Molecular and Human Genetics, [3]Howard Hughes Medical Institute, Baylor College of Medicine, Houston, TX 77030, USA. [4]Department of Biochemistry and Molecular Biology, University of Texas Health Sciences Center, Houston, TX 77030, USA.

*To whom correspondence should be addressed. E-mail: selledge@bcm.tmc.edu

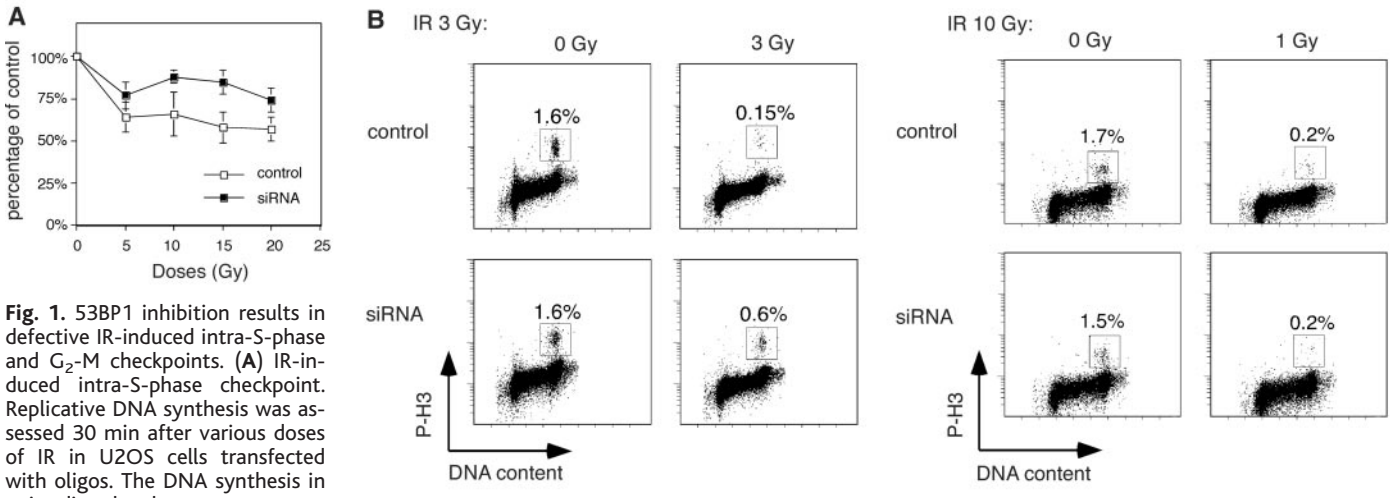

Fig. 1. 53BP1 inhibition results in defective IR-induced intra-S-phase and G_2-M checkpoints. (**A**) IR-induced intra-S-phase checkpoint. Replicative DNA synthesis was assessed 30 min after various doses of IR in U2OS cells transfected with oligos. The DNA synthesis in unirradiated cultures was set to 100% for cells transfected with control oligos or siRNA oligos targeting 53BP1 (*14*). Error bars represent the standard deviation of triplicate samples. (**B**) Analysis of the G_2-M DNA damage checkpoint. Cells were either untreated or irradiated with either 3 Gy or 10 Gy as indicated, then incubated for 1 hour at 37°C before fixation. Cells in mitosis were determined by staining with propidium iodide and antibody to phosphohistone H3 (P-H3) (Cell Signaling, Beverly, MA), followed by fluorescein isothiocyanate (FITC)–conjugated secondary antibody (Jackson Immunoresearch Laboratories, West Grove, PA), and the percentage of the M-phase cells was determined by flow cytometry.

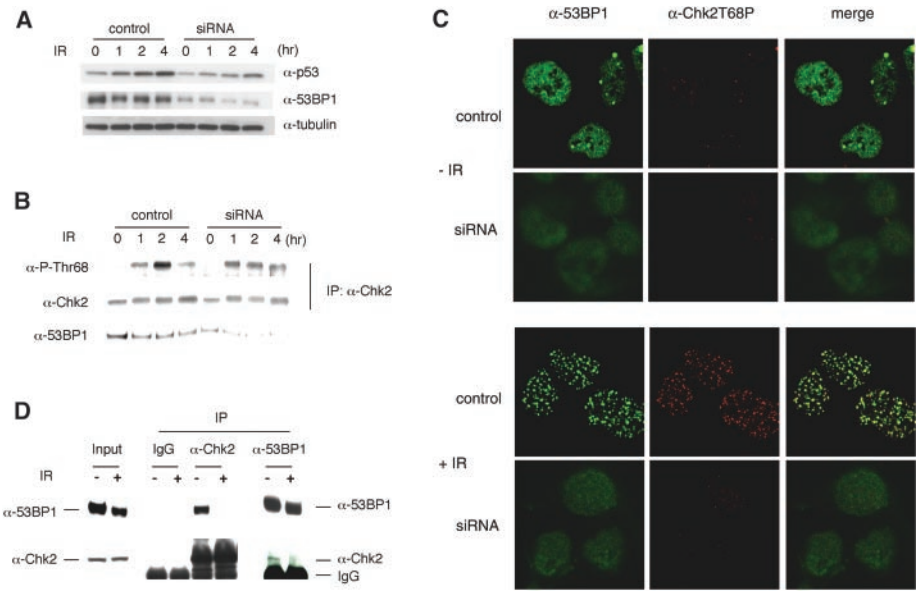

Fig. 2. 53BP1 regulates p53 and Chk2 in response to IR. (**A**) IR-induced p53 stabilization. U2OS cells were transfected with siRNA oligos targeting 53BP1 or control oligos for 2 days, then exposed to 10-Gy IR. Cell lysates were made from samples recovered from irradiation at the indicated times and separated by SDS-polyacrylamide gel electrophoresis (PAGE). Western blots were performed with the use of antibodies to 53BP1, tubulin, and p53 (Oncogene, San Diego, CA). (**B**) Chk2 phosphorylation at Thr^{68} is reduced in 53BP1-inhibited cells. Chk2 immunoprecipitates were prepared from U2OS cells at the indicated hours after exposure to 10-Gy irradiation. Western blots were performed using antibodies to Chk2 (*14*) and to T68P-Chk2 (*14*). (**C**) IR-induced phospho-foci recognized by antibodies to P-T68 of Chk2 depend on 53BP1. SiRNA-transfected U2OS cells were irradiated with 10-Gy irradiation and 2 hours later were fixed with paraformaldehyde, permealized with Triton X-100, and then immunostained with antibodies to Chk2T68P (*23*) and 53BP1 (*23*) and the appropriate FITC- (Molecular Probes, Eugene, OR) and Cy3-conjugated secondary antibodies (Amersham). (**D**) 293T cells were untreated (–) or treated (+) with 20-Gy IR and harvested after 1 hour. Cell extracts were incubated with antibodies to immunoglobulin G (IgG, control), Chk2, or 53BP1 and protein A Sepharose. Immunoprecipitates were separated by SDS-PAGE and then immunoblotted with antibodies to 53BP1 and Chk2 as indicated.

checkpoint, which reduces DNA synthesis. Unlike the control cells, 53BP1-inhibited cells showed radio-resistant DNA synthesis (Fig. 1A). This was also seen in Saos2 and HeLa cells with both siRNAs (*15*) and indicates a role of 53BP1 in the intra-S-phase checkpoint.

To assess the G_2-M checkpoint, we irradiated 53BP1-inhibited and control cells with 3 or 10 gray (Gy) of IR. About threefold more 53BP1-inhibited cells than the control cells treated with 3 Gy entered into mitosis (Fig. 1B). However, inhibition of 53BP1 had no effect after 10-Gy IR. Therefore, 53BP1-inhibited cells also displayed an IR-induced G_2-M checkpoint defect. The fact that 53BP1-inhibited cells were only defective in response to lower doses of irradiation indicates the existence of an alternative signaling pathway that operates at higher doses of IR.

Because 53BP1 binds p53, we asked whether 53BP1 was required for p53 activation in response to IR. The induction of p53 in response to IR was substantially decreased in 53BP1-inhibited cells (Fig. 2A). We then examined Chk2, a checkpoint protein implicated in p53 regulation that is phosphorylated on Thr^{68} and forms foci in response to IR (*16*, *17*). Quantification of the ratio of Chk2 phosphorylated on Thr^{68} to the total amount of Chk2 revealed that Chk2 phosphorylation at Thr^{68} was reduced twofold after 2 hours in response to IR in the 53BP1-inhibited cells (Fig. 2B). The reduction of Chk2 phosphorylation at Thr^{68} was reproducibly observed at 1 or 2 hours after IR in different experiments (*15*). A much stronger effect was observed in the formation of IR-induced foci recognized by antibodies to P-T68 of Chk2 (*17*), which were reduced in 53BP1 siRNA-treated cells but were unaffected in control cells (Fig. 2C).

53BP1 resembles the Rad9 BRCT-repeat protein of budding yeast, which binds to and is required for the DNA damage–induced activation of Rad53, a homolog of Chk2 (*16*). Like Rad9 and Rad53, we found that antibodies to Chk2 but not control antibodies could efficiently immunoprecipitate 53BP1 and that

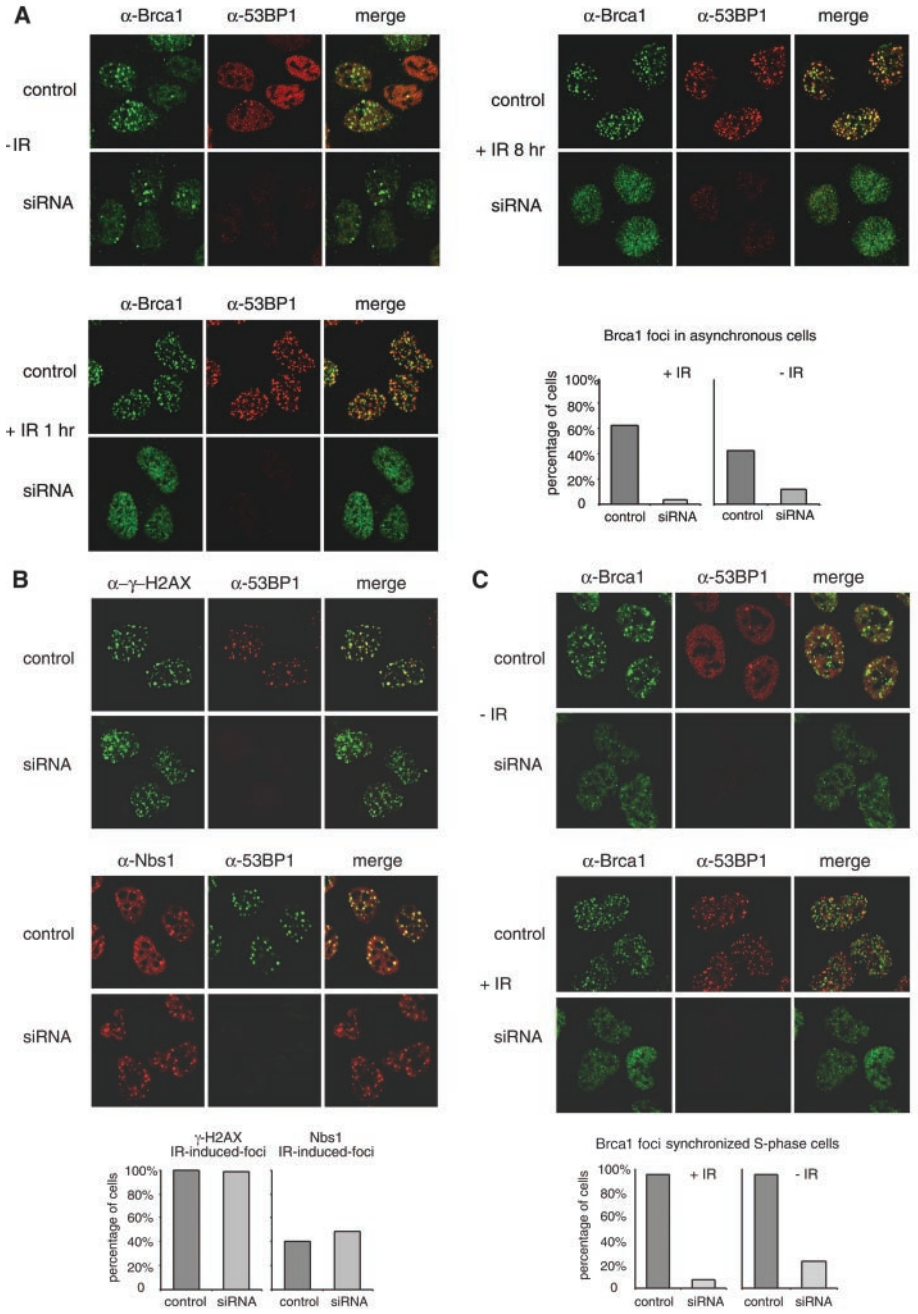

Fig. 3. Brca1 localization in S phase and relocalization in response to IR is dependent on 53BP1. (**A**) Brca1 localization in the presence and absence of 10-Gy IR. U2OS cells were transfected with siRNA targeting 53BP1 or control oligos and 2 days later exposed to 10-Gy IR. At the indicated times after IR, cells were permeablized with paraformaldehyde and fixed with Triton X-100. Immunostaining were performed with antibodies to 53BP1 and Brca1. Images were taken with a Zeiss confocal microscope. Quantitation of the BRCA1 foci are shown. These data were obtained with the use of siRNA oligo pair #1 targeting 53BP1. (**B**) IR-induced Nbs1 and γ-H2AX nuclear foci are independent of 53BP1. U2OS cells were treated and fixed as described in (A). Samples for γ-H2AX (*23*) staining were taken from cells recovered 2 hours after exposure to 10-Gy IR, and Nbs1 samples were cells recovered 6 hours after treatment with 10-Gy IR. Quantitation of foci are shown below. (**C**) Brca1 nuclear foci in synchronized S-phase cells in the presence and absence of 10-Gy IR are dependent on 53BP1. U2OS cells were sychronized using a double-thymidine block and released as described (14). At 4 hours after release, >80% of the cells were in S phase as indicated by flow cytometry. Cells at this stage were treated with 10-Gy irradiation and recovered for 1 hour at 37°C. Cells were fixed and immunostained as described. Quantitation of foci are shown below.

Chk2 dissociates from 53BP1 in response to IR (Fig. 2D). This association was also detected in the reciprocal immunoprecipitate with the use of 53BP1 antibodies. These data suggest that 53BP1 may act as an adaptor that facilitates Chk2 phosphorylation. It is likely that 53BP1 facilitates Chk2 activation in a transient complex and, upon activation, Chk2 dissociates from the 53BP1 complex.

The discrepancy between the partial dependency of 53BP1 for Chk2 phosphorylation and its major role in the formation of phospho-foci could be explained if only a subpopulation of phospho-Chk2 were responsible for the foci. A second explanation would be if other proteins phosphorylated by the 53BP1 pathway besides Chk2 were recognized by these antibodies, because the immunofluorescence specificity of these antibodies for phospho-Chk2 has not been fully established (*17*). Alternatively, 53BP1 might function as a general regulator of foci formation. To test this, we examined the ability of other proteins to form foci in the absence of 53BP1. Brca1, Nbs1, and γ-H2AX all form foci in response to IR (*16*). IR-induced Brca1 foci formation was largely abolished in 53BP1-inhibited cells. Brca1 showed diffuse staining and rarely formed distinctive foci in response to IR at different time points (Fig. 3A). In an asynchronous cell population, at 2 hours post-IR, only 4% of the cells formed Brca1 nuclear foci when cells were treated with 53BP1siRNA, as compared to 60% of the control cells (Fig. 3A). Similar results were obtained in Hct116 and HeLa cells with both oligo pairs (*15*). In contrast, formation of γ-H2AX foci or Nbs1 foci after IR remained unchanged in cells treated with control oligos or siRNA oligos (Fig. 3B). Rad51 foci were also unchanged (*15*).

When asynchronous control cells were analyzed for Brca1 foci formation in the absence of IR, about 40% contained more than 20 Brca1 foci, reflecting the S-phase and G_2 population. In 53BP1-inhibited cells, both the number of foci and the percentage of cells containing foci were reduced. Only 12% of 53BP1-inhibited cells contained more than 20 Brca1 foci (Fig. 3A). To control for cell cycle differences, we synchronized cells with the use of a double-thymidine block (*14*), and S-phase cells (4 hours after release from the block) were used for immunostaining. BRCA1 foci were also dependent on 53BP1 in S-phase cells in the presence or absence of IR (Fig. 3C).

Although the IR-induced foci formation of Brca1 is dependent on the presence of 53BP1, Brca1 foci did not show complete colocalization with 53BP1 foci at early times (Fig. 3A). The strong effect on BRCA1 foci formation, coupled with the fact that the 53BP1 and BRCA1 foci do not initially fully overlap, suggests that 53BP1 may regulate BRCA1 through a mechanism other than direct recruitment to foci. One means by which this might be achieved is through regulation of BRCA1 phosphorylation. In IR-treated cells, Brca1 phosphorylation was reduced in the samples prepared from cells treated with

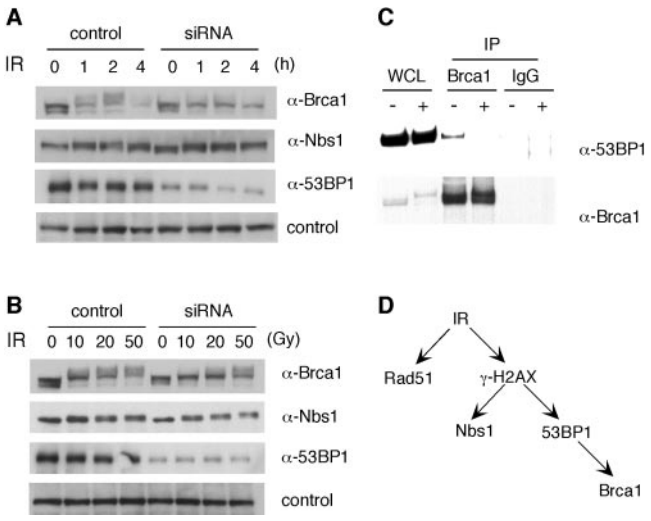

Fig. 4. 53BP1 regulation of Brca1. (**A**) Brca1 phosphorylation is reduced in the absence of 53BP1. U2OS cells were treated with siRNA oligos targeting 53BP1 or control oligos for 2 days. Cells were exposed to 10-Gy irradiation, and cell lysates were prepared at indicated times after irradiation. Immunoblots were performed with antibodies to Brca1 (Oncogene), Nbs1 (Norvus, Littleton, CO), and 53BP1. The control band is a nonspecific band from the same blot that was incubated with antibodies to Brca1. (**B**) Brca1 phosphorylation in response to different doses of irradiation. U2OS cells were transfected with siRNA oligos targeting 53BP1 or control oligos for 2 days, then treated with different doses of irradiation. Cell lysates were prepared at 2 hours after irradiation. (**C**) 53BP1 associates with Brca1. Cell lysates from untreated U2OS cells or 2 hours after exposure to 10-Gy IR were incubated with antibodies to Brca1 or rabbit IgG as a control. Western blots were performed with antibodies to 53BP1 and Brca1 (Oncogene). Ten percent of the cell lysate used for immunoprecipitation were loaded in the control lanes (WCL). (**D**) A schematic showing the genetic dependence for formation of nuclear foci for different proteins in response to IR.

siRNA oligos targeting 53BP1 relative to controls (Fig. 4A). As with the G_2-M checkpoint, the strongest dependency of Brca1 phosphorylation appeared to be at lower doses of IR (Fig. 4B). High levels of IR have been shown to obscure BRCA1 regulation by other proteins such as ATM (*18*). The loss of 53BP1 did not have a general effect on the DNA damage-inducible phosphorylation of other proteins; for example, Nbs1 phosphorylation was not affected (Fig. 4, A and B). Furthermore, although BRCA1 phosphorylation showed less dependency on 53BP1 at 50-Gy IR, these cells still failed to form foci (*15*).

Next we examined whether 53BP1 associated with BRCA1. Brca1 interacts with 53BP1 in vivo and, like Chk2, this interaction was abolished in response to IR (Fig. 4C). Thus, this dynamic association is likely to be important for regulation of 53BP1's ability to regulate both Chk2 and BRCA1 function in response to DNA damage.

An important finding of these studies is that 53BP1 is a critical transducer of the DNA damage signal and is required for both the intra-S-phase and G_2-M checkpoints; similar results have been obtained by others (*19*). It is part of a partially redundant branch of the signaling apparatus, and its loss results in a partial decrease in phosphorylation of key checkpoint target proteins. Because it binds to p53, Chk2, and Brca1 and controls the phosphorylation of at least two of these proteins, 53BP1 has the property of a mammalian adaptor or mediator that might recruit a subset of substrates to the ATM and ATR (ataxia telangiectasia and rad3-related) checkpoint kinases.

A second key finding of this study is that the pathway leading to the assembly of repair/signaling foci in response to damage is branched and shows a regulatory hierarchy in which H2AX is required for Nbs1 and 53BP1 foci (*20*), and 53BP1 controls the ability of at least BRCA1 but not Nbs1 to form foci as depicted in the pathway model shown in Fig. 4D. The nature of this disruption in foci formation is unknown but may be related to the role of 53BP1 in control of phosphorylation of these or other proteins. Regardless of the mechanism, it is clear that 53BP1 is a central transducer of the DNA damage signal to p53 and other tumor suppressor proteins and is likely to play an important role in the maintenance of genomic stability and prevention of cancer (*21*, *22*).

References and Notes

1. K. Iwabuchi, P. L. Bartel, B. Li, R. Marraccino, S. Fields, *Proc. Natl. Acad. Sci. U.S.A.* **91**, 6098 (1994).
2. K. Iwabuchi *et al.*, *J. Biol. Chem.* **273**, 26061 (1998).
3. I. Callebaut, J. P. Mornon, *FEBS Lett.* **400**, 25 (1997).
4. P. Bork *et al.*, *FASEB J.* **11**, 68 (1997).
5. Y. Saka, F. Esashi, T. Matsusaka, S. Mochida, M. Yanagida, *Genes Dev.* **11**, 3387 (1997).
6. X. Zhang *et al.*, *EMBO J.* **17**, 6404 (1998).
7. R. S. Williams, R. Green, J. N. Glover, *Nature Struct. Biol.* **8**, 838 (2001).
8. W. S. Joo *et al.*, *Genes Dev.* **16**, 583 (2002).
9. L. B. Schultz, N. H. Chehab, A. Malikzay, T. D. Halazonetis, *J. Cell Biol.* **151**, 1381 (2000).
10. I. Rappold, K. Iwabuchi, T. Date, J. Chen, *J. Cell Biol.* **153**, 613 (2001).
11. L. Anderson, C. Henderson, Y. Adachi, *Mol. Cell. Biol.* **21**, 1719 (2001).
12. Z. Xia, J. C. Morales, W. G. Dunphy, P. B. Carpenter, *J. Biol. Chem.* **276**, 2708 (2001).
13. S. M. Elbashir *et al.*, *Nature* **411**, 494 (2001).
14. Material and methods are available as supporting material on *Science* Online.
15. B. Wang and S. J. Elledge, unpublished observations.
16. B. B. Zhou, S. J. Elledge, *Nature* **408**, 433 (2000).
17. I. M. Ward, X. Wu, J. Chen, *J. Biol. Chem.* **276**, 47755 (2001).
18. D. Cortez, Y. Wang, J. Qin, S. J. Elledge, *Science* **286**, 1162 (1999).
19. R. DiTullio, T. Halazonetis, personal communication.
20. A. Celeste *et al.*, *Science* **296**, 922 (2002).
21. C. Lengauer, K.W. Kinzler, B. Vogelstein. *Nature* **396**, 643 (1998).
22. Y. Shiloh Y, M.B. Kastan, *Adv. Cancer Res.* **83**, 209 (2001).

23. Antibodies to Chk2T68P provided by J. Chen; 53BP1, T. D. Halazonetis; and γ-H2AX, W. M. Bonner.
24. We thank D. Cortez for helpful discussions; W. M. Bonner, T. D. Halazonetis, J. Qin, and J. Chen for providing antibodies; and T. Halazonetis for sharing unpublished checkpoint information and suggesting the use of 3GyIR. B.W. is a fellow of the U.S. Army Breast Cancer Postdoctoral Trainee Award, and S.J.E. is an Investigator with the Howard Hughes Medical Institute.

Supporting Online Material

www.sciencemag.org/cgi/content/full/1076182/DC1
Materials and Methods
Fig. S1

15 July 2002; accepted 23 September 2002
Published online 3 October 2002;
10.1126/science.1076182
Include this information when citing this paper.

21. Ahn, J.-H., Schwarz, J. K., Piwnica-Worms, H. & Canman, C. E. Threonine 68 phosphorylation by ataxia telangiectasia-mutated is required for efficient activation of Chk2 in response to ionizing radiation. *Cancer Res.* **60,** 5934–5936 (2000).
22. Chaturvedi, P. *et al.* Mammalian Chk2 is a downstream effector of the ATM-dependent DNA damage checkpoint pathway. *Oncogene* **18,** 4047–4054 (1999).
23. Elbashir, S. M. *et al.* Duplexes of 21-nucleotide RNAs mediate RNA interference in cultured mammalian cells. *Nature* **411,** 494–498 (2001).
24. Painter, R. B. & Young, B. R. Radiosensitivity in ataxia-telangiectasia: A new explanation. *Proc. Natl Acad. Sci. USA* **77,** 7315–7317 (1980).
25. Falck, J., Mailand, N., Syljuasen, R. G., Bartek, J. & Lukas, J. The ATM-Chk2-Cdc25A checkpoint pathway guards against radioresistant DNA synthesis. *Nature* **410,** 842–847 (2001).
26. Hirao, A. *et al.* DNA damage-induced activation of p53 by the checkpoint kinase Chk2. *Science* **287,** 1824–1827 (2000).
27. Hirao, A. *et al.* Chk2 is a tumour suppressor that regulates apoptosis in both an ataxia telangiectasia mutated (ATM)-dependent and an ATM-independent manner. *Mol. Cell. Biol.* **22,** 6521–6532 (2002).
28. Jack, M. T. *et al.* Chk2 is dispensable for p53-mediated G1 arrest but is required for a latent p53-meidated apoptotic response. *Proc. Natl Acad. Sci. USA* **99,** 9825–9829 (2002).
29. Chehab, N. H., Malikzay, A., Apple, M. & Halazonetis, T. D. Chk2/hCds1 functions as a DNA damage checkpoint in G1 by stabilizing p53. *Genes Dev.* **14,** 278–288 (2000).
30. Shieh, S. Y., Ahn, J., Tamai, K., Taya, Y. & Pricves, C. The human homologs of checkpoint kinases Chk1 and Cds1 (Chk2) phosphorylate p53 at multiple DNA damage-inducible sites. *Genes Dev.* **14,** 289–300 (2000).

Acknowledgements We thank L. Wang for technical support. We also thank Mayo Protein Core facility for synthesis of peptides. We are grateful to L. Karnitz and S. Kaufmann and members of the Chen and Karnitz laboratories for discussions and ongoing technical support. This work is supported in part by grants from the National Institute of Health, the Prospect Creek Foundation and the Breast Cancer Research Foundation. J.C. is a recipient of a DOD breast cancer career development award.

Competing interests statement The authors declare that they have no competing financial interests.

Correspondence and requests for materials should be addressed to J.C. (e-mail: chen.junjie@mayo.edu).

MDC1 is a mediator of the mammalian DNA damage checkpoint

Grant S. Stewart*, Bin Wang*, Colin R. Bignell†, A. Malcolm R. Taylor† & Stephen J. Elledge*‡§

** Verna & Mars McLean Department of Biochemistry and Molecular Biology, ‡ Department of Molecular and Human Genetics, and § Howard Hughes Medical Institute, Baylor College of Medicine, Houston, Texas 77030, USA*
† CRC Institute for Cancer Studies, University of Birmingham, Edgbaston, Birmingham B15 2TT, UK

To counteract the continuous exposure of cells to agents that damage DNA, cells have evolved complex regulatory networks called checkpoints to sense DNA damage and coordinate DNA replication, cell-cycle arrest and DNA repair[1]. It has recently been shown that the histone H2A variant H2AX specifically controls the recruitment of DNA repair proteins to the sites of DNA damage[2–4]. Here we identify a novel BRCA1 carboxy-terminal (BRCT) and forkhead-associated (FHA) domain-containing protein, MDC1 (mediator of DNA damage checkpoint protein 1), which works with H2AX to promote recruitment of repair proteins to the sites of DNA breaks and which, in addition, controls damage-induced cell-cycle arrest checkpoints. MDC1 forms foci that co-localize extensively with γ-H2AX foci within minutes after exposure to ionizing radiation. H2AX is required for MDC1 foci formation, and MDC1 forms complexes with phosphorylated H2AX. Furthermore, this interaction is phosphorylation dependent as peptides containing the phosphorylated site on H2AX bind MDC1 in a phosphorylation-dependent manner. We have shown by using small interfering RNA (siRNA) that cells lacking MDC1 are sensitive to ionizing radiation, and that MDC1 controls the formation of damage-induced 53BP1, BRCA1 and MRN foci, in part by promoting efficient H2AX phosphorylation. In addition, cells lacking MDC1 also fail to activate the intra-S phase and G2/M phase cell-cycle checkpoints properly after exposure to ionizing radiation, which was associated with an inability to regulate Chk1 properly. These results highlight a crucial role for MDC1 in mediating transduction of the DNA damage signal.

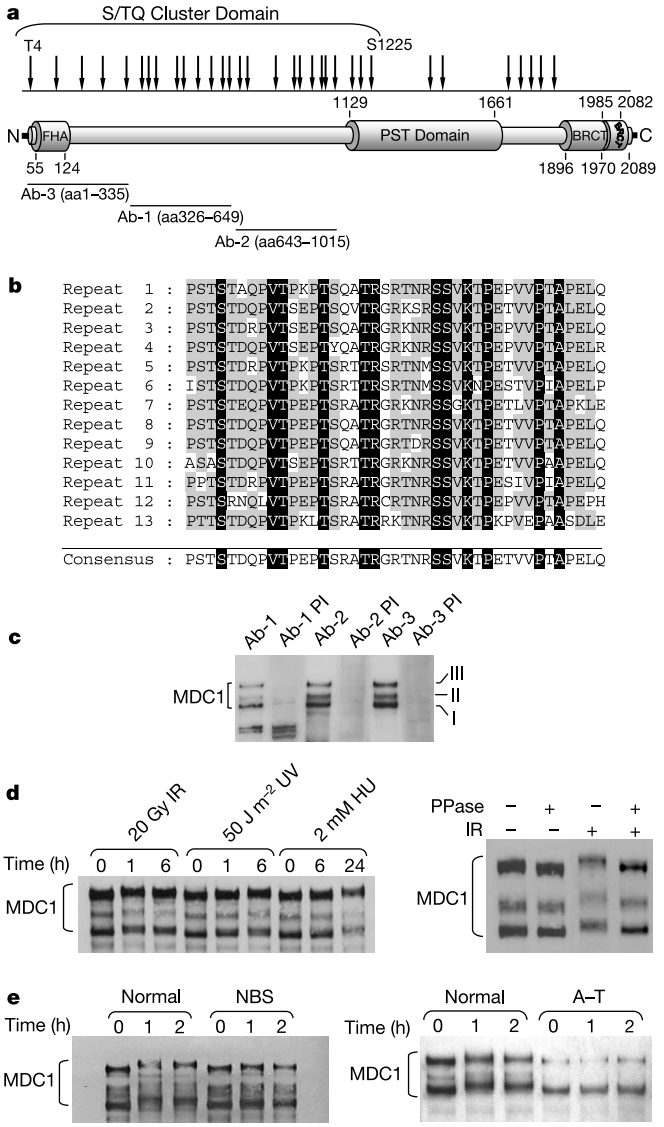

Figure 1 MDC1 is phosphorylated in response to DNA damage and DNA replication stress. **a**, A diagrammatic representation of the MDC1 protein. The amino acids encompassing each domain are indicated. PST indicates proline/serine/threonine repeat domain. The red arrows indicate potential phosphatidylinositol-3-OH kinase-like kinase phosphorylation motifs (SQ/TQ). The fragments of the MDC1 protein used to make anti-MDC1 antibodies (Ab-1, Ab-2, Ab-3) are indicated. **b**, Alignment of the 41-amino-acid repeat sequence that composes the PST domain. Black shaded boxes indicate conserved amino acids and grey boxes indicate similar amino acids. **c**, Recognition of three isoforms (I, II and III) of human MDC1. PI refers to pre-immune serum. **d**, DNA damage-induced phosphorylation of MDC1. Cells were treated with 20 Gy IR, 50 J m^{-2} UV or 2 mM HU and harvested at the times indicated. IR-treated cell extracts were also incubated with and without λ protein phosphatase (λ PPase). **e**, MDC1 is phosphorylated in response to IR in an ATM- and Nbs1-dependent manner. Normal, NBS and A–T lymphoblasts were irradiated with 20 Gy of IR and harvested at the times indicated.

Mediators are an emerging class of checkpoint proteins involved in transducing the DNA damage signal. The prototypical mediator

is the Rad9 protein in *Saccharomyces cerevisiae*. Rad9 is phosphorylated by the ATR (ataxia–telangiectasia and Rad3 related) homologue, Mec1, in response to DNA damage and controls the activation of the Chk1 and Chk2 (scRAD53) homologues[5,6]. Rad9 contains two BRCT motifs that are required for its checkpoint functions[7]. No clear mammalian homologue of *S. cerevisiae* Rad9 has been identified. However, several large BRCT-repeat-containing proteins, such as TopBP1, 53BP1 and BRCA1, which have been implicated in the cellular response to DNA damage, may compose this class of mediator protein in higher eukaryotic cells[8–11].

To search for proteins involved in various aspects of DNA repair, we investigated proteins with motifs common to DNA damage response proteins and found a protein (Kazusa DNA Research Institute clone KIAA0170) that possesses the characteristics of a DNA damage mediator and named it MDC1. MDC1 contained two carboxy-terminal BRCT-repeats and an amino-terminal phospho-amino-acid-binding motif called a FHA domain, which is also found in several DNA damage response proteins such as Chk2, Rad53, Cds1 and Nbs1 (refs 12–15). A large S/TQ cluster domain can be found encompassing the N-terminal half of the protein (Fig. 1a). Both BRCA1 and Chk2 have S/TQ cluster domains and are phosphorylated within these domains by ATM (ataxia–telangiectasia mutated) and ATR after DNA damage[16–19]. MDC1 also contains a large central proline/serine/threonine-rich repeat (PST) domain that has no significant homology to any other protein in the database (Fig. 1b).

To investigate the role of MDC1 in the DNA damage response, three polyclonal antisera generated to non-overlapping fragments of the MDC1 open reading frame (ORF) all specifically recognized three bands (I, II and III) of approximately 250 kDa, which were not recognized by the pre-immune sera (Fig. 1c). All three bands diminished in intensity when cells were pre-treated with three different MDC1-specific siRNA oligonucleotides but not control siRNAs demonstrating specificity (data not shown and see Fig. 5a). To address whether the expression or mobility of MDC1 was affected by DNA damage, cells were exposed to a variety of genotoxic agents and blotted for MDC1. All isoforms demonstrated a reduced mobility after exposure of cells to ionizing radiation (IR), ultraviolet radiation (UV) and hydroxyurea (HU) (Fig. 1d). The altered mobility was ablated by phosphatase treatment, indicating that MDC1 is modified by phosphorylation after DNA damage (Fig. 1d). Furthermore, the phosphorylation of MDC1 after IR is dependent on the presence of functional ATM and Nbs1 (Fig. 1e). Both ATM and ATR could be shown to phosphorylate a fragment of the MDC1 protein encompassing the S/TQ cluster domain *in vitro* (data not shown).

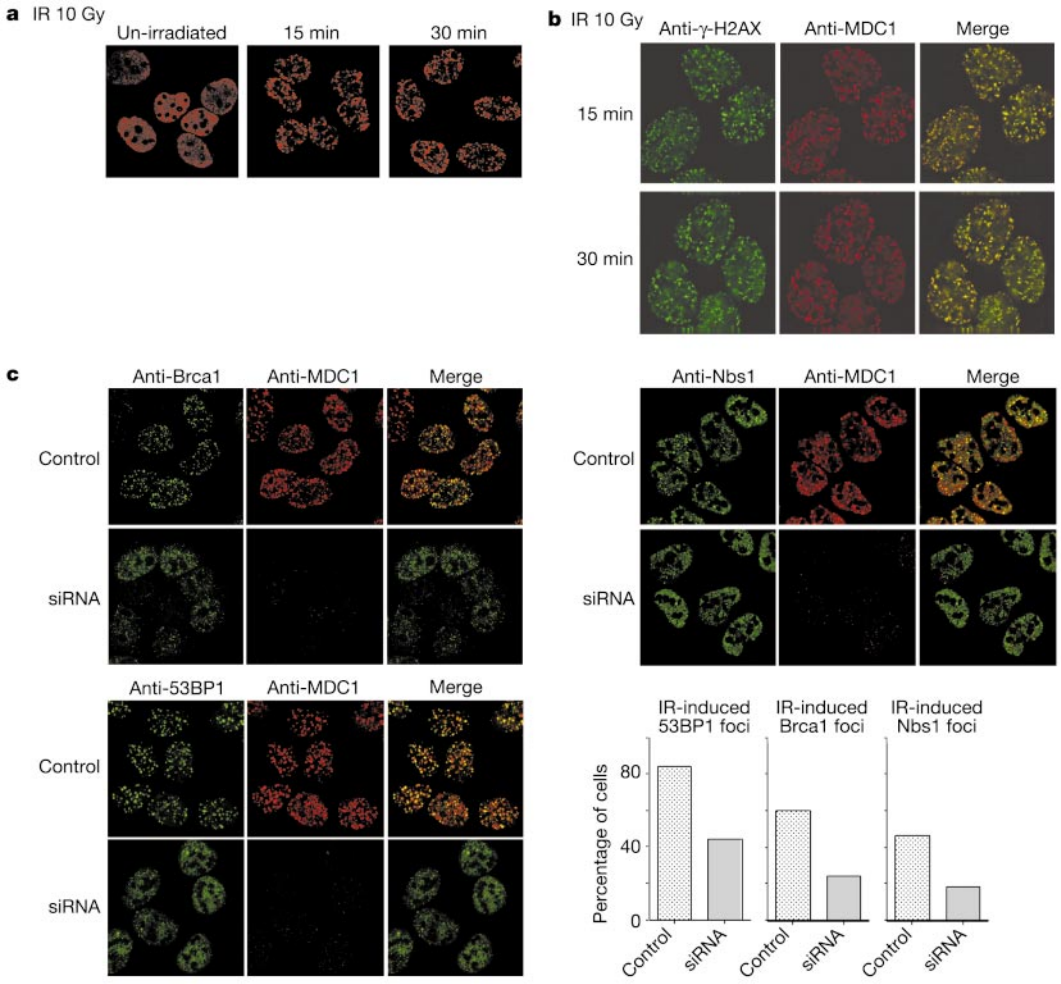

Figure 2 MDC1 regulates BRCA1, 53BP1 and Nbs1 foci formation. **a**, IR-induced MDC1 foci formation. Cells were untreated or irradiated with 10 Gy, fixed and stained with anti-MDC1 antibodies at the times indicated. **b**, Co-localization of MDC1 and γ-H2AX foci after 10 Gy IR. **c**, Inhibition of MDC1 results in defective BRCA1, 53BP1 and Nbs1 foci formation after IR exposure. U2OS cells were transfected with a control or MDC1 siRNA and irradiated with 10 Gy IR. Cells were fixed at 2 h post-irradiation and stained with the indicated antibodies. Cells were fixed at 6 h post-irradiation to visualize Nbs1 foci. The percentages of cells with the respective foci are indicated. When cells were treated with MDC1 siRNA, the percentage of cells listed refers to the percentage of cells that lack detectable MDC1 but contain the indicated foci. Images were taken with a Zeiss confocal microscope.

Many DNA damage-signalling proteins are recruited to sites of damage[20]. It has been suggested that the order and timing of these events are critical for normal DNA repair. To assess whether MDC1 could also localize to sites of damage, cells were treated with IR and stained with anti-MDC1 antiserum. MDC1 rapidly formed foci in over 95% of cells within 15 min after exposure to IR (Fig. 2a). A proportion of un-irradiated cells also contained MDC1 foci, indicating that MDC1 may be responding to endogenous damage or replication stress. No foci were observed in the cells stained with the pre-immune serum (Supplementary Information Fig. 1). MDC1 also formed foci after UV-irradiation (data not shown) indicating that MDC1 can respond to multiple types of DNA aberrations.

A time-dependent, sequential assembly of repair factors at the sites of damage has been demonstrated[20]; γ-H2AX (the phosphorylated form of H2AX) foci appear within minutes after irradiation. 53BP1, BRCA1 and Mre11/NBS1/hRad50 complex are subsequently recruited to γ-H2AX-positive repair foci. To determine the kinetics of MDC1 foci compared with other foci-forming proteins, co-localization studies were done. Strikingly, within 15 min of exposure to ionizing radiation, MDC1 foci extensively overlap with γ-H2AX foci and remain co-localized throughout the time course (Fig. 2b). MDC1 foci also significantly co-localize with 53BP1 and BRCA1 foci at 2 h post-irradiation, and at later times also exhibited co-localization with Nbs1 foci (Fig. 2c). The numbers of MDC1 foci per cell were in excess of 53BP1, BRCA1 and Nbs1 foci at corresponding times.

Several proteins that show co-localization in foci exist as pre-assembled complexes[21]. Therefore, we determined whether MDC1 could bind to the components of the MRN complex and other known damage response proteins. MDC1 could be shown to co-precipitate with Nbs1, hRad50 and hMre11 before and after DNA damage and to a lesser extent with ATM and the FANCD2 protein (Fig. 3). The prior exposure of cells to IR appears to reduce the interaction of MDC1 with these proteins slightly. Given that MDC1 binds tightly to chromatin after DNA damage (data not shown), it is likely that the reduction of co-immunoprecipitated protein after exposure to IR is due to a reduced ability to efficiently solubilize MDC1 protein before immunoprecipitation. MDC1 could also be shown to interact strongly with 53BP1 and SMC1 in a manner unaffected by DNA damage. It is therefore likely that MDC1 exists within a large complex consisting of several DNA repair proteins and cell-cycle checkpoint regulatory proteins.

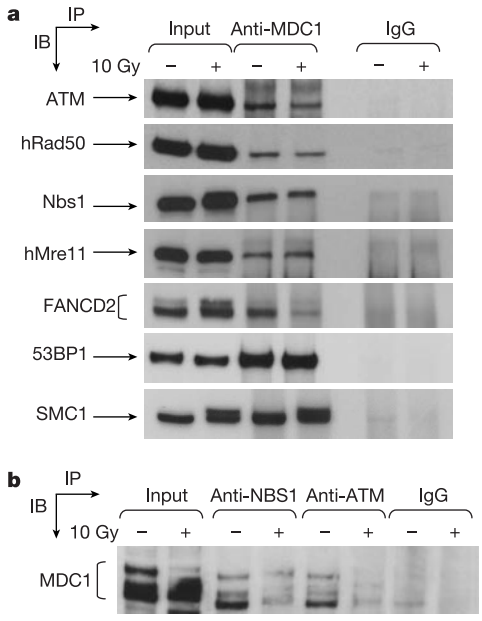

Figure 3 MDC1 associates with DNA damage checkpoint proteins. Cells were mock irradiated (−) or treated with 10 Gy IR (+) and harvested 1 h later. Immunoprecipitations (IP) or immunoblots (IB) were done with the antibody indicated or a non-specific, species-matched IgG control. Input represents 1% of total protein used in IPs. The unavailability of immunoprecipitating antibodies to 53BP1, SMC1 and FANCD2 prevented examination of the reciprocal co-immunoprecipitation with MDC1; however, the interaction was confirmed by using the two other anti-MDC1 antibodies generated to non-overlapping epitopes (data not shown).

There appears to be a hierarchy of proteins involved in the assembly of damage-responsive foci. H2AX is required for the formation of 53BP1, NBS1 and BRCA1 foci[10,22,23]. To determine whether MDC1 functions in this pathway, we asked if MDC1 was required for the ability of these repair proteins to form foci. Cells were treated with a control siRNA or MDC1 siRNA, irradiated and stained for 53BP1, BRCA1 and Nbs1 foci. Cells lacking MDC1 showed a significant reduction in the number of cells with Nbs1 foci, with the number of residual foci in each cell also being reduced (Fig. 2c). This suggests that MDC1 is required for efficient localization of the MRN complex after DNA damage. In addition, both 53BP1 and BRCA1 foci were similarly affected in the MDC1-siRNA-treated cells compared with the control siRNA-treated cells (Fig. 2c). These data demonstrate that MDC1 is likely to function upstream of 53BP1, BRCA1 and the MRN complex, possibly acting as a scaffold for protein recruitment. Consistent with this hypothesis, MDC1 foci were not affected in NBS or ATLD cells or when cells were treated with 53BP1-specific siRNA (data not shown). It should be noted that inhibition of MRN and 53BP1 foci was not complete, suggesting that either the siRNA treatment leaves residual functional MDC1 capable of limited foci formation, or that a partly redundant pathway exists to localize these proteins.

Because MDC1 and H2AX extensively co-localize and display similar kinetics of foci formation after IR, we examined the ability of MDC1 to form foci in the absence of H2AX and other checkpoint proteins. Mouse MDC1 showed a punctate nuclear staining pattern in wild-type mouse embryo fibroblasts (MEFs), which re-organized into large foci in response to DNA damage. MDC1 foci failed to form in H2AX null MEFs (Fig. 4a) but did form foci in Chk2 null MEFs (data not shown). Thus, H2AX acts upstream of MDC1. Surprisingly, the phosphorylation of MDC1 is also partly dependent on the presence of H2AX (Fig. 4b) but Chk2 loss has little or no effect on phosphorylation. Given that one of the functions of H2AX is to specifically recruit DNA repair proteins to sites of damage[2,3], this suggests that the modification of MDC1 by ATM and other kinases might be enhanced by recruitment to sites of DNA damage. In addition, the damage-induced phosphorylation of 53BP1 was also found to be partly dependent on H2AX (Fig. 4b), consistent with its interaction with MDC1. This contrasts with the ATM-dependent phosphorylation of Nbs1, which occurs normally in the absence of H2AX (ref. 2).

The fact that H2AX and MDC1 form completely overlapping foci with identical kinetics suggests that they might have a more intimate relationship. To examine this we immunoprecipitated MDC1 and tested for the presence of phospho-S139 H2AX. Phosphorylated H2AX co-immunoprecipitated with MDC1 and the association was increased in the presence of DNA damage (Fig. 4c). The presence of γ-H2AX in undamaged cells may represent intrinsic cellular damage. It is thought that the phosphorylation of H2AX on S139 triggers its ability to recruit factors such as MDC1 to foci. To examine this we used an S139-phosphorylated and unphosphorylated peptide from the C-terminal tail of H2AX coupled to beads to assess whether MDC1 could be pulled down from cellular extracts. MDC1 bound specifically to the phosphorylated H2AX peptide and not to the unphosphorylated H2AX peptide or a control-phosphorylated peptide from cyclin E (Fig. 4d). In addition to MDC1, 53BP1 was also pulled down by the phospho-H2AX peptide, confirming the previously published association of H2AX and 53BP1[23]. Not all DNA repair/checkpoint proteins were found to

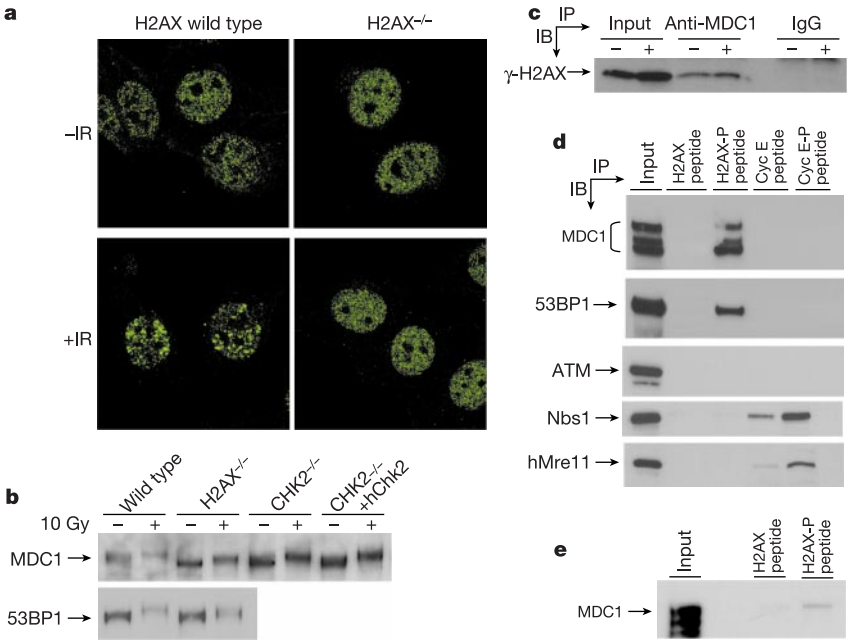

Figure 4 Interactions between MDC1 and H2AX. **a**, MDC1 foci formation is H2AX dependent. H2AX$^{-/-}$ MEFs and the corresponding wild-type MEFs were exposed to IR, fixed and stained with anti-MDC1 antibodies at 30 min post-irradiation. **b**, MDC1 and 53BP1 phosphorylation is dependent on H2AX. Wild type, H2AX$^{-/-}$ MEFs, CHK2$^{-/-}$ and human CHK2 complemented CHK2$^{-/-}$ MEFs were irradiated and harvested after 1 h. **c**, Association of MDC1 with γ-H2AX. Immunoprecipitations (IP) and immunoblots (IB) were done with the antibody indicated or a non-specific, species-matched IgG control. **d**, A phosphorylated H2AX peptide recruits MDC1. Cell extracts were incubated with a peptide from the C-terminal tail of H2AX. (P) indicates phosphorylation of the peptide on serine-139. A cyclin E peptide and its phosphorylated version (P) were used as specificity controls. **e**, *In vitro* binding of MDC1 to the phosphorylated H2AX peptide. Phosphorylated or unphosphorylated H2AX-coupled peptide was added to ^{35}S-methionine-labelled, *in vitro* translated MDC1 and incubated for 1 h. Peptide-bound proteins were detected by using autoradiography.

associate with H2AX as components of the MRN complex: ATM and hChk2 (data not shown) were not significantly enriched by the H2AX p-S139 peptide. As we previously detected Nbs1 and ATM in MDC1 IPs, we had expected to recover these proteins with MDC1; however, it is possible that these proteins exist in a complex with MDC1 that already has γ-H2AX in it or that the complex containing MRN and ATM cannot bind in the context of the bead for steric reasons.

To further assess the interaction of MDC1 and the H2AX phospho-peptide, MDC1 was translated *in vitro* by using a rabbit reticulocyte lysate system and incubated with the H2AX-peptide-coupled beads. The MDC1 translated *in vitro* was pulled down specifically by the H2AX phospho-peptide, again demonstrating that the interaction is phospho dependent (Fig. 4e). However, it is unclear whether this interaction is direct as the reticulocyte lysates may contain bridging proteins.

To examine the genetic role of MDC1 in the DNA damage response, siRNA was used to deplete MDC1. Cells were transiently transfected with either a control siRNA or one of three MDC1-specific siRNAs, harvested 48–72 h after transfection, and their protein expression determined. All three MDC1-specific siRNA oligonucleotides decreased by more than 80% in the overall MDC1 protein expression, compared with the mock or control siRNA-transfected cells (Fig. 5a). To examine the ability of MDC1-depleted cells to respond to damage, siRNA-transfected cells were plated at low density, irradiated with IR and assessed for their ability to form colonies. Cells with reduced MDC1 exhibited hypersensitivity to the killing effects of IR (Fig. 5b) when compared with the control cells. Furthermore, transfection with MDC1-specific siRNA also reduced the number of colonies formed from undamaged cells when compared with control cells, indicating that MDC1 function may be required to maintain cell viability.

The sensitivity to IR suggests an important role in responding to DNA damage; therefore we checked the integrity of cell-cycle checkpoints in these cells. To test whether MDC1 could function in regulating the intra-S-phase checkpoint, cells were either transfected with control siRNA or MDC1-specific siRNA oligonucleotides. After 48 h, cells were exposed to 15 Gy of IR and the rate of incorporation of tritiated thymidine was determined. Control cells exhibited a decrease of approximately 50% in the rate of DNA synthesis. In contrast, cells treated with MDC1 siRNA oligonucleotides 4 or 5 only decreased the rate of DNA synthesis by 25% (Fig. 5c). This demonstrates a role for MDC1 in regulating S-phase progression after DNA damage.

We next examined the integrity of the G2/M checkpoint. Cells treated with MDC1-specific siRNA were irradiated and labelled with an anti-phospho-histone H3 antibody as a marker of mitotic cells. A clear reduction in phospho-H3-positive cells was observed in the control-treated cells after IR exposure, whereas a significant number of the cells lacking MDC1 entered mitosis (Fig. 5d), indicative of a defect in the ability to arrest the cell cycle in G2 phase.

To gain insight into the precise mechanism by which MDC1 mediates both the S-phase and G2/M damage-activated cell-cycle checkpoints, cells were treated with MDC1-targeted siRNA and assessed for their ability to properly phosphorylate key effector molecules known to be critical for efficient checkpoint activation after DNA damage. We observed decreased phosphorylation of SMC1 S996 (more pronounced at 2 h) and Chk1 S345 in response to IR, and SMC1, Chk1 and RPA2 in response to UV (Fig. 5e). Nbs1 and Chk2 were not affected although we observed a small decrease in Chk2 T68 phosphorylation in response to UV in some experiments (data not shown). Chk1 is required for the G2/M checkpoint arrest[24,25] and this defect is likely to explain the checkpoint defect we observed. Both SMC1[26,27] and Chk1[28] have been implicated in the intra-S-phase checkpoint, and their defective regulation is likely to explain these defects as well. The fact that UV-induced signalling is impaired suggests that the ATR pathway depends in part upon MDC1 function, as ATR is the major regulator of Chk1 phosphoryl-

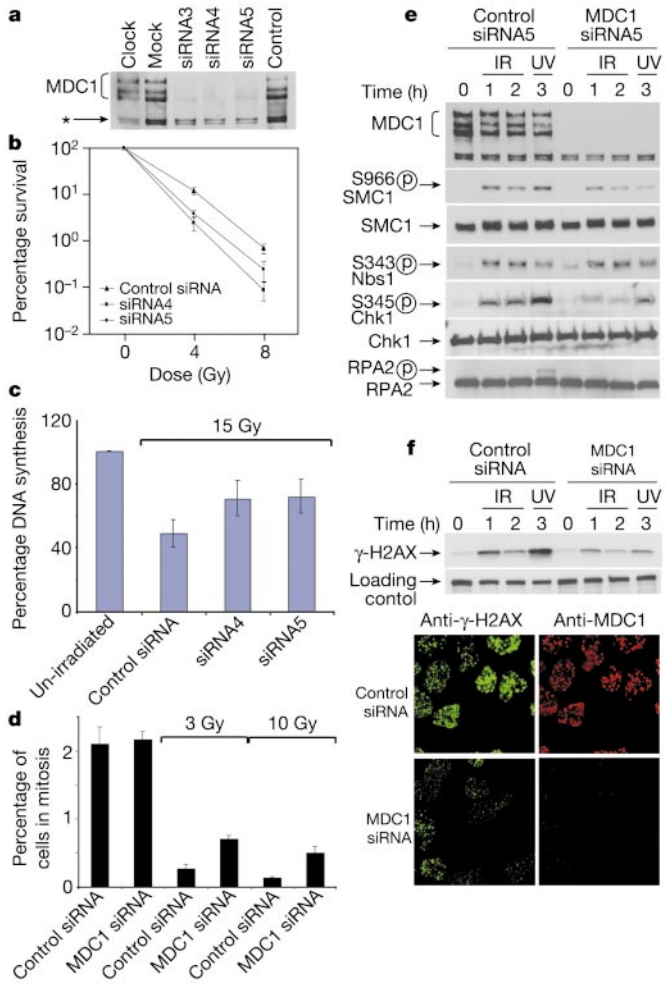

Figure 5 MDC1 inhibition results in defective IR-induced checkpoints and Chk1 and H2AX phosphorylation. **a**, siRNA-mediated reduction of MDC1 protein expression. Cells were transfected with a control or MDC1 siRNA and harvested at 48 h. Three different siRNAs to MDC1 were used. An asterisk indicates a cross-reacting band used as a loading control. **b**, Reduced MDC1 expression results in IR sensitivity. Control or MDC1 siRNA-treated cells were plated at low density, irradiated and colonies counted after 14 days. **c**, MDC1 prevents RDS. DNA synthesis was assessed 30 min after 15 Gy IR in U2OS cells transfected with a control or MDC1 siRNA oligonucleotides. **d**, Analysis of the G2/M checkpoint. Cells were untreated or γ-irradiated as indicated, then incubated for 1 h at 37 °C before fixation. Mitotic cells were determined by phospho-histone H3 staining and flow cytometry. **e**, MDC1 is required for DNA damage checkpoint signalling. Cells were transfected twice with siRNAs and irradiated 72 h later. The immunoblot with SMC1 as a control for protein loading shows a reduced mobility in extracts from damaged cells rather than increased protein loaded on the gel. **f**, MDC1 is required for H2AX phosphorylation. Control or MDC1 siRNA-treated cells were irradiated and the levels of H2AX phosphorylation detected by western blot and immunofluorescence 1 h post-irradiation.

ation. Together, these results indicate that MDC1 is a central transducer of the DNA damage checkpoint signal.

As MDC1 controls the phosphorylation of several checkpoint-responsive proteins, we sought to examine whether it might have a role in H2AX phosphorylation. Depleting cells of MDC1 protein significantly affected the phosphorylation of H2AX after both IR and UV radiation and the formation of phospho-H2AX foci (Fig. 5f). Thus MDC1 and H2AX share a mutual dependency for phosphorylation and foci formation.

In this study, we have identified a new DNA damage checkpoint protein, MDC1, which transduces the DNA damage signal and shares an intimate relationship with H2AX. In response to DNA damage, MDC1 and H2AX exist in a complex, are phosphorylated and co-localize to sites of DNA damage, all in a mutually dependent fashion. Both proteins are required for optimal formation of MRN, 53BP1 and BRCA1 foci. Furthermore, peptides representing the tail of H2AX specifically recruit MDC1 and 53BP1 protein in a phosphorylation-dependent manner, suggesting a model in which H2AX is phosphorylated in response to damage and the phospho-H2AX recruits MDC1 leading to its phosphorylation. However, we cannot determine whether MDC1 controls the initial phosphorylation of H2AX, or merely protects H2AX from dephosphorylation through formation of a complex with H2AX. It is possible that there is a self-reinforcing loop whereby MDC1 and H2AX mutually stimulate each other's phosphorylation and help larger complexes of proteins associate at these foci. Furthermore, this effect on H2AX phosphorylation may, in part, help to explain why the recruitment of 53BP1, BRCA1 and Nbs1 to damage foci partly depends on MDC1. The ability of MDC1 to form complexes with MRN and 53BP1 may also contribute to this dependency. Regardless, it is clear from the data presented here that H2AX and MDC1 are intimately related and work together to mediate the DNA damage response.

Although MDC1 and H2AX have many common features, there are some important differences. MDC1 is required for the intra-S-phase checkpoint and the G2/M DNA damage checkpoint. H2AX has recently been shown to have a mild G2/M defect in response to low doses of IR[3], much less severe than that observed in MDC1. MDC1 exists in complexes with several checkpoint-signalling proteins such as the MRN complex, SMC1, 53BP1 and FANCD2. Furthermore, MDC1 is required for the efficient phosphorylation of several checkpoint-signalling proteins including SMC1, RPA2 and the crucial checkpoint kinase Chk1. The defect in Chk1 phosphorylation explains the defects in both the intra-S-phase and G2/M checkpoints. The defect in MDC1 checkpoint signalling is more pronounced in response to UV than IR. This, together with the regulation of Chk1, suggests that MDC1 plays an important role in the ATR signalling pathway that controls Chk1 phosphorylation[25] and a less important role in the ATM pathway. This may explain the mild defect in the IR-induced phosphorylation of SMC1, which is primarily ATM dependent. The mild SMC1 phosphorylation defect becomes more pronounced at later times in the absence of MDC1, consistent with the late role of ATR in IR-induced phosphorylation of substrates shared by ATM. MDC1 may play a role in the recruitment of checkpoint kinases such as ATR to substrates such as H2AX and the pathway controlling Chk1, which may include BRCA1 and Claspin. Therefore, MDC1 plays a critical role in the DNA damage checkpoint response. MDC1 represents the third member of the mediator family of proteins in mammals. Each of these proteins plays important and potentially overlapping roles in transducing the DNA damage signal to promote genomic stability. As a new member of this family, MDC1 is also likely to be involved in tumorigenesis. □

Methods

Cells

Lymphoblastoid cell lines (LCLs) were routinely maintained in RPMI medium supplemented with 10% foetal bovine serum (FBS), glutamine and penicillin and streptomycin (pen/strep). U2OS cells were maintained in McCoy's 5A medium supplemented with 10% FBS, glutamine and pen/strep. All MEF cell lines were maintained in DMEM medium supplemented with 10% FBS, glutamine and pen/strep.

siRNA

The siRNA duplexes were 21 base pairs with a 2-base deoxynucleotide overhang (Dharmacon Research). The sequences of MDC1 siRNA4 and siRNA5 oligonucleotides were GUCUCCCAGAAGACAGUGAdTdT and ACAGUUGUCCCCACAGCCCdTdT, respectively. The control siRNA used was CGUACGCGGAAUACUUCGAdTdT against LacZ. Cells were transfected with siRNA duplexes by using Oligofectamine (Invitrogen), following the manufacturer's instructions.

MDC1 antibody generation

A full-length MDC1 clone (KIAA0170) was generously provided by the Kazusa DNA Research Institute. Fragments of the cDNA were subcloned into a glutathione *S*-transferase (GST) expression vector (Amersham Biosciences), expressed in bacteria and

purified by using glutathione-coupled sepharose beads (Amersham Biosciences). Purified GST fusion proteins were injected into rabbits and the antisera were affinity purified by using the respective antigen (Bethyl Laboratories). Ab-1 was generated to a fragment of MDC1 encompassing amino acids 326–649, Ab-2 was generated to a fragment of MDC1 encompassing amino acids 643–1015 and Ab-3 was generated to a fragment of MDC1 encompassing amino acids 1–335.

Immunoblot analysis

Cells were sonicated in UTB buffer (8 M urea, 150 mM β-mercaptoethanol, 50 mM Tris/HCl pH 7.5) and cellular debris removed by centrifugation. Protein concentration was determined by using the BioRad Bradford Protein determination reagent. Proteins were fractionated in 6% SDS–polyacrylamide gels. Proteins were transferred to nitrocellulose, and immunoblots were performed by using the appropriate antibody. Antibodies to Nbs1, hMre11 and hRad50 were obtained from Genetex, the phospho-Nbs1 (serine-343) antibody was obtained from Cell Signaling and the anti-phospho-H2AX (serine-139) antibodies were obtained from Upstate Biotechnology. The anti-FANCD2 and anti-Chk1 antibodies were purchased from Santa Cruz. J. Qin provided antibodies to SMC1 and phosphorylated SMC1 (ref. 21). P. Carpenter supplied antibodies to 53BP1.

Immunoprecipitation and phosphatase treatment

LCLs ($\sim 4 \times 10^7$) were either mock irradiated or irradiated with 10 Gy of ionizing radiation and incubated for 1 h at 37 °C. The cells were then lysed for 30 min in NETN lysis buffer (50 mM Tris/HCl pH 7.5, 150 mM NaCl, 1 mM EDTA, 1% NP40 supplemented with protease inhibitors (Roche) and Benzonase (Novagen)). The clarified extract was pre-cleared with the appropriate IgG (Dako) and protein A or G beads (Amersham Biosciences) for 1 h at 4 °C. Immunoprecipiting antibody (5 μg) was added with protein A or G beads to the pre-cleared supernatant and incubated for 3 h at 4 °C. The immunocomplexes were washed four times in NETN lysis buffer (containing 0.5% NP40), boiled in SDS sample buffer, loaded on an SDS–polyacrylamide gel. Proteins were analysed by immunoblotting using standard methods and detected as described above. For phosphatase treatment of cell extract, 1,200 units of λ protein phosphatase (New England Biolabs) were added to the extract in the presence of $MnCl_2$ and incubated for 30 min at 30 °C. The phosphatase was then heat inactivated.

H2AX peptide pull-down assay

Two peptides to the last C-terminal 10 amino acids of human H2AX (CKATQASQEY) were synthesized (Bethyl), one of which was phosphorylated on the serine residue. The peptides were coupled to beads by using the Sulfolink kit (Pierce). 20 μg of coupled peptide were used per pull-down. The assay was essentially identical to the immunoprecipitation protocol as described above.

H2AX peptide *in vitro* binding assay

MDC1 construct (2 μg) was translated *in vitro* for 90 min at 30 °C by using the TNT-coupled reticulocyte lysate system (Promega) containing 20 μCi of ^{35}S-labelled methionine (Amersham Biosciences). Half of each reaction was added to a volume of NETN lysis buffer containing 1% NP40. Coupled H2AX peptide (20 μg) was added and incubated for 1 h at 4 °C. The beads were washed thoroughly with NETN and the bound proteins analysed by western blotting.

Colony-forming assay

U2OS cells transfected with siRNA were seeded at low density and irradiated with various doses of ionizing or UV radiation. Cells were left for 14 days at 37 °C to allow colonies to form. Colonies were stained with 2% methylene blue/50% ethanol and counted. Colonies were defined as containing 50 or more cells.

Radio-resistant DNA synthesis assay

The RDS assay was done as described as before. Briefly, cells were transfected with siRNA oligonucleotides, and 4 h later were placed into McCoy's 5A medium containing 10 nCi of ^{14}C-labelled thymidine (NEN Life Science Products Inc.) per millilitre overnight. The medium containing ^{14}C-labelled thymidine was then replaced with normal McCoy's 5A medium, and the cells were incubated for another 24 h. Cells were irradiated, incubated for 30 min at 37 °C, and then pulse-labelled with 2.5 μCi [3H]thymidine (NEN Life Science Products Inc.) per millilitre for 15 min. Cells were harvested, washed twice with PBS, and fixed in 70% methanol for 30 min. After the cells were transferred to Whatman filters and fixed sequentially with 70% and then 90% methanol, the filters were air-dried and the amount of radioactivity was assayed in a liquid scintillation counter. The resulting ratios of ^{3}H counts per minute to ^{14}C counts per minute, corrected for those counts per minute that were the result of channel crossover, were a measure of DNA synthesis.

Immunofluorescence

Cells were fixed with 3% paraformaldehyde/2% sucrose for 10 min, permeablized with 0.5% Triton X-100 solution, and then immunostained with primary antibodies against various proteins and the appropriate Alexa488- (green, Molecular Probes) and Cy3- (red) conjugated secondary antibodies (Amersham Biosciences). Images were taken with a Zeiss confocal microscope.

Received 12 December 2002; accepted 24 January 2003; doi:10.1038/nature01446.

1. Zhou, B. B. & Elledge, S. J. The DNA damage response: putting checkpoints in perspective. *Nature* **408,** 433–439 (2000).
2. Bassing, C. H. *et al.* Increased ionizing radiation sensitivity and genomic instability in the absence of histone H2AX. *Proc. Natl Acad. Sci. USA* **99,** 8173–8178 (2002).
3. Celeste, A. *et al.* Genomic instability in mice lacking histone H2AX. *Science* **296,** 922–927 (2002).
4. Fernandez-Capetillo, O. *et al.* DNA damage-induced G(2)-M checkpoint activation by histone H2AX and 53BP1. *Nature Cell Biol.* **4,** 993–997 (2002).
5. Vialard, J. E., Gilbert, C. S., Green, C. M. & Lowndes, N. F. The budding yeast Rad9 checkpoint protein is subjected to Mec1/Tel1-dependent hyperphosphorylation and interacts with Rad53 after DNA damage. *EMBO J.* **17,** 5679–5688 (1998).
6. Gilbert, C. S., Green, C. M. & Lowndes, N. F. Budding yeast Rad9 is an ATP-dependent Rad53 activating machine. *Mol. Cell.* **8,** 129–136 (2001).
7. Soulier, J. & Lowndes, N. F. The BRCT domain of the S. cerevisiae checkpoint protein Rad9 mediates a Rad9-Rad9 interaction after DNA damage. *Curr. Biol.* **9,** 551–554 (1999).
8. Schultz, L. B., Chehab, N. H., Malikzay, A. & Halazonetis, T. D. p53 binding protein 1 (53BP1) is an early participant in the cellular response to DNA double-strand breaks. *J. Cell Biol.* **151,** 1381–1390 (2000).
9. Venkitaraman, A. R. Functions of BRCA1 and BRCA2 in the biological response to DNA damage. *J. Cell Sci.* **114,** 3591–3598 (2001).
10. Wang, B., Matsuoka, S., Carpenter, P. & Elledge, S. J. 53BP1, a mediator of the DNA damage checkpoint. *Science* **298,** 1435–1438 (2002).
11. Yamane, K., Wu, X. & Chen, J. A DNA damage-regulated BRCT-containing protein, TopBP1, is required for cell survival. *Mol. Cell. Biol.* **22,** 555–566 (2002).
12. Callebaut, I. & Mornon, J. P. From BRCA1 to RAP1: a widespread BRCT module closely associated with DNA repair. *FEBS Lett.* **400,** 25–30 (1997).
13. Ozaki, T. *et al.* NFBD1/KIAA0170 is a novel nuclear transcriptional transactivator with BRCT domain. *DNA Cell Biol.* **19,** 475–485 (2000).
14. Huang, M. & Elledge, S. J. in *Cold Spring Harbor Symposia on Quantitative Biology* Vol. LXV, 1–9 (Cold Spring Harbor Laboratory Press, New York, 2000).
15. Durocher, D. & Jackson, S. P. The FHA domain. *FEBS Lett.* **513,** 58–66 (2002).
16. Matsuoka, S., Huang, M. & Elledge, S. J. Linkage of ATM to cell cycle regulation by the Chk2 protein kinase. *Science* **282,** 1893–1897 (1998).
17. Cortez, D., Wang, Y., Qin, J. & Elledge, S. J. Requirement of ATM-dependent phosphorylation of brca1 in the DNA damage response to double-strand breaks. *Science* **286,** 1162–1166 (1999).
18. Matsuoka, S. *et al.* Ataxia telangiectasia-mutated phosphorylates Chk2 in vivo and in vitro. *Proc. Natl Acad. Sci. USA* **97,** 10389–10394 (2000).
19. Tibbetts, R. S. *et al.* Functional interactions between BRCA1 and the checkpoint kinase ATR during genotoxic stress. *Genes Dev.* **14,** 2989–3002 (2000).
20. Paull, T. T. *et al.* A critical role for histone H2AX in recruitment of repair factors to nuclear foci after DNA damage. *Curr. Biol.* **10,** 886–895 (2000).
21. Wang, Y. *et al.* BASC, a super complex of BRCA1-associated proteins involved in the recognition and repair of aberrant DNA structures. *Genes Dev.* **14,** 927–939 (2000).
22. Rogakou, E. P., Boon, C., Redon, C. & Bonner, W. M. Megabase chromatin domains involved in DNA double-strand breaks in vivo. *J. Cell Biol.* **146,** 905–916 (1999).
23. Rappold, I., Iwabuchi, K., Date, T. & Chen, J. Tumor suppressor p53 binding protein 1 (53BP1) is involved in DNA damage-signaling pathways. *J. Cell Biol.* **153,** 613–620 (2001).
24. Takai, H. *et al.* Aberrant cell cycle checkpoint function and early embryonic death in Chk1$^{-/-}$ mice. *Genes Dev.* **14,** 1439–1447 (2000).
25. Liu, Q. *et al.* Chk1 is an essential kinase that is regulated by Atr and required for the G_2/M DNA damage checkpoint. *Genes Dev.* **14,** 1448–1459 (2001).
26. Kim, S. T., Xu, B. & Kastan, M. B. Involvement of the cohesin protein, Smc1, in Atm-dependent and independent responses to DNA damage. *Genes Dev.* **16,** 560–570 (2002).
27. Yazdi, P. T. *et al.* SMC1 is a downstream effector in the ATM/NBS1 branch of the human S-phase checkpoint. *Genes Dev.* **16,** 571–582 (2002).
28. Zhao, H., Watkins, J. L. & Piwnica-Worms, H. Disruption of the checkpoint kinase 1/cell division cycle 25A pathway abrogates ionizing radiation-induced S and G2 checkpoints. *Proc. Natl Acad. Sci. USA* **99,** 14795–14800 (2002).

Supplementary Information accompanies the paper on *Nature*'s website (**http://www.nature.com/nature**).

Acknowledgements We thank A. Nussenzweig for the gift of the H2AX null MEFS and the corresponding wild-type MEFs. We thank P. Cooper, J. Chen and S. Jackson for sharing unpublished information and helpful discussions. We thank D. Lou for excellent technical assistance and N. Foray for technical advice. This work was supported by a National Institutes of Health Grant to S.J.E. B.W. is a fellow of the US Army Breast Cancer Postdoctoral Trainee Award, and S.J.E. is supported by a grant from the NIH, is an Investigator with the Howard Hughes Medical Institute and is a Senior Scholar of the Ellison Foundation. C.R.B. is supported by the Leukemia Research Fund. G.S.S. is supported by the European Molecular Biology Organization (EMBO).

Competing interests statement The authors declare that they have no competing financial interests.

Correspondence and requests for materials should be addressed to S.J.E. (e-mail: selledge@bcm.tmc.edu).

THE JOURNAL OF BIOLOGICAL CHEMISTRY
Vol. 278, No. 17, Issue of April 25, pp. 14971–14977, 2003

Printed in U.S.A.

Role for the BRCA1 C-terminal Repeats (BRCT) Protein 53BP1 in Maintaining Genomic Stability*

Received for publication, December 9, 2002, and in revised form, January 24, 2003
Published, JBC Papers in Press, February 10, 2003, DOI 10.1074/jbc.M212484200

Julio C. Morales‡, Zhenfang Xia‡, Tao Lu§, Melissa B. Aldrich‡, Bin Wang¶‖, Corina Rosales‡, Rodney E. Kellems‡, Walter N. Hittelman§, Stephen J. Elledge¶‡‡§§¶¶, and Phillip B. Carpenter‡‖‖**

From the ‡Department of Biochemistry and Molecular Biology, University of Texas Health Sciences Center, Houston, Texas 77030, the §Department of Experimental Therapeutics, University of Texas M. D. Anderson Cancer Center, Houston Texas 77030, and the ¶Verna and Mars McLean Department of Biochemistry and Molecular Biology, ‡‡Department of Molecular and Human Genetics, and §§Howard Hughes Medical Institute, Baylor College of Medicine, Houston, Texas 77030

p53-binding protein-1 (53BP1) is phosphorylated in response to DNA damage and rapidly relocalizes to presumptive sites of DNA damage along with Mre11 and the phosphorylated histone 2A variant, γ-H2AX. 53BP1 associates with the BRCA1 tumor suppressor, and knockdown experiments with small interfering RNA have revealed a role for the protein in the checkpoint response to DNA damage. By generating mice defective in *m53BP1* (*m53BP1*$^{tr/tr}$), we have created an animal model to further explore its biochemical and genetic roles *in vivo*. We find that *m53BP1*$^{tr/tr}$ animals are growth-retarded and show various immune deficiencies including a specific reduction in thymus size and T cell count. Consistent with a role in responding to DNA damage, we find that *m53BP1*$^{tr/tr}$ mice are sensitive to ionizing radiation (γ-IR), and cells from these animals exhibit chromosomal abnormalities consistent with defects in DNA repair. Thus, 53BP1 is a critical element in the DNA damage response and plays an integral role in maintaining genomic stability.

DNA damage-response mechanisms ensure the fidelity of chromosomal transmission, and their failure may lead to the development of diseases such as cancer (1). In response to γ-IR,[1] phosphoinositide-like kinases (PIKs) such as ATM (mutated in ataxia-telangiectasia) transduce damage signals to kinases, transcription factors, and DNA repair proteins by targeting (S/T)Q motifs (2). A second PIK, ATR (ATM- and Rad3-related), also responds to γ-IR, but it appears to respond primarily to agents that create replicational stress (*i.e.* hydroxyurea and aphidicolin) (2). ATM and ATR have distinct but overlapping substrate specificities including the ability of both enzymes to target p53 serine residue 15 (Ser-15) as well as the product of breast cancer susceptibility gene 1, BRCA1, at Ser-1423 (3, 4). BRCA1 is a major target of the DNA damage response, and mutations in *BRCA1* contribute to nearly 50% of familial forms of breast and ovarian cancer (5). BRCA1 had been found associated with RNA polymerase II (6), chromatin-remodeling factors (7), and a variety of DNA repair and replication factors (8–10). Indeed, BRCA1 has been shown to function in genomic stability by controlling homologous recombination, transcription-coupled repair of oxidative DNA damage, and cell cycle checkpoints (11–14).

One protein that contains numerous (S/T)Q motifs and two C-terminal BRCT repeats is p53-binding protein 1 (53BP1). 53BP1 was discovered as a p53-interacting factor in a two-hybrid screen (15) and was subsequently proposed to function as a transcriptional co-activator of p53 (16). Although the relationship between 53BP1 and p53 has not been fully established, 53BP1 and p53 from both *Xenopus* and humans have been shown to interact either directly or indirectly in experimental settings that express high levels of 53BP1 protein from plasmids or that naturally occur in eggs (15, 17). We, as well as others, have demonstrated previously that 53BP1 is involved in the DNA damage-response network (17–20). 53BP1 proteins are phosphorylated in response to γ-IR, and this is likely governed by the action of PIKs like ATM (17, 19, 20). γ-IR also induces 53BP1 to rapidly relocalize to DNA repair foci, and this response is delayed or inhibited by treatment with the PIK inhibitors caffeine and wortmannin. 53BP1 foci also overlap with those formed by the Mre11 complex, BRCA1, and the phosphorylated form of the histone variant H2AX (γ-H2AX; see Refs. 18–20). As both the Mre11 complex and γ-H2AX are believed to localize to physical sites of DNA damage (21–23) and to recruit various DNA repair factors to these sites, 53BP1 has been inferred to localize to these sites as well. This notion is further supported by the fact that γ-H2AX recruits 53BP1 to nuclear foci and physically interacts with 53BP1 (20, 24). Recent studies have revealed a role for 53BP1 in cell cycle checkpoints (25–27) as well as in maintaining p53 levels in response to γ-IR (27). Here we show that a 380-amino-acid region of 53BP1 that includes a recently described kinetochore-binding domain (28) is necessary for the formation of irradiation-in-

* This work was supported by grants from The Robert A. Welch Foundation (to P. B. C.) and The Ellison Medical Foundation (to P. B. C.) as well as National Institute of Health Grants GM65812-01 (to P. B. C.), DK46207 (to R. E. K.), and 5P30 CA16672 (to W. N. H.). The costs of publication of this article were defrayed in part by the payment of page charges. This article must therefore be hereby marked "*advertisement*" in accordance with 18 U.S.C. Section 1734 solely to indicate this fact.

‖ A fellow of the U. S. Army Breast Cancer Postdoctoral Trainee Award.

** A Sophie Caroline Steves Distinguished Professor in Cancer Research.

¶¶ An investigator with the Howard Hughes Medical Institute, an Ellison Medical Foundation Senior Scholar, and the Welch Professor of Biochemistry.

‖‖ An Ellison Medical Foundation Junior Scholar who is grateful for their support. To whom correspondence should be addressed. Fax: 713-500-0652; E-mail: Phillip.B.Carpenter@uth.tmc.edu.

[1] The abbreviations used are: γ-IR, ionizing radiation; PIK, phosphatidyl inositol-like kinase; BRCT, BRCA1 C-terminal repeats; MEF, murine embryonic fibroblast; ATM, mutated in ataxia-telangiectasia; ATR, ATM- and Rad3-related; RT, reverse transcription; HA, hemagglutinin; IP, immunoprecipitation; WB, Western blotting; DN, double negative.

duced foci. We further deciphered the role of 53BP1 in the DNA damage response by generating mice defective in *m53BP1*. We report that murine animals expressing a truncated form of *m53BP1* (*m53BP1*$^{tr/tr}$) exhibit a pleiotropic phenotype that includes growth retardation, immune deficiencies including defects in T cell maturation, sensitivity to γ-IR, as well as increased chromosomal aberrations. Taken together, these results reveal that 53BP1 is an integral component of the DNA damage-response network and indicate that the protein plays an important role in maintaining genomic stability.

EXPERIMENTAL PROCEDURES

Antibodies and Indirect Immunofluorescence—Three antibodies that recognize both the human and murine 53BP1 proteins were generated for this study. We found that our 53BP1 antibodies recognize both the murine and human proteins. Polyclonal antibodies raised against glutathione *S*-transferase fusion proteins encoding the first 524 amino acids of human 53BP1 (α53BP1) or the last 200 residues of the protein (α53BP1-C) were affinity-purified by established procedures and used as described in the text. α53BP1-N is a polyclonal, anti-peptide antibody that was raised against an N-terminal sequence GVLELSQSQDVEE that is conserved between human and murine 53BP1 proteins. Polyclonal antibodies were affinity-purified by standard methods. Anti-HA antibodies were purchased from Covance, and anti-ATR antibodies were obtained from Oncogene Research Products.

Mouse Genetics and Genotyping of m53BP1$^{tr/tr}$ Animals—Murine animals defective in *m53BP1* (*m53BP1*$^{tr/tr}$) were generated with a random retrovirus as described previously (29). Genomic DNA was isolated from mouse tail snips by standard methods. Insertion of VICTR54 introduces new *Xba*I sites into the intron preceding exon 14 of the wild-type allele. Therefore, a disrupted *m53BP1* allele will be broken into multiple *Xba*I fragments including a 5′-proximal, 1.5-kb fragment. To detect this fragment, we PCR-amplified and labeled with ^{32}P a probe downstream of the 5′ naturally occurring *Xba*I site but upstream of the one introduced by VICTR54, as shown in Fig. 2*A*. The primers used to amplify the 700-base pair probe for Southern analysis were 5′-CTCAGCATCCATGCTGGGC-3′ and 5′-TACTTAATGAGGCTAGAGCACAGC-3′. The sequences of the primers used for RT-PCR analysis were as follows: A, 5′-CCTCAGGCAGAGTGAACA-3′; B, 5′-CTCTGTGTCGTCCACGGGAGCACT-3′; C, 5′-GTGGCGATGCAAGACATGGCCA-3′; D, 5′-GCCAAGAACAGATGGAACAGCTGA-3′. Either poly(A)$^+$ or total RNA was isolated by standard methods and used to prepare cDNA with the Superscript one-step PCR system (Invitrogen).

Immune System Analysis—Bone marrow, thymus, and spleen tissue were analyzed in 8-week-old male and female mice. Bone marrow was flushed with Hank's balanced salt solution (Invitrogen) from two femurs per animal. Cells were counted in 3.0% acetic acid with a hemocytomter. Bone marrow cells were stained in Hank's balanced salt solution/2.0% fetal bovine serum, with Fc block, CD11b (Mac-1), Gr-1, ter119, CD19, anti-IgM, CD45R/B220, and CD43 (all from Pharmingen). Flow cytometric analysis was performed on a BD Biosciences FACScan, with CellQuest software, and appropriate negative isotype control antibodies (Pharmingen) were used in all analyses. Spleens and thymuses were excised and gently crushed through 100-μm cell strainers (Falcon) in Hank's balanced salt solution/fetal bovine serum. Red blood cells were lysed with ACK buffer (0.15 M NH_4Cl, 1.0 mM $KHCO_3$, 0.1 mM EDTA, pH 7.2) (5 ml/spleen or thymus, 5 min at room temperature). After centrifugation and washing with phosphate-buffered saline/2.0% fetal bovine serum, the cells were counted as above and stained for flow cytometric analysis. Thymic cells were stained with CD4, CD8, CD25, CD44, and CD3 (Pharmingen). Flow cytometry was performed as above.

Chromosome Aberration Studies—Exponentially growing passage 2 MEFs were irradiated at room temperature with 0, 0.5, or 1.5 Gy of γ-IR using a Nasatron irradiator, returned to 37 °C for 30 min to allow cells irradiated in mitosis to exit, and then incubated with 1 μg/ml colcemid for 2 h prior to cell harvest, hypotonic (0.075 M KCl) fixation (3:1 methanol:glacial acetic acid), and metaphase spread preparation. Dried slide preparations were stained with Giemsa and examined for the presence of chromatid gaps, breaks, and exchanges by light microscopy. Between 50 and 100 metaphases were scored for each treatment.

RESULTS AND DISCUSSION

Dynamic Nuclear Localization of 53BP1 in the Absence and Presence of DNA Damage—It has been recently shown that 53BP1 localizes to the kinetochore during mitosis (28). However, the behavior of 53BP1 during interphase in the absence of extrinsic DNA damage has not been fully investigated. To examine the interphase behavior of 53BP1 during the course of normal, unperturbed MCF-7 cell cycles, we used a laser scanning cytometer to determine the nuclear localization of 53BP1 and the cellular DNA content for any given cell. In G_1, 53BP1 exists in a diffuse nuclear pattern as well as in large nuclear "dots" (Fig. 1*A*). In S-phase, 53BP1 can be found in a discrete, punctate pattern (Fig. 1*A*). The nuclear distribution pattern of 53BP1 in G_2 cells appeared in two types, one similar to S-phase but with fewer foci (Fig. 1*A*) and one that exhibited few, if any, large dots (not shown). It is well established that 53BP1 relocalizes to nuclear foci in response to DNA damage (17–20). We found that 53BP1 and ATR co-localized to nuclear foci in response to hydroxyurea (Fig. 1*B*). We also found that 53BP1 physically associates with ATR in nuclear extracts derived from K562 cells (Fig. 1*C*). 53BP1 can be detected in ATR immunoprecipitates and ATR is present in 53BP1 immunoprecipitates, and the association occurs independently of DNA damage (Fig. 1*C*). Moreover, ATR phosphorylates 53BP1 *in vitro* (not shown). Thus, 53BP1 interacts with various factors implicated in genomic stability including ATR, p53, H2AX, BRCA1, and Chk2. To address which structural elements of 53BP1 are required for the formation of irradiation-induced foci, we created a series of mutant constructs in the 53BP1-expression vector pCMH6K53BP1 (16). We generated mutant forms of 53BP1 that deleted the C-terminal BRCT motifs (ΔBRCT), the kinetochore-binding region (ΔKINET), the N-terminal 1,234 residues except for the initiation codon (ΔNH3), and a protein mutated at 15 potential phosphorylation sites (15AQ), some of which are known to be targeted during the DNA damage response.[2] All constructs maintained the nuclear localization signal. Transient tranfections with these various constructs into MCF-7 cells revealed that the mutant proteins were being expressed (not shown). We confirmed that the wild-type, HA-tagged version of 53BP1 encoded by pCMH6K53BP1 generated nuclear foci in response to DNA damage when immunostained with an antibody specific for the HA tag (Fig. 1*D*). Untransfected cells were found to stain negative with anti-HA antibodies (not shown). Our results indicate that the majority of 53BP1 appears dispensable for DNA damage-inducible focus formation, including the N-terminal 1,234 residues (which includes numerous (S/T)Q motifs) as well as the C-terminal BRCT motifs (Fig. 1*D*). Surprisingly, ΔKINET, a 380-amino-acid deletion (residues 1,236–1,615) that removes the kinetochore binding region (28) of 53BP1, failed to form irradiation-induced foci as the protein persisted in a diffuse nuclear pattern after irradiation (Fig. 1*D*).

Generation of Mice Defective in m53BP1 (m53BP1$^{tr/tr}$)—To begin to decipher the functional role for 53BP1 in the DNA damage response, we identified embryonic stem cells (OST94324) from Omnibank (29) containing a single, ~5.0-kb retroviral insertion (VICTR54; Fig. 2*A*) in murine 53BP1 (m53BP1; 1,957 amino acids; 80% identity to human 53BP1; see Ref. 28). VICTR54 was found inserted within a 4.9-kb intron located between exons 13 and 14 (Fig. 2*A*). VICTR54, and its related vectors, are usually found within introns and contain splice acceptor (*SA*) and donor (*SD*) sequences such that a neomycin (*NEO*) resistance gene and flanking sequences are spliced into the mature transcript as an exon (Fig. 2*A*) (29). These transcriptional fusions disrupt the coding sequence through the introduction of premature stop codons. Such gene trapping methodologies have been applied previously to understanding gene function (29). OST94324 cells were used to gen-

[2] Z. Xia, J. C. Morales, and P. B. Carpenter, unpublished data.

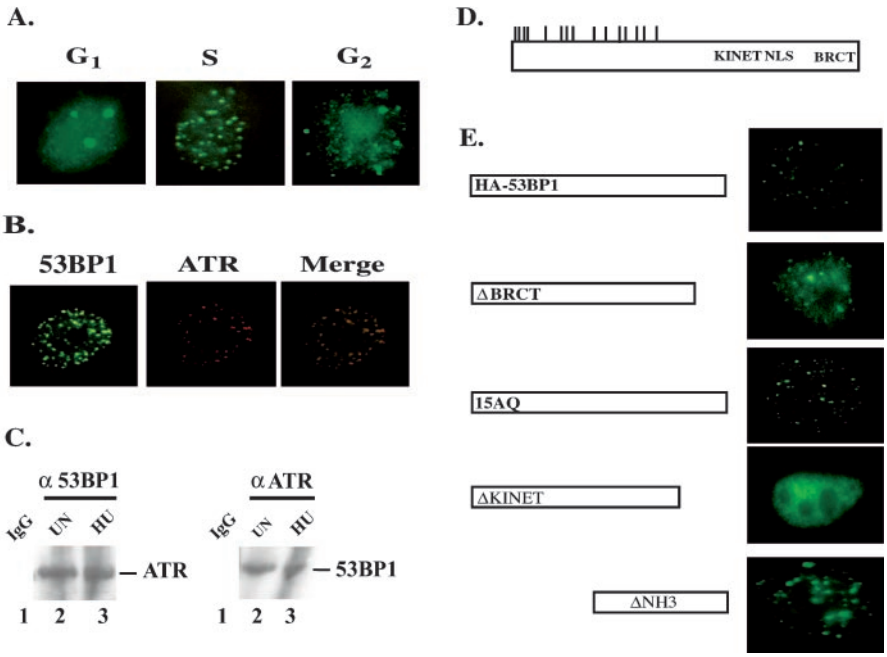

FIG. 1. **Dynamic nuclear localization of human 53BP1 during interphase, association with ATR, and structural requirements for DNA damage inducible focus formation.** As shown in *A*, immunofluorescence analysis with an antibody specific for 53BP1 (α53BP1; see "Experimental Procedures") reveals the nuclear staining pattern for cells unambiguously assigned to the G_1-phase (*left*), S-phase (*middle*), and G_2-phase (*right*) of the cell cycle as determined by DNA content with a lasing scanning cytometer. Black and white images were captured with a ×100 objective on a Zeiss Axiophot and pseudocolored in Adobe PhotoShop. As shown in *B*, ATR and 53BP1 co-localize to nuclear foci in response to hydroxyurea (2.0 mM). *Left panel*, immunostaining for 53BP1. *Middle*, immunostaining with an antibody specific for ATR (see "Experimental Procedures"). *Right*, merged images to show co-localization between 53BP1 and ATR. As shown in *C*, ATR and 53BP1 physically interact before and after DNA damage. K562 cells were grown and either left untreated (*lanes 1* and *2*) or treated with 2.0 mM hydroxyurea (*HU*; *lane 3*) for 18 h prior to the preparation of nuclear extracts for immunoprecipitation with an antibody against 53BP1 (*left panel*) or ATR (*right panel*). Immunoblotting was then performed with the reciprocal antibodies as shown. *D*, schematic representation of primary structure of 53BP1 (not drawn to scale). *Hatched lines* represent locations of (S/T)Q sites mutated in 15AQ. *KINET*, kinetochore-binding region (28); *NLS*, nuclear localization signal (28). *E*, identification of a region of 53BP1 required for irradiation-induced focus formation. Wild-type, HA-tagged 53BP1 and various mutant derivatives were transfected into MCF7 cells and treated with 10 Gy of ionizing radiation prior to fixation and immunostaining with an antibody specific for the HA tag (Covance). The following constructs expressing in-frame 53BP1 deletions or mutations were made: ΔBRCT (deletes amino acid residues 1,786–1,964), ΔKINET (deletes amino acid residues 1,236–1,615), ΔNH3 (deletes the first 1,234 amino acids residues except for the initiation codon), and 15AQ, a construct with mutations in 15 (S/T)Q sites. The following serine or threonine residues were mutated to alanines in 15AQ: Ser-6, Ser-13, Ser-25, Ser-29, Ser-105, Ser-166, Ser-176, Ser-178, Thr-302, Ser-452, Ser-523, Ser-543, Ser-625, Ser-784, Ser-892. All constructs were verified by DNA sequencing and expressed in either 293T or MCF7 cells (not shown).

erate transgenic animals heterozygous in *m53BP1* (m53BP1+/tr) as described previously (29). Southern blotting with DNA isolated from tail biopsies confirmed the disruption in m53BP1 and was used to genotype the animals (Fig. 2*B*; see "Experimental Procedures"). Crosses between heterozygous animals produced *m53BP1*$^{tr/tr}$ progeny born at the expected frequencies. The *m53BP1*$^{tr/tr}$ animals were found to be fertile, but we did observe that crosses between mutant animals produced smaller litters as some embryos spontaneously aborted and were reabsorbed by the mother (data not shown). RT-PCR analysis with various primers 5′ and 3′ to the insertion demonstrated that exon 13 failed to properly splice next to exon 14 in the *m53BP1*$^{tr/tr}$ mice (Fig. 2*C*). Rather, the "artificial" exon containing neomycin from VICTR54 was spliced adjacent to exon 13 as verified with primers specific for exon 13 and the neomycin gene (primer set D/A; Fig. 2*C*). Sequencing of a cloned RT-PCR product spanning the insertion event revealed that the natural coding sequence of m53BP1 had stopped after residue 1,205, where it then fused to 21 residues derived from VICTR54 before terminating (Fig. 2*D*). Therefore the disrupted allele of *m53BP1* encodes a truncated 1,226 residue protein (m53BP1^{tr}), and notably, m53BP1^{tr} is missing over 700 residues including its functional nuclear localization signal, kinetochore binding domain (KINET), and two BRCT motifs (Fig. 2*D*). To determine whether m53BP1^{tr} was expressed, we performed immunoprecipitation/Western blotting (IP/WB) analysis from brain extracts derived from *m53BP1*$^{+/+}$, *m53BP1*$^{+/tr}$, and *m53BP*$^{tr/tr}$ animals. By using antibodies specific for the N and C termini of 53BP1 (α53BP1-N and α53BP1-C, respectively; see "Experimental Procedures"), we determined that a truncated m53BP1 protein corresponding to m53BP1^{tr} appeared in heterozygous and mutant extracts but not in wild-type ones (Fig. 2*E*). The levels of m53BP1^{tr} appeared much lower than the full-length protein and, in some cases, we observed an apparent isoform of m53BP1 in wild-type and heterozygous animals (Fig. 2*E*). The disappearance of full-length m53BP1 in the mutant samples was accompanied by the appearance of a smaller protein corresponding to m53BP1^{tr} (Fig. 2*E*). We observed that α53BP1-N cross-reacted with m53BP1^{tr} but not with α53BP1-C, demonstrating that m53BP1 is indeed truncated in *m53BP1*$^{tr/tr}$ animals (Fig. 2, *E* and *F*).

Immune Deficiencies in m53BP1$^{tr/tr}$ *Mice*—We observed that *m53BP1*$^{tr/tr}$ animals were growth-retarded as the males and females were found on average to weigh 25 and 15% less, respectively, than their wild-type littermates (Fig. 3*A*). We found that thymuses derived from *m53BP1*$^{tr/tr}$ animals were significantly smaller and possessed fewer cells than those from *m53BP1*$^{+/+}$ animals (Fig. 3*B*). This suggests that defects in *m53BP1* may contribute to immune deficiencies, a result that has been observed for various DNA damage-response factors, including H2AX (24). We found that the lymphoid organ architecture of thymuses, as assayed by hematoxylin and eosin staining of tissue sections, appeared normal in *m53BP1*$^{tr/tr}$ mice (data not shown). In addition, flow cytometric analysis

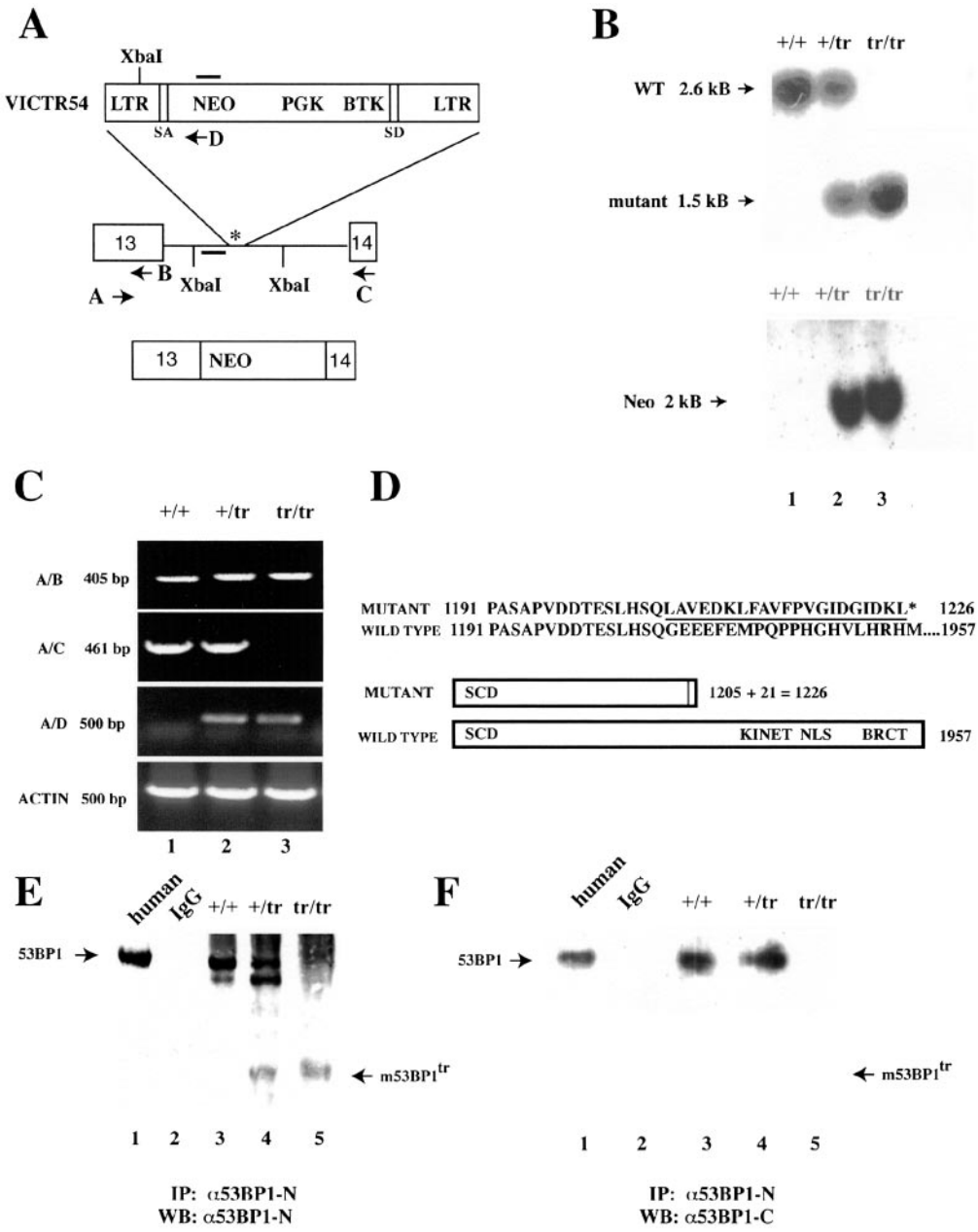

FIG. 2. **Generation and characterization of mice defective in *m53BP1* (*m53BP1*$^{tr/tr}$).** *A*, schematic diagram of insertion event in *m53BP1* (not drawn to scale). The *thick horizontal lines* represent positions of probes for Southern blotting as described in *B*. *Arrows* represent the position and orientation of PCR primers used in *C*. The insertion of VICTR54 was determined by DNA sequencing to reside within the intron preceding exon 14 at nucleotide position 1,730 (marked by *). Splicing of the neomycin gene and flanking DNA produces a transcript that potentially disrupts the proper splicing of exons 13 and 14. *LTR*, long-terminal repeat; *NEO*, neomycin resistance gene; *PGK*, phosphoglycerate kinase-1; *BTK*, Bruton's tyrosine kinase; *SA* and *SD*, splice acceptor and donor, respectively. *B*, *top*, Southern blotting to determine the genotype of *m53BP1*-defective animals. 10 μg of genomic DNA was digested with *Xba*I and was probed with a radiolabeled fragment (see "Experimental Procedures") capable of discerning wild-type (*WT*) and mutant alleles as discussed under "Experimental Procedures." *Bottom*, a 700-bp probe derived from the neomycin gene was used to help genotype the animals. +/+, wild type; +/*tr*, heterozygous; *tr/tr*, homozygous. As shown in *C*, RT-PCR analysis indicates that improper splicing occurs between exons 13 and 14 in *m53BP1*$^{tr/tr}$ mice. Positions and orientation of primers for PCR are indicated in *A*. Control reactions without reverse transcriptase showed essentially no amplified products (not shown). As shown in *D*, *m53BP1*$^{tr/tr}$ encodes a truncated protein of 1,226 amino acids. RT-PCR products derived from primer set A/D (as shown in *C*) using RNA isolated from *m53BP1*$^{tr/tr}$ animals as template were cloned into the TA vector (Invitrogen). DNA sequencing and conceptual translation indicated that *m53BP1*$^{tr/tr}$ animals potentially encode a truncated m53BP1 protein (m53BP1^{tr}) of 1,205 natural residues along with an additional 21 residues derived from the VICTR54 vector. m53BP1^{tr} is missing over 700 C-terminal residues, including those that specify the kinetochore binding domain (*KINET*; amino acids 1,220–1,601), the nuclear localization signal (*NLS*; mapped to amino acids 1,601–1,703; ref), and the C-terminal BRCT repeats (amino acids, 1,665–1,957). The small, vertical rectangle in m53BP1^{tr} represents the additional vector-derived 21 residues. *E* and *F*, detection of m53BP1^{tr} protein by IP/WB analysis. 1.0 mg of total brain protein extracts derived from +/+, +/tr, and tr/tr animals was immunoprecipitated with 5 μg of affinity-purified antibody (α53BP1-N) raised against an N-terminal peptide sequence (see "Experimental Procedures") and split into two equal parts. One part (*E*) was blotted with α53BP1-N, and the other (*F*) was immunoblotted with an affinity-purified antibody specific for the C terminus (α53BP1-C). *E*, *lane 1*, IP from 100 μg of MCF-7 nuclear extract. *Lane 2*, IP with nonspecific IgG control. *Lanes 3–5*, IP with +/+, +/tr, and tr/tr animals as determined in *B*. IP/WB analysis shows the presence of m53BP1^{tr} in *m53BP1*$^{+/tr}$ and *m53BP1*$^{tr/tr}$ animals but not of *m53BP* $^{+/+}$ ones. In some cases, we observed an apparent isoform of m53BP1 in brain tissue, as designated by the *asterisk*. *F*, WB with α53BP1-C, an affinity-purified antibody against the C-terminal 200 residues of human 53BP1. As shown, α53BP1-C recognizes full-length m53BP1 but fails to immunoreact with m53BP1^{tr}, indicating that the protein is indeed missing C-terminal residues of m53BP1.

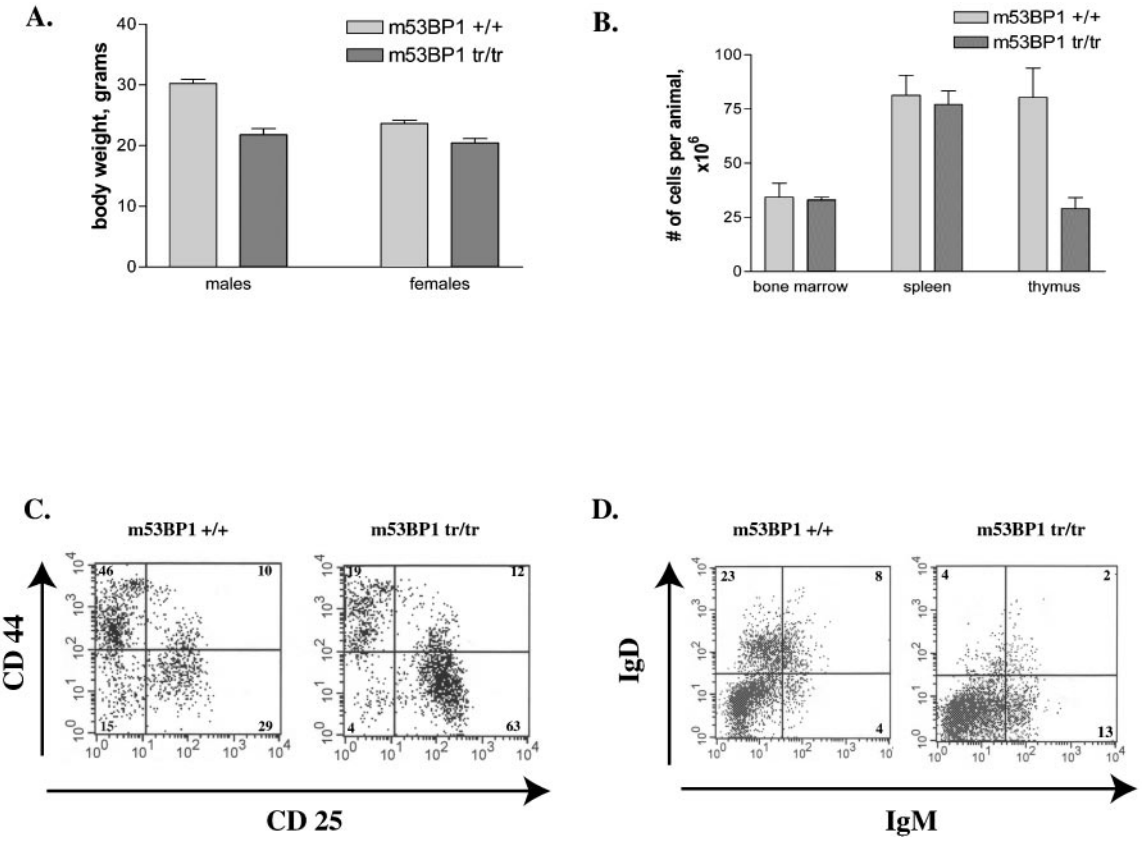

FIG. 3. **Growth retardation and immune deficiencies in mice defective in *m53BP1*.** *A*, mean body weight, in grams, of *m53BP1*$^{+/+}$ and *m53BP1*$^{tr/tr}$ mice. ($n = 10$). As shown in *B*, reduced thymus size in *m53BP1*$^{tr/tr}$ animals results in lower tissue cell count. Mean cell numbers are $\times 10^6$ (per mouse) of bone marrow (two femurs per mouse), spleens, and thymuses from *m53BP1*$^{+/+}$ and *m53BP1*$^{tr/tr}$ mice ($n = 4$). *C*, defective T cell development in *m53BP1*$^{tr/tr}$ mice as revealed by double-negative thymocyte populations. $CD4^+$ and $CD8^+$ cells were removed by gating, leaving DNI ($CD44^+CD25^-$), DNII ($CD44^+CD25^+$), DNIII ($CD44^-CD25^+$), and DNIV ($CD44^-CD25^-$) thymocytes. *Numbers* in the histogram quadrants are average percentages for four mutant or control animals. *D*, defective B cell development in *m53BP1*$^{tr/tr}$ animals. Immature ($IgM^{hi}IgD^{lo}$), transitional ($IgM^{hi}IgD^{hi}$), and mature ($IgD^{hi}IgM^{lo}$) B cells in *m53BP1*$^{+/+}$ and *m53BP1*$^{tr/tr}$ mouse spleens. *Numbers* in the histogram quadrants are average percentages for four mutant or control mice.

with a variety of markers (*e.g.* B220, CD43, Gr-1, CD11a, and Ter119) revealed that bone marrow pro-B, pre-B, myeloid, and erythroid progenitor populations were normal in *m53BP1*$^{tr/tr}$ mice (not shown). Although CD4 and CD8 T cell populations were proportionately similar in *m53BP1*$^{tr/tr}$ and *m53BP1*$^{+/+}$ thymuses, we observed that progression out of the DNIII stage of early thymocyte development was impaired in *m53BP1*$^{tr/tr}$ animals (Fig. 3*C*), the stage at which β-gene rearrangement occurs. This indicates that m53BP1 participates in proper T cell development, a process known to require various DNA repair factors (30). We also found that spleens derived from *m53BP1*$^{tr/tr}$ animals were similar in size and organ architecture to those from *m53BP1*$^{tr/tr}$ animals and that the lack of functional m53BP1 did not affect the proportions of B and T lymphocytes (data not shown). We did observe, however, that *m53BP1*$^{tr/tr}$ spleens were deficient in mature B cells ($IgM^{lo}IgD^{hi}$; Fig. 4*D*), suggesting that deficiencies in m53BP1 may also result in defective B lymphocyte development.

Genomic Instability in m53BP1$^{tr/tr}$ Mice—Mice with defects in double-stranded break repair are highly sensitive to γ-IR. To evaluate whether *m53BP1* contributes to increased sensitivity to DNA damage, we treated *m53BP1*$^{tr/tr}$ or wild-type animals with 7 Gy of γ-IR. After this whole body irradiation treatment, we found that 100% of the mutant animals died between 9 and 15 days post-irradiation in contrast to only 16% of the control littermates (Fig. 4*A*). This shows that animals defective in *m53BP1* are highly sensitive to γ-IR, a result that parallels previous observations with H2AX-deficient mice (24). Despite this, we found that *m53BP1*$^{tr/tr}$ animals treated with lower doses of γ-IR (1.5 Gy) remained viable (Fig. 4*B*). To further explore m53BP1 function, we generated embryonic fibroblasts (MEFs) from wild-type and *m53BP1*$^{tr/tr}$ animals. *m53BP1*$^{tr/tr}$ MEFs proliferated more slowly than their wild-type counterparts (Fig. 5*A*). Immunofluorescence analysis indicated that the truncated m53BP1 protein expressed in *m53BP1*$^{tr/tr}$ animals failed to form foci in response to DNA damage as it was essentially absent from the nucleus (data not shown). This result is consistent with our transfection studies, which have shown that C-terminal determinants (ΔKINET) are necessary for focus formation. The relative growth of the mutant and the wild-type MEFs was reminiscent of what has been recently described for H2AX (24). To further characterize cells defective in *m53BP1*, we examined the cytological consequences of impaired m53BP1 function in early passage MEFs derived from *m53BP1*$^{tr/tr}$ and *m53BP1*$^{+/+}$ animals. For this, exponentially growing MEFs (passage 2) were treated with 0, 0.5, or 1.5 Gy of γ-IR, and metaphase preparations were examined 2.5 h post-irradiation. Untreated MEFs derived from *m53BP1*$^{tr/tr}$ animals showed increased levels of chromatid gaps, breaks, and, to a lesser extent, exchanges when compared with those derived from *m53BP1*$^{+/+}$ mice, suggesting an intrinsic genomic stability defect in the mutant cells (Fig. 5, *B* and *C*). More strikingly, irradiated MEFs derived from *m53BP1*$^{tr/tr}$ animals showed an ~2-fold increase in levels of chromatid breaks and gaps when compared with MEFs derived from wild-type mice (Fig. 5, *B* and *C*). Although MEFS from *m53BP1*$^{tr/tr}$ animals showed relatively high chromatid exchange rates at 0.5 Gy when compared with those from *m53BP1*$^{+/+}$ animals, this difference was

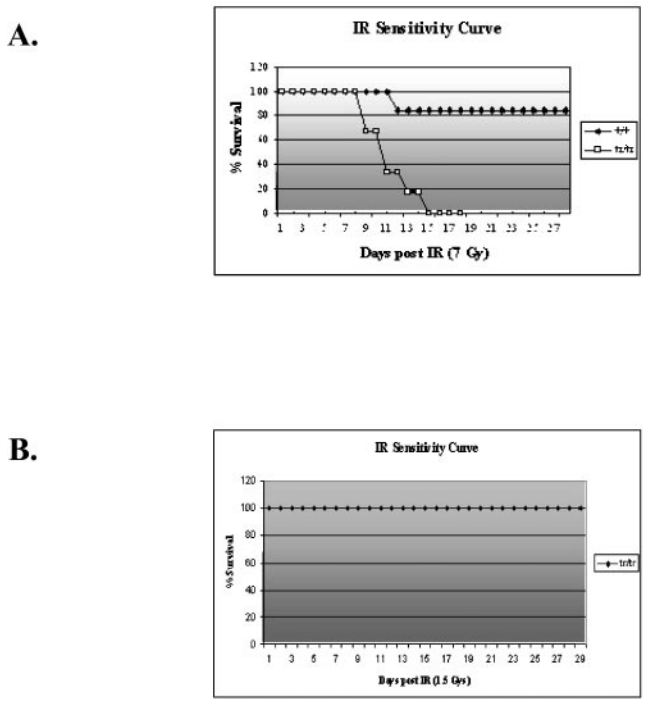

FIG. 4. **Characterization of animals and cells defective in *m53BP1*$^{tr/tr}$.** *A*, survival of 4–6-week-old *m53BP1*$^{tr/tr}$ and *m53BP1*$^{+/+}$ mice after exposure to 7 Gy of γ-IR. Six animals from each genotype were used in the experiment. *B*, survival of 4–6-week-old *m53BP1*$^{tr/tr}$ animals after exposure to 1.5 Gy of ionizing radiation.

less apparent at 1.5 Gy, perhaps due to the limited progression to mitosis of the most damaged cells from both populations during this time frame. One possible explanation for the increased frequencies of chromosomal aberrations observed in the *m53BP1*$^{tr/tr}$ MEFs following irradiation might be a deficiency in a G_2 checkpoint response whereby more damaged cells would still be permitted to enter mitosis and would be available for chromosome analysis. In fact, recent reports have implicated 53BP1 in the G_2/M checkpoint (25–27). To examine this in our MEFs, either *m53BP1*$^{tr/tr}$ or wild-type MEFs were treated with 0, 1.5, or 10 Gy of γ-IR, and cultures were analyzed for the fraction of cells showing phospho-histone H3 immunostaining (mitotic cells) either after 1 or 16 h post-irradiation (in the presence of colcemid). Although all cell types showed evidence of a partial G_2/M block following irradiation, MEFs derived from *m53BP1*$^{tr/tr}$ mice showed only a slight decrease, if any, in the G_2 block when compared with MEFs derived from wild-type mice (data not shown). The minimal effects on the G_2/M checkpoint observed in our *m53BP1*$^{tr/tr}$ MEFs may be due to the nature of the truncated protein produced from the *m53BP1*$^{tr/tr}$ allele that is expressed in our mutant animals described here.

53BP1 interacts with a variety of factors known to be involved in the maintenance of genomic stability including ATR, p53, H2AX, BRCA1, Chk2, and ATM (15, 20, 25, 27). The generation of murine animals defective in *m53BP1* provides a valuable tool to further understand the role of the protein in the DNA damage response. The *m53BP1*$^{tr/tr}$ allele expresses a truncated version of m53BP1, and this likely represents a

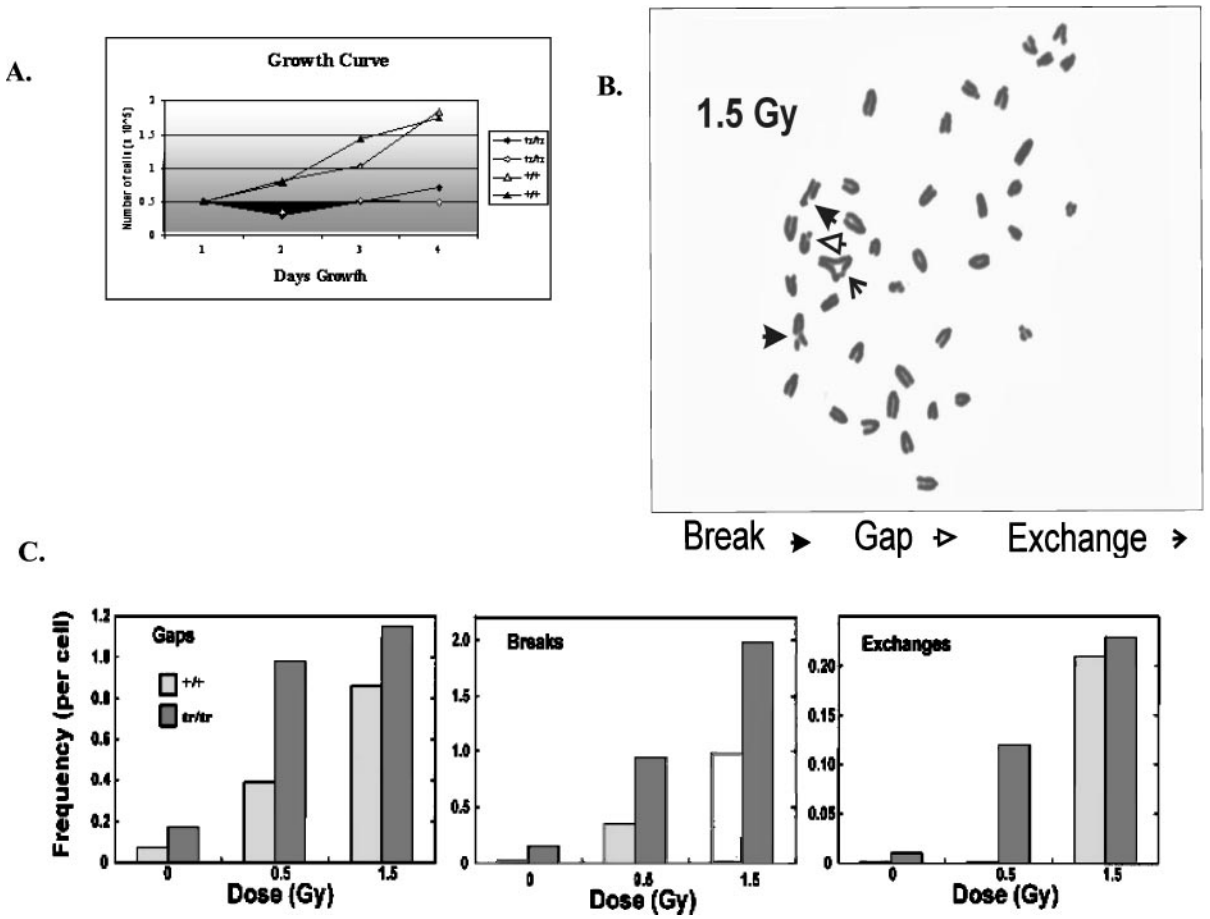

FIG. 5. **Chromosomal abnormalities in *m53BP1*$^{tr/tr}$ cells.** *A*, growth curve of MEFs derived from *m53BP1*$^{tr/tr}$ (*open diamonds*) and *m53BP1*$^{+/+}$ (*closed circles*). *B*, metaphase preparation of mutant MEF following 1.5 Gy of γ-IR. Note the presence of a chromatid gap, two chromatid breaks, and one chromatid exchange in the metaphase sample. *C*, relative frequencies of chromatid gaps, breaks, and exchanges in metaphases of wild-type and mutant MEFs following 0, 0.5, and 1.5 Gy of ionizing radiation.

significant impairment in some aspects of its function. *m53BP1*$^{tr/tr}$ is missing over 700 amino acids including the nuclear localization signal, the C-terminal BRCT motifs, and a kinetochore-binding domain. We have observed that this domain is also necessary for forming irradiation-induced nuclear foci. Indeed, the lack of detectable, irradiation-induced foci in mutant MEFs suggests that the protein cannot fully perform its functions as a DNA damage-response element. Moreover, the lethality observed for *m53BP1*$^{tr/tr}$ mice at higher doses of radiation (7 Gy) suggests that there are no other factors acting redundantly with m53BP1 with respect to this aspect of radiation resistance and indicates that m53BP1 is a critical element for double-stranded break repair. Therefore, the C-terminal 700 amino acids of m53BP1 encode important, functional determinants of the protein.

We observed that *m53BP1*$^{tr/tr}$ animals are growth-retarded as the males weigh, on average, 25% less than their wild-type littermates. The decreased thymus size, reduced T cell count, immature B cell population, and lack of progression out of DNIII for thymus T cells reveal that *m53BP1*$^{tr/tr}$ animals are immune-deficient. How m53BP1 contributes to this process remains to be established, but one possibility is that the protein participates in the maturation of T-cell receptors and immunoglobulins during V(D)J recombination, a process known to utilize DNA repair proteins (30). This is particularly interesting given the involvement of m53BP1 in double-stranded break repair as revealed by several factors including, most notably, the sensitivity of *m53BP1*$^{tr/tr}$ animals after exposure to 7 Gy of ionizing radiation. Indeed, sensitivity to ionizing radiation often correlates with impaired V(D)J joining (30). Moreover, H2AX defective-animals are also immune-deficient (24). As H2AX is required for the formation of 53BP1 foci and because it physically associates with 53BP1 (20), it is possible that an ordered pathway of assembly of DNA damage-response proteins at these programmed breaks may facilitate V(D)J recombination and maximize antibody diversity.

Our results show that genetic defects in *m53BP1* result in a pleiotropic phenotype consistent with defects in DNA repair and checkpoint control. The phenotype of 53BP1-defective animals is quite similar to H2AX-deficient ones, consistent with the notion that H2AX operates upstream of 53BP1 in a DNA damage-response pathway. When such pathways are defective, cells cannot properly repair damaged DNA, a situation that may lead to increased genomic instability and the development of diseases such as cancer. For example, given the immune deficiencies in *m53BP1*$^{tr/tr}$ mice, one may anticipate the generation of lymphomas. In light of this, we have not observed the development of any cancerous phenotypes in our *m53BP1*-defective mice. Although there are a variety of possible reasons for this (*i.e.* genetic background, allele, etc.), it is interesting to note that mice nullizygous for H2AX also apparently fail to generate cancers.[3] As H2AX and 53BP1 are not required for viability, it is possible that mutations in 53BP1, when combined with other mutations in critical DNA damage-response elements (*i.e.* H2AX, ATM, and p53) will lead to more severe defects in genomic stability, a process that may then lead to the development of cancer. The analysis of cells derived from these crosses is likely to provide more insight into how 53BP1 functions in the DNA damage response in concert with its various interacting partners.

[3] Dr. A. Nussenzweig, personal communication.

Acknowledgments—We thank Jian Kuang and Randy Legerski for help in setting up our makeshift laboratory at M. D. Anderson in the aftermath of Hurricane Allison. We thank Heladio Ibarguen for help with the metaphase spreads. We are grateful to David Cortez for providing useful suggestions during the course of the project. We are also indebted to Mike Blackburn, Rob Kirken, Jeff Frost, Hays Young, and Jose Molina for technical advice. We thank Jungie Chen for communicating results prior to publication.

REFERENCES

1. Zhou, B. S., and Elledge, S. J. *Nature* (2000) **408,** 433–439
2. Abraham, R. T. (2001) *Genes Dev.* **15,** 2177–2196
3. Cortez, D., Wang, Y., Qin, J., and Elledge, S. J. (1999) *Science* **286,** 1162–1166
4. Tibbetts, R. S., Mrumbaugh, K. M., Williams, J. M., Sarkaria, J. N., Cliby, W. A., Shieh, S.-Y., Taya, Y., Prives, C., and Abraham, R. T. (1999) *Genes Dev.* **13,** 152–157
5. Scully, R., and Livingston, D. (2000) *Nature* **408,** 429–432
6. Scully, R., Anderson, S. F., Chao, D., Wei, M., Ye, W., Young, R. A., Livingston, D. M., and Parvin, J. D. (1997a) *Proc. Natl. Acad. Sci. U. S. A.* **94,** 5605–5610
7. Bochar D. A., Wang L., Beniya H., Kinev A., Xue Y., Lane W. S., Wang W., Kashanchi F., and Shiekhattar R. (2000) *Cell* **102,** 257–265
8. Scully, R., Chen, J., Plug, A., Xiao, Y., Weaver, D., Feunteun, J., Ashley, T., and Livingston, D. M. (1997b) *Cell* **88,** 265–275
9. Chen, J., Silver, D. P., Walpita, D., Cantor, S. B., Gazdar, A. F., Tomlinson, G., Couch, F. J., Weber, B. L., Ashley, T., Livingston, D. M., and Scully, R. (1998) *Mol. Cell* **2,** 317–328
10. Wang, Y., Cortez, D., Yazdi, P., Neff, N., Elledge, S. J., and Qin, J. (2000) *Genes Dev.* **14,** 927–939
11. Gowen, L. C., Avrutskaya, A. V., Latour, A. M., Koller, B. H., and Leadon, S. A. (1998) *Science* **281,** 1009–1012
12. Moynahan, M. E., Chiu, J. W., Koller, B. H., and Jasin, M. (1999) *Mol. Cell* **4,** 511–518
13. Xu, X., Weave, Z., Linke, S. P., Li, C., Gotay, J., Wang, X. W., Harris, C. C., Ried, T., and Deng, C. X. (1999) *Mol. Cell* **3,** 389–395
14. Xu, B., Kim, S.-T., and Kastan, M. B. (2001) *Mol. Cell Biol.* **21,** 3445–3450
15. Iwabuchi, K., Bartel, P. L., Li, B., Maraaccino, R., and Fields, S. (1994) *Proc. Natl. Acad. Sci. U. S. A.* **91,** 6098–6102
16. Iwabuchi, K., Li, B., Massa, H. F., Trask, B. J., Date, T., and Fields, S. (1998) *J. Biol. Chem.* **273,** 26061–26068
17. Xia, Z., Morales, J. C., Dunphy, W. G., and Carpenter, P. B. (2001) *J. Biol. Chem.* **276,** 2708–2718
18. Schultz, L. B., Chehab, N. H., Malikzay, A., and Halazonetis, T. (2000) *J. Cell Biol.* **151,** 1381–1390
19. Anderson, L., Henderson, C., and Adachi, Y. (2001) *Mol. Cell. Biol.* **21,** 1719–1729
20. Rappold, I., Iwabuchi, K., Date, T., and Chen, J. (2001) *J. Cell Biol.* **153,** 613–620
21. Nelms, B. E., Maser, R. S., MacKay, J. F., Lagally, M. G., and Petrini J. H. (1998) *Science* **280,** 590–592
22. Rogakou, E. P., Boon, C., Redon, C., and Bonner, W. M. (1999) *J. Cell Biol.* **146,** 905–916
23. Rogakou, E. P., Pilch, D. R., Orr, A. H., Ivanova, V. S., and Bonner, W. M. (1998) *J. Biol. Chem.* **273,** 5858–5868
24. Celeste, A., Petersen, S., Romanienko, P. J., Fernandez-Capetillo, O., Chen, H. T., Sedelnikova, O. A., Reina-San Martin, B., Coppola, V., Meffre, E., Difilippantonio, M. J., Redon, C., Pilch, D. R., Olaru, A., Eckhaus, M., Camerini-Otero, R. D., Tessarollo, L., Livak, F., Manova, K., Bonner, W. M., Nussenzweig, M. C., and Nussenzweig, A. (2002) *Science* **296,** 922–927
25. DiTullio, R. A., Mochan, T. A., Venere, M., Bartkova, J., Sehested, M., Bartek, J., and Halazonetis, T. D. (2002) *Nature Cell Biol.* **12,** 998–1002
26. Fernandez-Capetillo, O., Chen, H. T., Celeste, A., Ward, I., Romamienko, P. J., Morales, J. C., Naka, K., Xia, Z., Camerini-Otero, R. D., Motoyama, N., Carpenter, P. B., Bonner, W. M., Chen, J., and Nussenzweig, A. (2002) *Nature Cell Biol.* **12,** 993–997
27. Wang, B., Matsuoka, S., Carpenter, P. B., and Elledge, S. J. (2002) *Science* **298,** 1435–1438
28. Jullien, D., Vagnarelli, P., Earnshaw, W. C., and Adachi, Y. (2002) *J. Cell Sci.* **115,** 71–79
29. Zambrowicz, B. P., Friedrich, G. A., Buxton, E. C., Lilleberg, S. L., Person, C., and Sands, A. T. (1998) *Nature* **392,** 608–611
30. Gellert, M. (2002) *Annu. Rev. Biochem.* **71,** 101–113